Republic of Iraq
Ministry of Higher Education and Scientific Research
University of Kerbala - College of Science
Department of Chemistry

Preparation, Characterization and study of Complexes Containing Beta-lactam group with Some Transitional Elements and their Biological Activity Against Pathogenic Bacteria

A Thesis

Submitted to council of the College of Science/ University of Kerbala as a Partial Fulfillment of the Requirements for the MS.c.Degree in Chemistry

By

Ibtisam Mohammed Ali

Supervised by

Prof. Dr. Mohammed Hamid Said **Prof. Dr. Wafaa Sadiq Mohsin Al-Wazni**

2021 AD **1443 AH**

Supervisor Certification

I certify that this thesis is conducted under my supervision at the Department of Chemistry, College of Science for women, University of Babylon, University of Kerbala /College of Science/ Department of Chemistry as partial fulfillment of the requirements for the degree of Master in Chemistry.

Signature:

Name: **Prof. Dr. Mohammed Hamid Said**

Address: University of Babylon / College of Science for Women

Date: / /2021

Signature:

Name: **Prof. Dr. Wafaa Sadiq Mohsin Al-Wazni**

Address: University of Kerbala /College of Science/Department of Biology

Date: / /2021

Report of the Head of Chemistry Department
Chairman of Postgraduate Studies Committee

According to the recommendation presented by the Chairman of the Postgraduate Studies Committee, I forward this thesis for discussion.

Signature:

Name: **Assist. Prof. Dr. Adnan Ibrahim Mohammed**

Address: University of Kerbala/College of Science

Date: / /2021

Examination Committee Certification

We, the examining committee, certify that we have read this thesis **"Preparation, Characterization and study of Complexes Containing Beta-lactam group with Some Transitional Elements and their Biological Activity Against Pathogenic Bacteria"** and examined the student (**Ibtisam Mohammed Ali**) in its contents and that in our opinion; it is adequate as a thesis for the degree of Master of Science in chemistry.

Signature:

Name: **Dr Hayder Hamied Mihsen**

Title: Professor

Address: University of Kerbala , College of Science, Department of Chemistry.

Date: / / 2021

Signature:
Name: **Dr**. **Khalid Abdulkareem Mohammad**
Title: Assistant Professor
Address: University of Baghdad, College of Science, Department of Chemistry.
Date: / / 2021

(**Member**)

:Signatur
Name**:Dr.Tariq Hussein mgheer almamory**
Title: Assistant Professor
Address:
Date: / / 2021

(**Member**)

Signature:
Name: **Dr. Mohammed Hamid Said**
Title: Professor
Address: University of Babylon / College of Science for Women
Department of Chemistry.
Date: / / 2021

Signature:
Name: **Dr. Wafaa Sadiq Mohsin Al-Wazni**
Title: Professor
Address: University of Kerbala /College of Science
Department of Biology
Date: / / 2021

(**Member & Supervisor**)

(**Member & Supervisor**)

Signature:
Name: **Dr. Jasem Hanoon Hashim Al-Awadi**
Title: Assistant Professor
Address: **Dean of College of Science, University of Kerbala**.
Date: / / 2021

Dedication

This thesis would not be possible without the support of Allah, who has always given me the strength, health, and ability to complete this project.

Specifically, I would like to dedicate this thesis to my father, mother, brothers, and sisters for their endless support, patience, and goodness. Another special dedication is also given to my friends, colleagues, and to all those who have supported me throughout my journey to complete this thesis.

To put it briefly, I dedicate this work to everyone who has contributed to this study.

Ihtisam

2021

Acknowledgment

First of all, great thanks to Allah for the uncountable gifts and help to complete this thesis.

I also would like to express endless and sincere thanks and appreciation to my supervisors **Prof. Dr. Mohammed Hamid Said, Prof. Dr. Wafaa Sadiq Mohsin Al-Wazni** for his kind interest, the project suggestion, encouragement, and guidance throughout this work.

Besides, I want to thank all faculty members of the Department of Chemistry, College of Science at the University of Kerbala for their exceptional support of this work. Great thanks to the staff of Central Health lablab in Kerbala city for their assistance in antibacterial potency measurements.

With affection and deep appreciation, I thank my father, mother, and brothers for their patience, support, and enthusiastic encouragement during the completion of the thesis.

Last, I would like to express my thanks to all those who have helped me in a way or another to make this work come true.

Abstract

In this work, four new ligands have been prepared by the reaction of 6-amino penicillanic acid (6-APA) with Schiff bases to produce azo-azomethine ligands HL_1, HL_2,HL_3 ,and HL_4 respectively. Its includes preparation of 6-amino-penicillinic acid derivative from the reaction of Schiff base compound (Z)-3-((3-hydroxybenzylidene) amino) phenol) with 6-amino-penicillinic acid and linking them by the Azo bond To form ligand (HL_1),and use The“(Z)-3-((3-hydroxybenzylidene) amino) phenol) Schiff base in the preparation of (HL_2) ligand ,(HL_3) ligand was prepared by reaction the of 3-(((4-hydroxyphenyl) imino) methyl) phenol with 6-amino penicillanic acid (6-APA),and use the 3-((4-(dimethylamino) benzylidene) amino) phenol (Schiff base compound)to formation of (HL_4) , also study the physical properties of the ligands (azo-azomethine ligands) and identifies there composition by various techniques such as ^{1}HNMR, mass spectroscopy, UV-visible, and FTIR. The result indicates that the prepared ligands acted as a tridentate ,New complexes have been prepared by the reaction of the above derivative ligands with metal ions Cu (II), Ni (II), and Fe (II) that HL_1, HL_2, HL_3, and HL4 have interacted with these metal ions in mole ratio [1:2]. The synthesized complexes are characterized using , CHNs, atomic Absorption, Uv-Visible, and FT-IR, Magnetic Moment, and Molars Conductivity for all prepared compound. The results show that the complexes suggested be with octahedral geometry with d^2sp^3 and sp^3d^2. The antibacterial activity of the synthesized compounds is studied against (*Staphylococcus aureus*) using the minimum inhibitory concentration (MIC). The results show that (MIC) of the prepared compounds has inhibition activity against (*Staphylococcus aureus*) bacteria and obviously affects the ability of pathogenic bacteria (*S. aureus*) to attain virulence factors such as biofilm and hemolysin toxin.

Table of Contents

No.	Subject	Page
	Dedication	
	Acknowledgment	
	Abstract	I
	Table of Contents	II
	List of tables	V
	List of figures	V
	Chapter One ***Introduction***	
1.1	Introduction	1
1.2	Schiff base	2
1. 2.1	Synthesis of Schiff bases	2
1.2.2	Methods for Preparing Schiff bases	4
1.2.3	Classification of Schiff Bases Complexes According to no. of atoms Donor:	5
1.1.4	Applications of Schiff bases:	11
1.2	AZO compound:	14
1.2.1	synthysis of Azo dye:	14
1.2.2	Classification of Azo Dyes:	15
1.2.3	Azo dye applications	17
1.3	Azo-azomethine compound	19
1.4	6-amino pencillanic acid	21
	Chapter Two ***Experimental part***	
2.1	The chemicals	27
2.2	Apparatus:	28
2.3.1	Preparation of the ligand (HL_1)	30
2.3.2	Preparation of ligand (HL_2)	32

No.	Subject	Page
2.3.3	Preparation of the ligand (HL_3)	34
2.3.4	Preparation of the ligand (HL_4)	36
2.4	The biological activity of ligand and its complexes on some bacteria	39
2.4.1	The apparatus and instruments used in the experiments	39
2.4.2	Methods of preparation Culture media	40
2.4.3	Collection of samples:	43
2.4.4	Identification of Isolated Bacteria	
2.4.5	Morphological and Culture Characteristic	44
2.4.6	Biochemical Tests	44
2.4.7	Vitek Diagnosis System	44
2.4.8	Minimum inhibitory concentration (MIC)	42
2.4.9	Antibacterial activity of the ligand and complexes	42
2.4.10	Effect ligands and complexes on isolated bacteria to procedure virulence factors	43
	Chapter Three ***Results and Discussion***	
3.1	Solubility tests:	48
3.2	Infrared Spectra:	50
3.2.1	Infrared spectrum Ligand (HL_1)	51
3.2.2	Infrared spectrum Ligand (HL_2)	51
3.2.3	Infrared spectrum Ligand (HL_3)	51
3.2.4	Infrared spectrum Ligand (HL_4)	52
3.2.5	Infrared spectrum of complexes with (HL_1)	55

No.	Subject	Page
3.2.6	Infrared spectrum of complexes with (HL_2)	56
3.2.7	Infrared spectrum of complexes with (HL_3)	56
3.2.8	Infrared spectrum of complexes with (HL_4)	57
3.3	Micro-elemental Analysis	70
3.4	Molar Conductivity Measurements	72
3.5	Magnetic Susceptibility Measurements	73
3.6	Study of the electronic spectra of ligands and metal complexes	76
3.6.1	Ligand Spectra	76
3.6.1	Charge-transfer Spectra:	76
3.6.2	Transition Spectra (d-d)	76
3.6.3	Counter-ion Spectra	76
3.6.4	Ligand Spectra	76
3.7	Nuclear magnetic Resonance spectrum	91
3.8	Mass spectroscopy	95
3.9	Proposed molecular structures of Ligands complexes	105
3.9.1	Copper, nickel and iron complexes derived from ligand (HL_1)	105
3.9.2	Complexes of copper , nickel and iron of ligand (HL_2)	106
3.9.3	Copper, nickel and iron complexes derived from ligand (HL_3)	107
3.9.4	Complexes of copper, nickel and iron of ligand (HL_4)	108
3.10	Biological activity of ligands and complexes	110
3.10.1	Determination of the minimum inhibition concentration (MIC)for ligand and complexes	111
3.10.2	The antibacterial activity of ligands and complexes	115
3.10.3	Effect of the ligand and complexes on biofilm formation	120
3.10.4	Effect of the ligand and complexes on Hymolysin formation	122
	Conclusion	123

No.	Subject	Page
1-2	Purity of the chemicals and their sup Pliers	28
2-2	Schiff base and Azo-Azomethine color m.pt. And yield%	39
2-3	Tools and instruments	40
2-4	Culture media	38
3-1	Solubility of organic ligands and their complexes in different solvents	41
3-2	FT-IR spectra bands of the synthesized ligands and complexes	49
3-3	the results of the element analysis(CHN) of the ligands (HL_1), (HL_2), (HL_3), (HL_4).	71
3-4	the atomic absorption of the metal in their complexes	71
3-5	The molar conductivity values of some of the electrolytes in solvents When ($1x10^{-3}$) Concentration	73
3-6	Values of molar conductivity (mol^{-1} ohm^{-1} cm^2) for ligands and there complexes In DMSO solvent at ($1x10^{-3}$) molar concentration at laboratory temperature.	82
3-7	Electronic Spectra and Magnetic susceptibility of ligands and complexes in DMSO solvent at laboratory temperature.	110
3-7	Minimum Inhibition Concentration (MIC)for ligand and complexes	113
3-9	Antibacterial Activity of ligands and complexes against *S. aureus* bacteria	106

List of Figures

No.	Subject	Page
1-1	Mechanism of Schiff Bases in an Acidic Medium	3
1-2	Complexes of Monodentate Schiff Bases	6
1-3	Monodentate Schiff Bases	7
1-4	Bidetate Schiff Base:	8
1-5	Tridentate Schiff Bases	9
1-6	Titradentate Schiff Base:	10
1-7	Ligand and Complex	11
1-8	Macrocyclic Schiff Bases	12
1-9	Complex of HL_1	14
1-10	Preparing Mono Azo Dye	16
1-11	Synthesis of the Monomers	17
1-12	Spatial Composition of the Compounds.	18
1-13	Preparing Azo-azomethine Ligand and Complex	21
1-14	Proposed Spatial	22
1-15	6-amino penicillanic acid	24
1-16	Ligand and complexes	25
1-17	Ligand complexes	26
1-18	Scheme Structures of b-lactam derivatives	24
1-19	L2 complexes	25
3-1	FTIR Ligand (HL_1)	46
3-2	FT-IR spectrum (HL_2)	47
3-3	FT-IR spectrum (HL_3)	48
3-4	FT-IR spectrum (HL_4)	49
3-5	FTIR spectra of the copper complex[$Cu(L_1)_2$]	52
3-6	FTIR spectra of Nickel complex [$Ni(L_1)_2$]	53
3-7	FTIR spectra of iron complex [$Fe(L_1)_2$]	54
3-8	FT-IR spectrum copper complex [$Cu(L_2)_2$]	55
3-9	FT-IR spectrum of Nickel complex [$Ni(L_2)_2$]	56
3-10	FT-IR spectrum of iron complex [$Fe(L_2)_2$]	57

3-11	FT-IR spectrum of copper complex $[Cu(L_3)_2]$	58
3-12	FT-IR spectrum of Nickel complex $[Ni(L_3)_2]$	59
3-13	FT-IR spectrum of iron complex $[Fe(L_3)_2]$	60
3-14	FT-IR spectrum of copper complex $[Cu(L_4)_2]$	61
3-15	FT-IR spectrum of Nickel complex $[Ni(L_4)_2]$	62
3-16	FT-IR spectrum of iron complex $[Fe(L_4)_2]$	63
3-18	Electronic spectra of ($C_{24}H_{26}N_4O_4S$) HL_1	83
3-19	Electronic spectra of ($C_{22}H_{21}N_3O_5S$) HL_2	83
3-20	Electronic spectra of ($C_{22}H_{21}N_3O_5S$) HL_3	84
3-21	Electronic spectra of ($C_{22}H_{21}N_3O_5S$) HL_4	84
3-22	Electronic spectra of copper complex$[Cu(C_{24}H_{25}N_4O_4S)_2]$	85
3-23	Electronic spectra of copper complex$[Cu(C_{22}H_{20}N_3O_5S)_2]$	85
3-24	Electronic spectra of copper complex$[Cu(C_{22}H_{20}N_3O_5S)_2]$	86
3-25	Electronic spectra of copper complex$[Cu(C_{24}H_{25}N_4O_4S)_2]$	86
3-26	Electronic spectra of nickel complex$[Ni(C_{24}H_{25}N_4O_4S)_2]$	87
3-27	Electronic spectra of nickel complex$[Ni(C_{22}H_{20}N_3O_5S)_2]$	87
3-28	Electronic spectra of nickel complex$[Ni(C_{22}H_{20}N_3O_5S)_2]$	88
3-29	Electronic spectra of nickel complex$[Ni(C_{24}H_{25}N_4O_4S)_2]$	88
3-30	Electronic Spectra of iron $[Fe(C_{24}H_{25}N_4O_4S)_2$	89
3-31	Electronic spectra of iron complex$[Fe(C_{22}H_{20}N_3O_5S)_2]$	89
3-32	Electronic spectra of iron complex$[Fe(C_{22}H_{21}N_3O_5S)_2]$	90
3-33	Electronic spectra of iron complex $[Fe(C_{24}H_{26}N_4O_4S)_2]$	90
3-34	HNMR spectrum of HL_1 ligand	93
3-35	HNMR spectrum of HL_3 ligand	94
3-36	HNMR spectrum of HL_4 ligand	95
3-37	Mass spectrum of ligand (L_1)	97

3-38	Mass spectrum of ligand (L_2)	98
3-39	Mass spectrum of ligand (L_3)	99
3-40	Mass spectrum of ligand (L_4)	100
3-41	Fragmentation pattern of ligand (L_1)	101
3-42	Fragmentation pattern of ligand (L_2)	102
3-43	Fragmentation pattern of ligand (L_3)	103
3-44	Fragmentation pattern of ligand (L_4)	104
3-45	Structure suggested of the copper (II), nickel (II) and iron (II) complex $[M(L_1)_2]$	106
3-46	Structure suggested of the copper (II), nickel (II) and iron(II) complex $[M(L_2)_2]$	107
3-47	Structure suggested of the copper (II), nickel (II) and iron (II) complex $[M (L_3)_2]$.	108
3-48	Structure suggested of the copper (II), nickel (II) and iron(II) complex $[M(L_4)_2]$	109
3-49	Inhibition zone diameter of ligand and complexes	114
3-50	Inhibition zone diameter of ligand and complexes	115
3-51	Antibacterial activity of (Cu_1)against S .aureus Biofilm	116
3-52	Antibacterial activity of (Ni_1)against S .aureus Biofilm	117
3-53	Antibacterial activity(Cu_2) against S .aureus Biofilm	117
3-54	Antibacterial activity (Ni_2)against S .aureus Biofilm	118
3-55	Antibacterial activity(Cu_3) against S .aureus Biofilm	118
3-56	Antibacterial activity (Ni_3)against S .aureus Biofilm	118
3-57	Antibacterial activity(Fe_3) against S .aureus Biofilm	119

3-58	Antibacterial activity (Cu_4)against S .aureus Biofilm	120
3-59	Effect MIC of [$Ni(L_2)_2$] on hemolysin	121
3-60	Effect of MIC of [$Cu(L_3)_2$] on hemolysin	121

List of Abbreviations and Symbols

Abbreviations and Symbols	The Meaning
1. 6-APA	6- amino pencillinic acid
2. HL_1	Ligand L1
3.HL_2	Ligand L2
4.HL_3	Ligand L_3
5.HL_4	Ligand L_4
5. UV-visible	Ultra Violate – visible
6. FTIR	Fourier Transformation Infrared
7. CHNs	Micro-elemental Analysis
8. MIC	minimum inhibitory concentration

Chapter One

1.1 Introduction

Coordination chemistry refers to the study of compounds that have a central atom (often metallic) surrounded by molecules or anions, known as ligands. The ligands are attached to the central atom by unusual bonds known as coordinated bonds, in which both electrons in the bond are supplied by the same atom on the ligands [1]. In coordination chemistry, a structure is first described by its coordination number, the number of ligands attached to the metal, specifically, the number of donor atoms. Although counting the ligands attached is attainable, the counting is still ambiguous. Coordination numbers are normally between two and nine, but large numbers of ligands are not uncommon for the lanthanides and actinides. The number of bonds depends on the size, charge, and electron configuration of the metal ion and the ligands. [2].

Researchers have developed this branch of inorganic chemistry by preparing different ligands carrying atoms capable of forming coordination bonds stable with metallic elements and other elements. The coordination compounds are of interest to many researchers and scholars because coordination compounds play an important role in various fields, including the analytical side to extract metals [3]. Coordination compounds are used in the spectral assessments of the transition elements. And the representative elements as well. The researchers' previous studies and processes of qualitative and quantitative estimation of low concentrations of ions are used in industrial, biological, and agricultural fields [4]. Coordination compounds are considered the inexhaustible aid in everything new in synthetic chemistry, and therefore the chemistry of coordination compounds has become a world in itself that includes many topics among its folds for each new coordination complex generating new understanding, new challenges, and a new wealth of scientific knowledge in its various useful fields [5].

1.2 Schiff Base

In coordination chemistry, there are important compounds, namely: Schiff base compounds that show great symmetry and produce stable compounds. Schiff base compounds are coordinated to metal ions via the Azomethine nitrogen. Schiff base ligands have been extensively studied in the field of coordination chemistry because of their facile syntheses, easy availability, and electronic properties. Schiff base compounds related to coordination chemistry have attracted much attention because of their significance in inorganic synthesis, analytical chemistry, refining metals, metallurgy, electroplating, and photograph [6]. Ligand compound consists of several kinds of Schiff base and azo-azomethine ligands, i.e. the Azo-azomethine ligand, which includes several active groups such as Azomethine (C=N) and azo group (N=N) that are discussed in the next sections.

Schiff base is the condensation product of aldehydes or ketones with the primary amines. The compounds are stable if there is at least one aryl group on the nitrogen or carbon. Schiff bases contain a group of azomethine and have the general syntactic formula RHC = N-R_1. The groups (-R) may be aliphatic, aromatic, homogeneous, or heterogeneous, and other various substitutes for Schiff bases [7]. The preparation of the Schiff base for the first time has been done by (Hugo Schiff) from the reaction of carbonyl compounds (dehydrates or ketones) with the primary amine [8]. Azomethine is the typical structural characteristic of these compounds. R' and R" are alkyl, aryl, cycloalkyl, or heterocyclic groups which have a general formula RHC = N- R' that can be differently replaced. These compounds are also considered to involve anile, imines, or azomethines.

The Schiff bases have a variety of names depending on the source of the primary carbonyl and amine complex. They are called aldimines if derived from aldehyde, Ketimines if derived from a ketone, while they are called (Anils), Benzanils, and Imines if the primary amine is aniline or a derivative of [9]. Schiff base ligands have comprehensive applications in several areas such as biological, inorganic, and analytical chemistry. The application of many new analytical devices requires the presence of organic reagents as essential compounds of the measuring system. Schiff base ligands are used in optical and electrochemical

sensors, and in several chromatographic methods to make the required detection to enhance selectivity and sensitivity [10].

1.2.1 Synthesis of Schiff Bases

To prepare Schiff base, there are several methods used by the researcher to prepare this type of organic compound. However, the most common among them is the use of the acidic medium as an aid addition and elimination. In the first step (the addition step), the reaction is accelerated by using acid as a catalyst (glacial acetic acid, or concentrated hydrochloric acid) as suggested by Hammett [11]. This process is called protonation of the carbonyl group followed by an attack of the nitrogen atom of the primary amine (nucleophile) on the positive partial charges of the carbon (electrophile) to form an unstable intermediate compound, where the process of re-arranging takes place. For the intermediate compound, the second step is to remove a water molecule. It is not preferable to add a large amount of acid, as this will lead to the restoration of the primary amines used, resulting to lose its nucleophilic property by occupying the unpaired electron with the acid proton to form the R-NH3 + ion, as shown in Figure (1-1) [12].

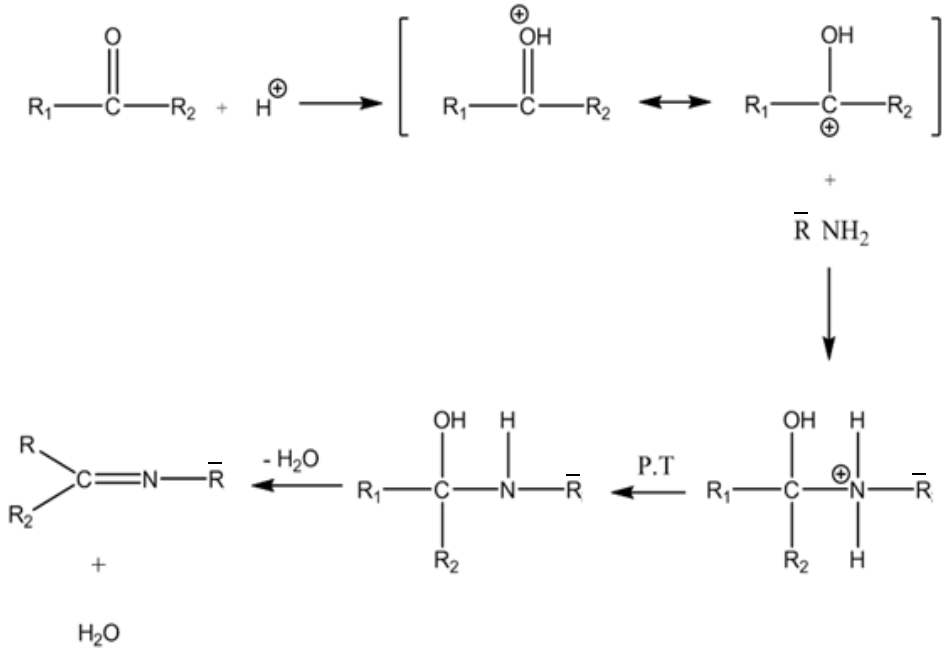

Scheme (1-1) Mechanism of Schiff Bases in an Acidic Medium

1.2.2 Methods for Preparing Schiff Bases

A. Condensation Reaction Method

The condensation reaction method is regarded as one of the most popular methods for preparing Schiff bases in which the reaction is stimulated with the presence of droplets from snow acetic acid, hydrochloric acid, or Para-sulfonic acid colorant reflux for carbonyl compounds with amine. Several researchers have explained that the acid gives a proton to the carbonyl group to form the carbonate ion which is added later to the amine in a rapid step. The limited step is the DE protonation step of the intermediate compound which is unstable and quickly loses a water molecule to form an amine as shown in Scheme (1-1) [13]. Aliphatic ketones and aldehydes rapidly have a condensation with the primary amines. To form corresponding bases, there is no spatial obstruction of the aryl and phenyl groups as for the aromatic. Thus, it reacts more slowly with amines. Then, it needs to add acid as a factor to help in heating to high temperatures to make the reaction take place [14].

B. Microwave Irradiation Method

Microwaves are known as electromagnetic waves falling between the far-infrared and radio rays that have a wavelength range. They are between 0.1 and 100 cm, corresponding to frequencies 0.3 and 300 kHz. The waves of microwaves are non-ionizing rays of insufficient energy to break the bonds and form photons. They are not thermal energy and turn into heat during their interaction with the medium in which they are reflected, implemented, or absorbed via the ability of some liquid or solid materials to convert electromagnetic radiation into heat which leads to chemical reactions. The interest in chemical synthesis with the help of microwaves makes it grow rapidly [15] .The new opportunities of technology for the chemical synthesis of compounds for using heat do not work. Microscopic radiation interactions have become an intensive research method since their early applications by Gedye and Majetich in 1986. It has quickly become a necessary technique in the rapid synthesis of inorganic compounds and membership, especially in the preparation of various cyclic compounds which have high

biological efficacy [16]. It is maintained that the microwave has main features as follows [17]:

1. The reaction times are extremely shorter compared to conventional heat such as reducing carbonyl compounds to alcohol by using borohydride. Also, Sodium with the presence of alumina as a catalyst under the influence of microwave radiation takes from 5.1 to 8 minutes, while in traditional methods it takes 5 days.

2. The microwave can supply energy without direct contact between source and sample.

3. The power supply to the model starts and stops immediately when the electrical power is shed and cut off.

4. The energy penetrates the model, not on its surface.

5. This technique can be used for sequential synthesis.

1.2.3-Classification of Schiff Bases Complexes According to No. of Atoms Donor:

This classification explains that coordination is the product of a Lewis acid-base reaction in which neutral molecules or anions (called ligands) are bound to a central metal atom (or ion) by coordinate covalent bonds. Ligands are Lewis bases that contain at least one pair of electrons to donate to a metal atom/ion. The factors on which the consistency depends are the nature of the metal ion, the charge, the radius, and the location of the metal ion in the periodic table [18].

a- Complexes of Monodentate Schiff Bases:

They are the complexes in which the ligand is bound through the nitrogen atom of the azomethine group that is part of the molecule. These complexes have relatively low stability, and this is possibly due to the basic characteristic of the nitrogen atom of the azomethine group [19].

Joseph and Ayisha (2013) have prepared copper, nickel, and cobalt binary complexes. They also have prepared one of the ligands that behave in a

Monodetate. The researchers have used CHN, FTIR, UV-Vis techniques, and magnetic sensitivity measurements to diagnose the prepared complexes, suggesting the tetrahedral shape of the complexes as shown in Figure (1-2) [20].

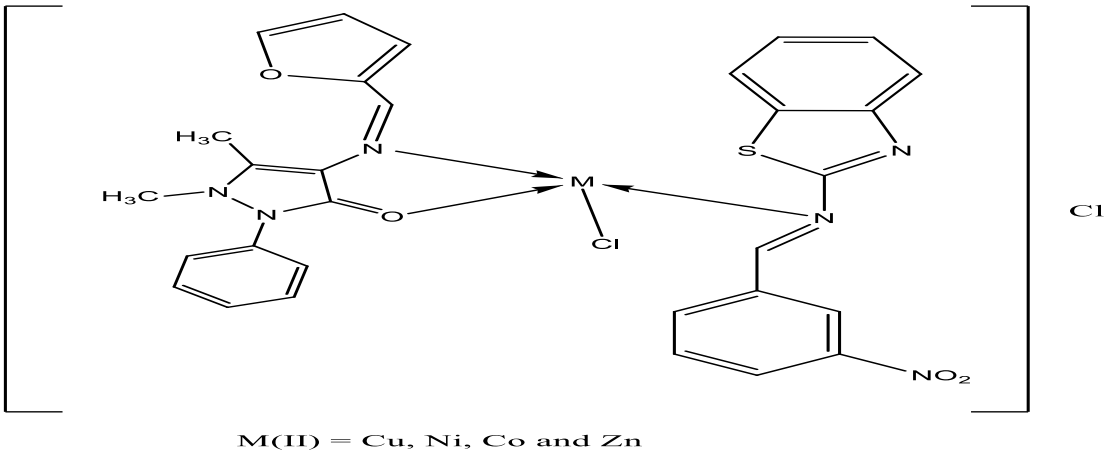

Figure (1-2) Complexes of Monodentate Schiff Bases

Muhammet Köse and et al. (2015) have prepared two ligands and studied their properties by the analytical and spectroscopic methods. The electrochemical photoluminescence properties of the Schiff bases have been investigated in different conditions. In their study, single crystals of the compounds (L1) and (L2) have been obtained from the methanol solution and structurally diagnosed by the X-ray crystallography technique. In the course of the complexation, the nitrogen and oxygen atoms of the azomethine ,the results of the study show that the molecule L2 is centrosymmetric whereas the L1 has no crystallographically imposed molecular symmetry [21].

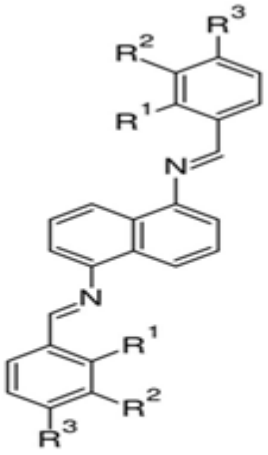

R^1: -OCH_3; R^2, R^3: H(L^1);R^1, R^2, R^3: -OCH_3 (L^2).

Figure (1-3) Monodentate Schiff Bases

b- Bidetate Schiff Base:

Chandrasekhar Vidya Rani, and his team (2020) have prepared and diagnosed new Schiff base ligands (HL1), (HL2) nickel, and metallic copper complexes by employing different analytical spectroscopic techniques and analyses. It is found that the single crystal XRD analysis confirms the proposed structure of ligands such as HL1 and HL2. It is also shown that EPR spectral analysis gives evidence about the tetrahedrally coordinated geometry that complexes show more binding towards HSA, may have good bioavailability and are likely to act as drug candidates [22].

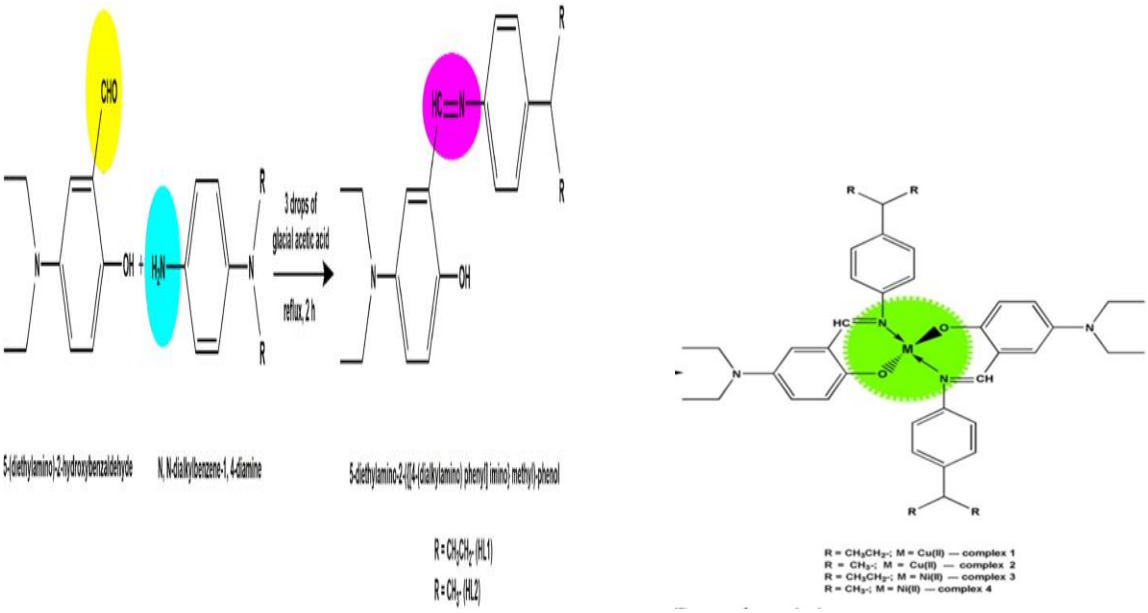

Figure (1-4) Bidetate Schiff Base:

Mohammad Azam (2020) has prepared a novel zinc complex by using the reaction of one equivalent of a bidentate Schiff base of interaction N, N0-bis (2-chlorobenzylidene)-2, 2-dimethylpropane-1, 3-diamine with one equivalent of zinc chloride in methanol diagnosed by elemental analyses, NMR, IR, and single-crystal X-ray crystallography. The crystallographic studies reveal that the zinc ion in the complex is coordinated to two imine nitrogen atoms of L and two chloride ions of zinc chloride. Besides, the anti-inflammatory activity of the studied zinc complex has also been evaluated. The results obtained show the studied complex is a good candidate in the treatment of inflammatory disorders [23].

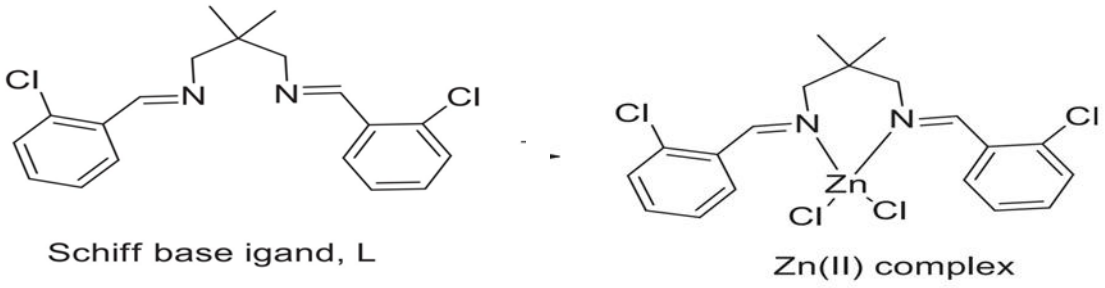

Figure (1-5) Bidentate Schiff Bases

c- Tridetate Schiff Base:

Carolina Manzur & Néstor Novoa (2020) conducted pieces of research and prepared synthesis and new developments of unsymmetrically substituted multi-dentate Schiff bases with electronic characteristics. They have also examined the electronic properties of complex and ligands of the synthesis of unsymmetrically substituted tetradentate Schiff bases and their transition metal (V, Mn, Fe, Co, Ni, Cu, Zn, Ru, Pd, Pt), and uranyl complexes [24].

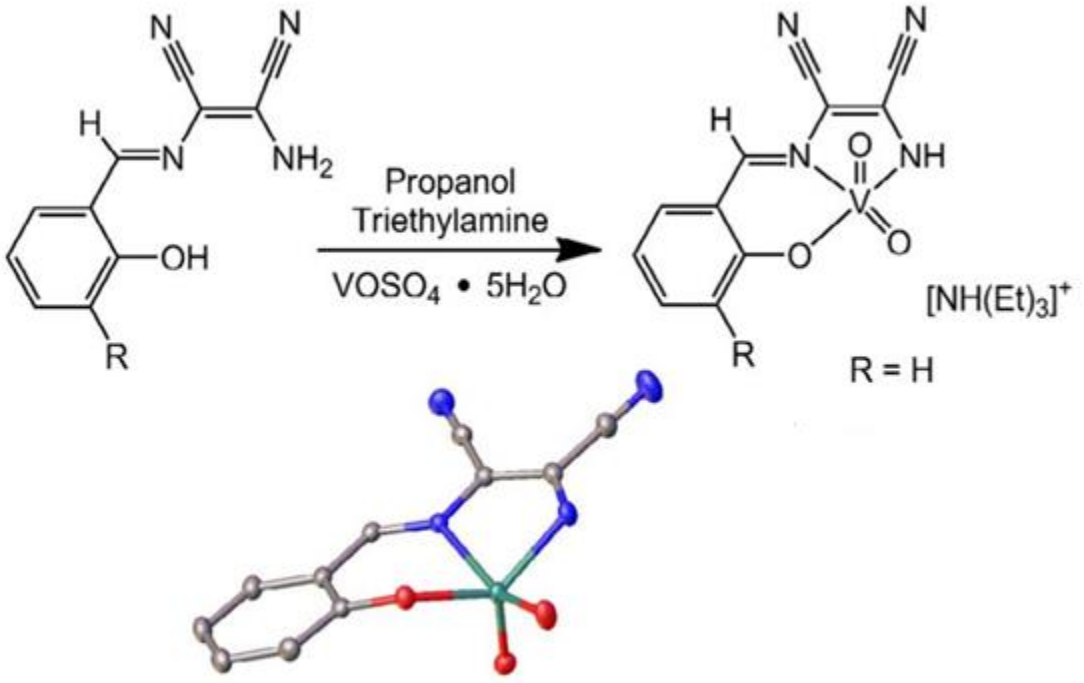

Figure (1-6) Tridentate Schiff Base:

d- Tetradentate Schiff Base

Khatereh Abdi and et al., (2020) have synthesized the Tetra aza macrocyclic Schiff base complex of Zn (II). They have also studied the interaction between the Zn (II) complex with calf thymus-deoxyribonucleic acid (CT-DNA) and bovine serum albumin (BSA) through the use of ultraviolet-visible absorption spectroscopy. The results show that the values of the binding constant of the metal complex to CT-DNA are more compared to BSA. The study also shows that the concentration of Zn (II) complex at the midpoint of transition from with CT-DNA is lower compared to BS [25].

e- Macro Schiff Bases:

Xiang Liu, Carolina Manzur C, & Néstor Novoa (2018) have conducted pieces of research on the synthesis and new chiral mononuclear complexes. They have found that all complexes are diagnosed by elemental analysis, circular dichroism, electronic, and IR spectroscopy. In their study, 1 H NMR complexes showed that Schiff bases are coordinated to the MoO22+ cation to create facial (Fac) and meridional (Mer) types of geometrical isomers [26].

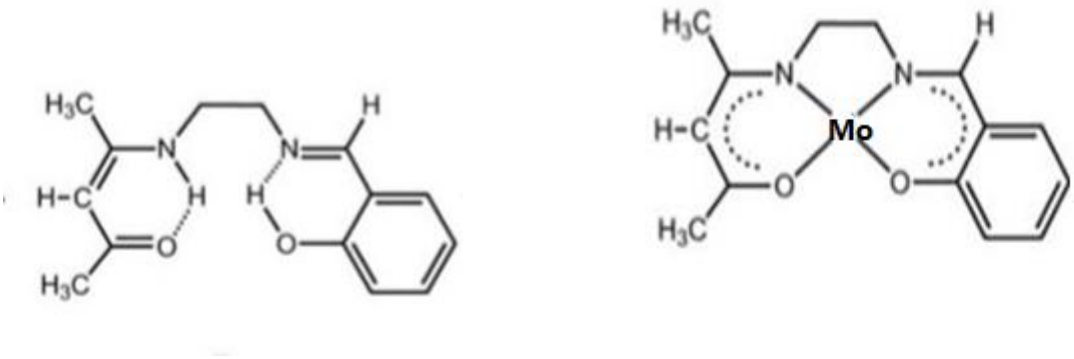

Figure (1-7) Ligand and Complex

Xiang Liu A& Jean-René Hamon (2019) have synthesized a new pentadentate, hexadentate, heptadentate, and macrocyclic Schiff base ligands containing various donor sets O, N, S, or P donor atoms and their metal complexes (essentially mononuclear). They have also synthesized ligands, prepared some of the transition metal complexes, and used spectroscopic techniques for their chemical structures. The results of the study confirm the efficacy of the synthesized compounds against cancer diseases [26].

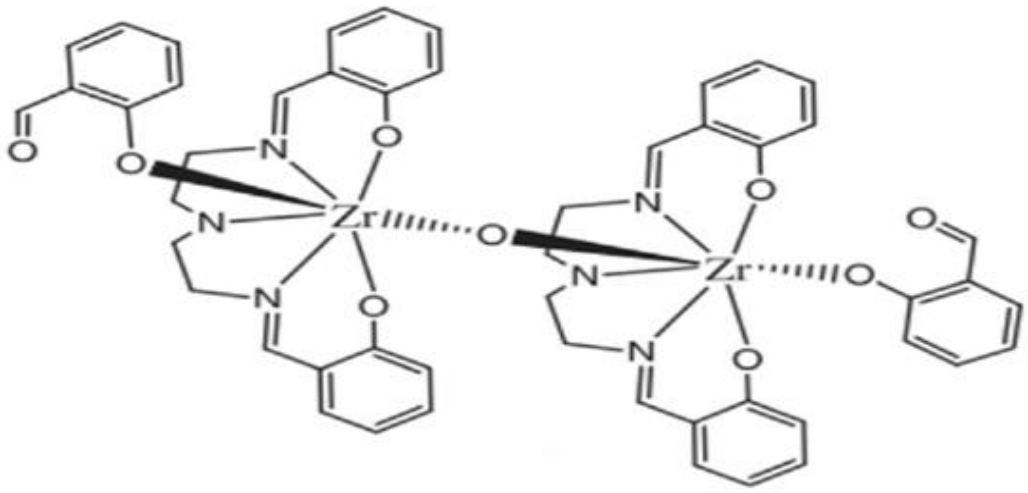

Figure (1-8) Macrocyclic Schiff Bases

1.1.4-Applications of Schiff Bases:

Schiff bases are one of the important areas in chemistry because they are employed in various fields and applications as inorganic compounds. The Schiff bases' uses and applications are countless but some applications are discussed as follows:

a- Industrial Applications:

Schiff bases are of great importance within the industrial field due to their extensive use in many fields such as working as a corrosion inhibitor that can form a protective layer on surfaces. These compounds have been tested on copper, iron, acetylated surfaces in acid and base media. They are used in lighting devices and as sensors in optical and electrochemical devices. These bases are utilized as plasticizers and stabilizers for polymers and gasoline, precursors for the polymerization process, antioxidants, and catalysts in the preparation of epoxy compounds [28].

Importantly, for the first time, an X3BA antiperovskite ferroelectric [(CH3)3NH] 3(MnBr3) (MnBr4) (where (CH3)3NH is X, MnBr3 is B, and MnBr4 is A) is reported in this study. Its significance lies in showing outstanding ferroelectricity with a significantly high phase transition temperature of 458 K as well as fascinating photoluminescence properties with two intense emissions. This chemical outcome opens a new avenue to explore the golden area of Antiperovskites for high-performance functional materials [29].

As synthetic compounds, they are employed as versatile tools in numerous applications such as fluorescent turn-on/turn-off sensors to determine diverse analysts (e.g., metallic components). As such, they can offer a new method to prepare toxic ions and/or to provide their speciation in environmental media. This review covers a broad range of Schiff bases used in sensing applications for metallic cations and anions in various kinds of environmental and biological media.[30]

b- Analytical Applications:

Due to Schiff bases' ability to form stable complexes with the ions of the elements, they have been recently used in the extraction and estimation of these elements. Recent studies and pieces of research have shown the analytical applications of the Schiff bases. Wang, Y., Ma (2018) has designed and synthesized new types of fluorescent chemosensor HL1. This sensor displays high selectivity and sensitivity for Al3+ compared to other competing metal ions. This study has also suggested a new type of fluorescence chemosensor based on quinoline-base. With the synthesis of the Schiff base, it displays high selectivity, good linear relationship, and low detection limit (8.08 × 10−8 mol/L) [31].

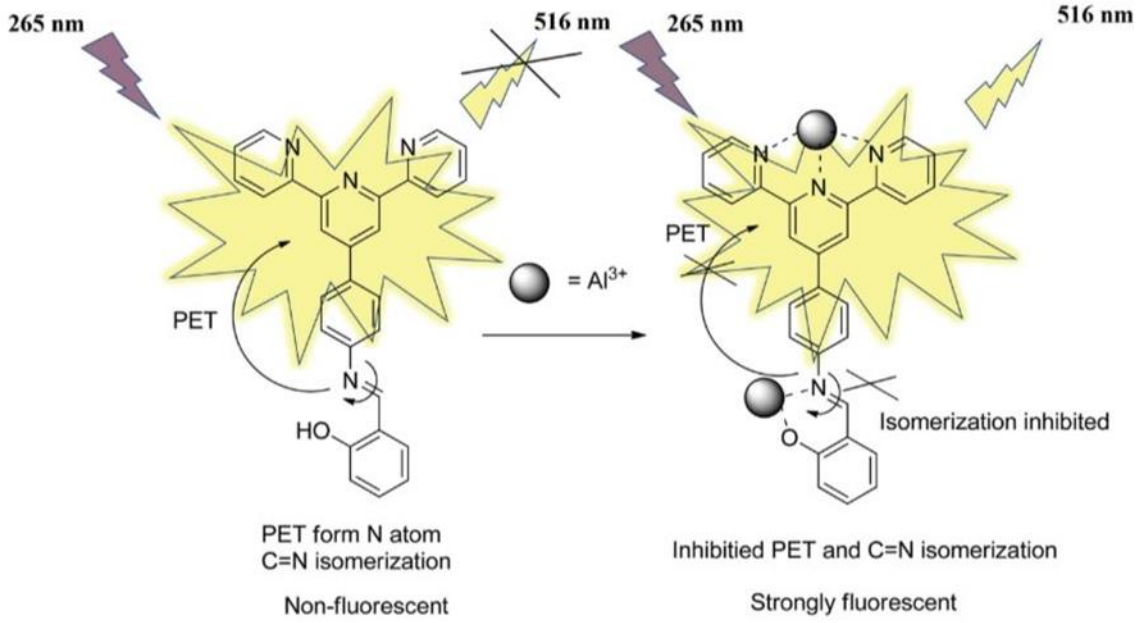

Figure (1-9) Complex of HL1

c- Medical and Biological applications:

Schiff bases are distinguished by their vital effectiveness in several biological and medical uses. They are used in preparing various drugs because their compounds play an important role in treating common diseases at present. In many cases, the cofactors of biologically important proteins are linked to their apoproteins by Schiff bases. In the next review, three classes of proteins in which Schiff bases are crucial for their function and catalytic mechanisms are discussed. First, there was a focus on retinylidene proteins where the cofactor retinal is fixed to the apoproteins by a protonated Schiff base [32]. Several studies have shown the biological applications of the Schiff bases in several areas. Al-Khathami, N. D., Al-Rashdi, K. S., New (2019) prepared to have Schiff base reacted with cis-[$PtCl_2$ (DMSO) $_2$], generating platinum (II) complexes. They have also prepared and diagnosed ligands and platinum (II) complexes by using IR and NMR spectroscopic methods. Besides, they show that single-crystal XRD presents structural confirmation for three of the organic compounds and two platinum complexes. Moreover, they have

tested ligand and its complexes on microorganisms such as Escherichia coli, Bacillus subtilus, Salmonella typhimurium, and Klebsiella pneumonia. The study has found that the biological applications show various inhibitory effects on different human pathogenic bacteria [33].

1.2 AZO Compound:

One of the known chemical compounds is the azo compound, the name azo coming from azote, which is the French name for nitrogen derived from the Greek language. Many textile materials and leather are dyed with azo dyes. Azo compounds are compounds carrying the functional group R^1 - N = N - R′, where R^1 and R can be either aryl or alkyl. The IUPAC defines AZO compounds as "Diazine derivatives (diimide), HN = NH such as PhN = NPh azobenzene or diphenyldiazene, where more stable derivatives contain two aryl groups". The group N = N is called the azo group. The azo compounds (R-N = N-R') are either an aliphatic R group (unknown for their lack of stability) or aromatic (known for the full stability) [34].

Of the most important compounds in many industrial and medical fields are the Azo compounds. It is extensively used by the field of manufacturing food and industrial dyes due to its bright colors, varied advantage, and its entry into dyeing tissues and fibers, alongside the role of its derivatives comprising the effective groups on the site that owns electrons and form them with double electronic azo-nitrogen clamp rings (pentagonal or Hexagonal) stable. They can also form stable complexes by using massive amounts of metal ions [35].

1.2.1 Classification of Azo Dyes:

Azo dyes are classified either according to the number of azo groups such as mono-azo dyes, di-azo, tri-azo, or poly-azo dyes or according to the nature of the oxychromic groups in them to acid dye, if they contain groups such as (-COOH-SO3H -OH) or basic if they contain groups such as)NR2 -NRH -NH2-). If the dye contains both types of groups, the classification depends on the number and strength of these groups [36]. Azo compounds are divided according to the type of the ring where it has two similar or aromatic groups on both ends and hence are called Homogeneous Azo. If the azo compounds have two heterogeneous organic

groups, they are called heterogeneous azo compounds, and this type of pigment is specific as (Heterocyclic azo dyes) are relatively recent reagents [37]. They are widely used in the field of chemical analyses because they contain heterozygous aromatic rings located on one or both sides of the azo group with the presence of an atom or donor atoms such as (S, N), O) or the aromatic rings are replaced by a different group (acidic or basic) or it may contain the two previous types together and in the same ring [38]. Many studies are conducted on the classification of Azo dyes and making the groups. Çiğdem Karabacak Atay & et al., (2019) have synthesized a new mono azo dye 5-amino-4-[4-(dimethylamino) phenyl] diazenyl]-pyrazol-3-ol (A) and 5-amino-4-[4-(dimethylamino) phenyl] diazenyl]-2-phenyl-pyrazol-3-one (B) and have studied their FT-IR, 1H NMR, and UV–Vis properties. The study shows that the good agreement between the results of the experiment and computation indicates that DFT and HF methods can provide satisfactory results for structural, spectroscopic, and electronic properties of mono azo dyes [39].

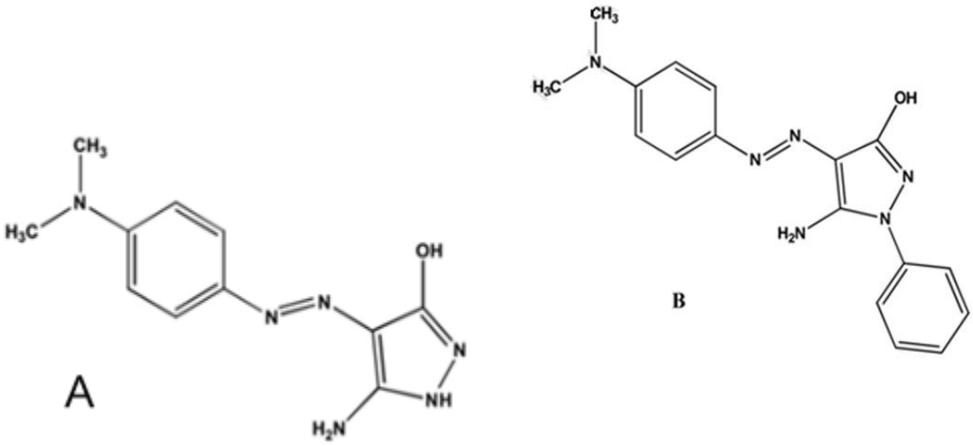

Figure (1-10) Preparing Mono Azo Dye

Khalid Hakkoustudy (2019) has designed and synthesized degradable linear azo polymers catalyzed polymerization of diynes and diazides to obtain a novel type of linear copolymer prepared from monomers derived from poly (ethylene glycol), 5, 50-azodisalicylic acid [olsalazine], and 1, 4-butanediol diglycidyl ether. All of them are diagnosed by Fourier transform infrared, nuclear magnetic resonance (NMR), gel permeation chromatography (GPC), and Differential scanning calorimetry (DSC). The result has been degraded by azoreductase

enzymes present in the colonic microbiota. It is found that a biodegradation experiment of a water-soluble prototype polymer shows that they are biodegradable via a strain of Enterococcus faecalis [40].

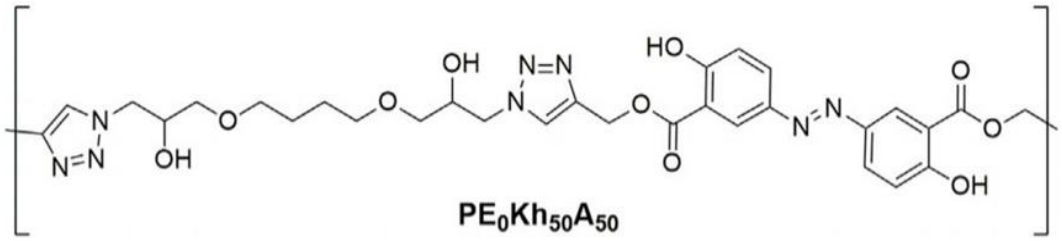

Figure (1-11) the Synthesis of the Monomers

1.2.2 Synthysis of Azo Dye:

The synthesis of an azo dye requires two organic compounds a diazonium salt and a coupling component. The diazonium salt reacts as an electrophile with an electron-rich coupling component such as the β-naphthol and naphthaline derivative through an electrophilic aromatic. Synthesis of most azo dyes involves diazotization of a primary aromatic amine followed by coupling with one or more nucleophiles. Amino- and hydroxy- groups are commonly used coupling components because of the diversity of dye components available for synthesis, as a large number of structurally different azo dyes are used in industry [41].

Azo dyes are prepared in a two-step reaction; the first is the synthesis of an aromatic diazonium ion from an aniline derivative. The next step is the coupling of the diazonium salt with an aromatic compound as shown below with the preparation of methyl yellow. The colors of azo dyes include different shades of yellow, red, orange, brown, and blue. The stoichiometry (a 1:1 mole ratio) shall be kept the same and due to changing molecular weights of the starting materials, different amounts of starting materials are used, thus there are separate procedures for each combination. The literature review of studies contains 16 different combinations but one of the starting materials is very expensive. However, it is found that the resulting colors are not very different from other colors [42].

1.2.3 Azo Dye Applications:

Azo dyes are widely used in textile, fiber, cosmetic, leather, paint, and printing industries. Along with their characteristic coloring function, azo compounds are reported as antibacterial, antiviral, antifungal, and cytotoxic agents. They can be used as drug carriers, either by acting as a 'cargo' that entrap therapeutic agents or by a prodrug approach [43].

A-Biological Application:

The biological activity of azo compound mostly results from the specific pathway of their metabolism. An enzyme-mediated reduction of the azo bond occurs in vivo. In mammalian organisms, it is found in the liver, digestive tract bacteria, and skin bacteria such as Staphylococcus aureus. The result of this reaction is the cleavage of the azo bond and the release of the corresponding aromatic amines originating from the azo dye [44]. Among the studies conducted on the biological application is a study by Siham Sami Al-Muhanaa & Abbas Hmood Al-Khafagy (2018) where they have prepared and synthesized new azo ligand, 2[(Aminoantipyren) azo]-4,5-bis(4-Methoxyphenyl)-H imidazole, (AAMPI) Then, complexation of the ligand with ions Co(II), Ni(II), Cu(II), Zn(II), Cd(II) and Hg(II) to yield six complexes with the general formula $[M(L)_2]$ Cl2.H2O, finding that the azo ligand is tridentate. They have prepared the structures of the ligand with complexes by using ultraviolet-visible spectroscopy (UV-Vis), Fourier-transform infrared spectroscopy (FT-IR), and proton nuclear magnetic resonance (1HNMR). They have tested synthesized compounds against the gram-negative, gram-positive bacteria and fungus. The results of the study show that the metal complexes exhibit antibacterial and antifungal activities compared with free ligand [45]. The spatial composition of these compounds is shown in Figure (1-12).

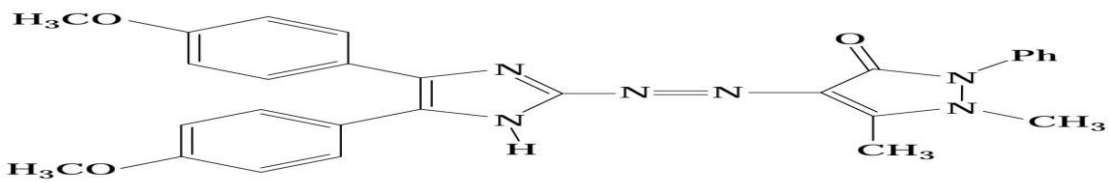

Figure (1-12) Spatial Composition of the Compounds.

B-Analytical Applications:

Despite the scientific and technological progress of the devices used to analyze and prepare trace amounts of ions, it has been found that azo compounds are the best in the of analyze very small quantities that are safe for these ions due to their high ability to form stable complexes[46]. Many studies are conducted on analytical applications. Nabeel Sabeh Othman & Safaa Abdul Aleem Zakaria (2018) have assayed micro amounts of paracetamol by using a method based on the reaction of p–aminophenol which results from the acid hydrolysis of paracetamol, with nitrite ion to form the corresponding diazonium salt followed by coupling reaction in an alkaline medium with phloroacetophenone to form a stable and soluble orange azo dye. The method has been successfully applied to assay paracetamol in various pharmaceutical preparations [47].

c- Industrial Applications:

Azo dyes are the most important synthetic colorants widely used in textile, printing, and paper manufacturing. Azo dyes are the largest group of synthetic aromatic dyes used in the textile industry for dyeing purposes and as a high water colorant soluble in nature. In textile azo dyes, they use synthetic dye, reactive dye, acid dye, sulfur dye, basic dye, oxidation dye, and other different colorants. Azo dyes are also known as azoic or nepthol dyes. The azo dyes are chiefly of red, brown, and yellow colors. The chemicals from which these dyes are manufactured are called fragrant amines. Dyes used in the food and textile industry consist of 60-70% of azo dyes. They are synthetic colors and most of them contain only one azo group. However, some azo dyes contain more than one azo group. In opposition to the belief, azo dyes are not made from coal or tar. The specialty of this dye is that it can provide almost all colors. The aromatic compounds in the azo dyes are the reason that they produce a strong and variety of colors. Manufacturing azo dyes is easy and cheap as the components of the dyes are cheap and easily available [48].

1.3. Azo-azomethine Compound

The class of compounds is regarded as derivatives of methylimine and is diagnosed by grouping −CH=N− or >C=N−. Schiff base —used especially of dyes important in color photography. Both Schiff bases and azo compounds are important structures in medicinal and pharmaceutical fields because the azo-azomethine compounds might be responsible for the biological activities. These compounds have also received special attention because of their mixed soft-hard donor characteristics, versatile coordination behavior optical and pharmacological properties, and thermal properties. Among the studies done on the Azo-azomethine compounds is a study by Azam, M., Al-Resayes (2018) as he has used the azo compound to synthesize new azo-azomethine, HL and its complexes with Cu(II) and Fe(III) ions. They have diagnosed and studied the azo compound by using various physicochemical techniques such as C, H, N analyses, FT-IR, 1H-NMR, ESI-MS, and UV-V. They have also tested the ligand and its complexes for antimicrobial activity against bacterial and fungal strains by determining inhibition zone, minimal inhibitory concentration (MIC), and minimal bactericidal concentration (MBC). The study has found that the complexes show moderate antimicrobial activity when tested against Gram +ve and Gram −ve bacterial strains [49].

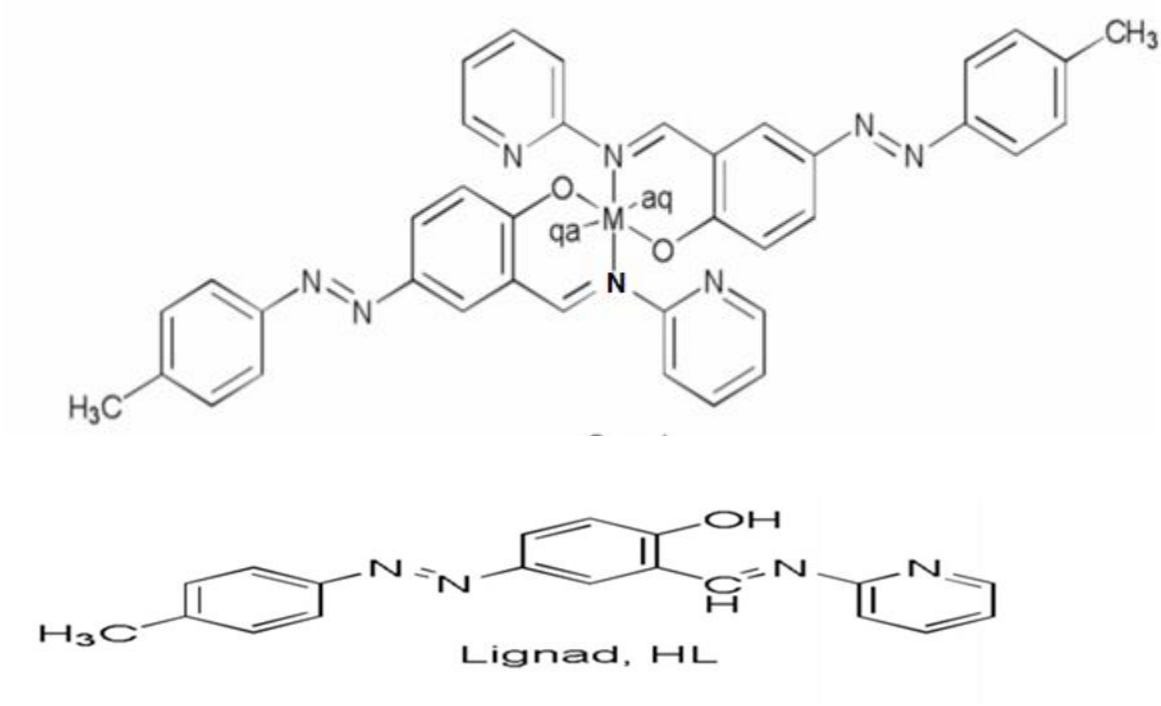

Figure (1-13) Scheme of Preparing Azo-azomethine Ligand and Complex

Fatma Sahan & Muhammet Kose (2019) have prepared and synthesized a tetrahedral derived from heterogeneous rings and a novel tetradentate azoazomethine ligand (H_2L) by using 2:1 molar condensation of an azo-aldehyde and ethylenediamine. They have also diagnosed ligand Cu (II), Ni (II), Co (II), and Zn (II) complexes by using techniques of NMR, infrared and UV–visible spectroscopies, and molar conductivity measurements. The results show that the metal ion is bound to the tetradentate ligand through phenolic oxygen and imine nitrogen of the ligand. Figure (1-14) shows the proposed spatial Figure [50].

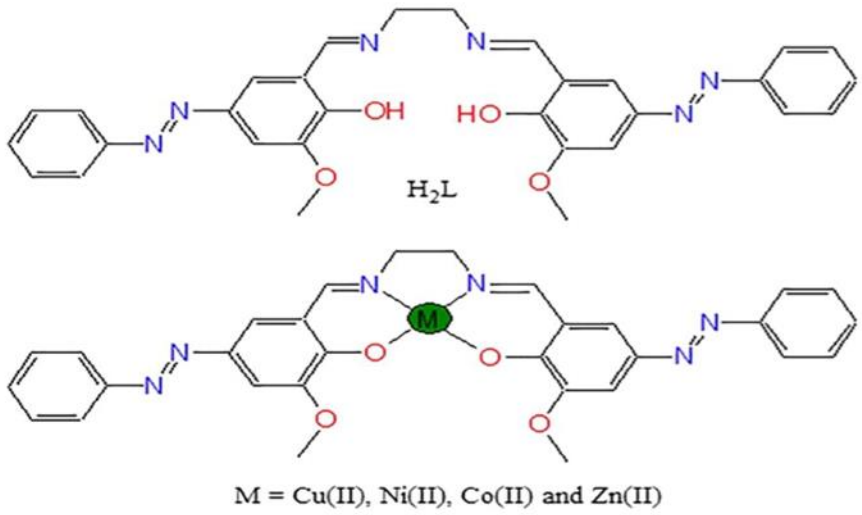

Figure (1-14) Proposed Spatial

1.4. 6-Amino Pencillanic Acid:

6-amino pencillanic acid is considered one of the most important antibiotics, and the biological effectiveness of this compound is due to the presence of a beta-lactam ring. This ring is highly effective against bacteria [51] 6-aminopenicillanic acid that has the basic structure of 5-membered thiazolidine ring connected to a 4-membered β-lactam ring attached amine group as shown in Figure (1-15). The key structural feature of the 6-aminopenicillanic acid is the four membered β-lactam ring; this structural moiety is essential for penicillin's antibacterial activity [52].

With the bacteria continuing to develop mechanisms reducing the effectiveness of these antibiotics, it is very important to continue research in the field of development and improvement of the composition and action of antibiotics. Several recent researches have been interested in developing these antibiotics by adding active groups to their composition or linking them with metal ions and forming complexes that have biological activity.

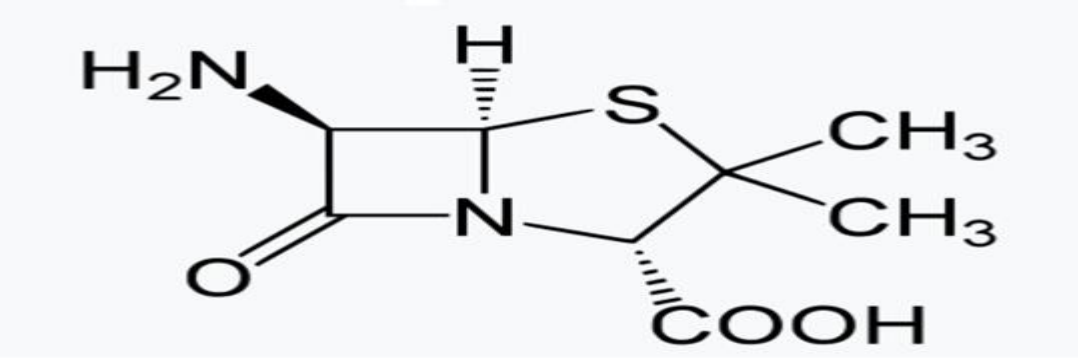

Figure (1-15) 6-Amino Penicillanic Acid

Ammar J. Alabdali and Yasser H. Saba (2016) studied the behavior of two new ligands and prepared them from the interaction of bifunctional aldehyde (terephthaldehyde and glyoxal) with the antibacterial 6-amino penicillanic acid (6-APA). The bifunctional bidendate-ligands L1 and L2 interacted with Co (II), Cu (II), and Zn (II). The resulting products are characterized using ^{1}H-NMR, Uv-Vis, and IR-spectroscopy. Metal and elemental analysis has been performed, along with molar conductivity and thermal analysis. The results show that the complexes could be with distorted octahedral geometry. The microbiological activity of the synthesized compounds has been evaluated in minimum inhibitory concentration (MIC) of the raw material 6-APA. They also found the compounds are more active and sensitive against both Gram-positive and Gram-negative organisms at the selected concentration (10^{-3}M) [53] as the complexes illustrated in Figures (1-16) and (1-17).

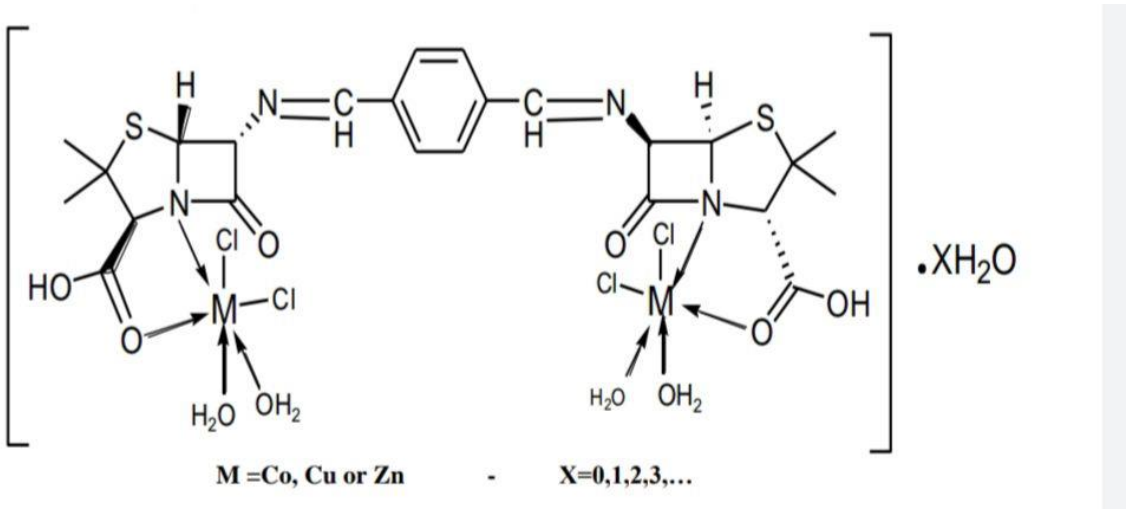

Figure (1-16) Ligand and Complexes

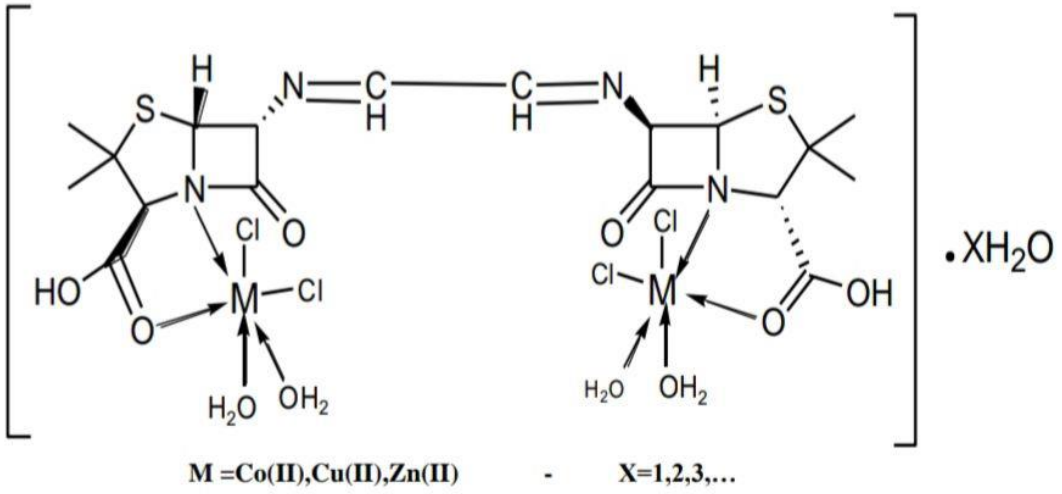

Figure (1-17) Ligands Complexes

Özdemir, Ö, Gürkan, P., Özçelik, B., & Oyard (2016) have conducted a research using new beta-lactam derivatives with higher amino acid reaction Schiff bases 6-APA and the presence of the 7-ethyl chloroformate of the ACA. The study aims to plan, analyze modern and complicated ligands, and diagnose them by using a wide variety of techniques, such as HNmr UV-visi, mass sclerosis, and atomic absorption to establish their spatial composition [54].

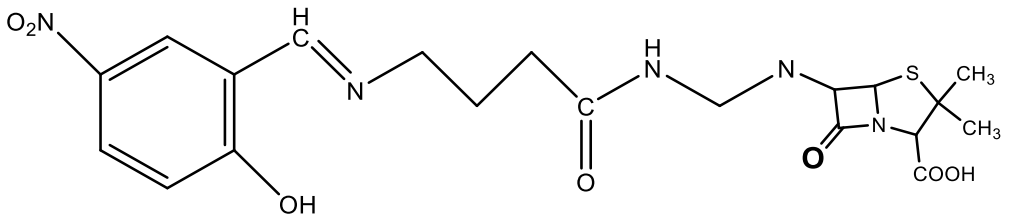

(*E*)-6-(((4-((2-hydroxy-5-nitrobenzylidene)amino)butanamido)methyl)-λ^2-azaneyl)-3,3-dimethyl-7-oxo-4-thia-1-azabicyclo[3.2.0]heptane-2-carboxylic acid

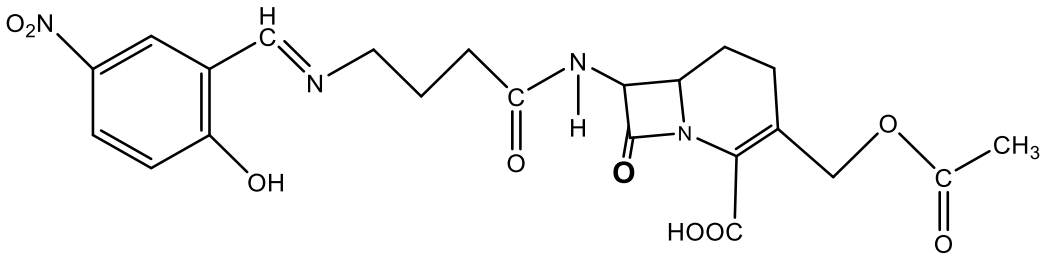

(*E*)-3-(acetoxymethyl)-7-(4-((2-hydroxy-5-nitrobenzylidene)amino)butanamido)-8-oxo-1-azabicyclo[4.2.0]oct-2-ene-2-carboxylic acid

Figure (1-18) Scheme Structures of B-lactam Derivatives

Rasha Hasan Jasim (2017) has studied the synthesis of the novel Schiff base ligands by condensing 6-Amino Penicillinic acid with Salicyldehyde. The characteristics are studied by using ^{1}H-NMR, ^{13}C-NMR, mass spectrometry, UV-Vis, and FT-IR. The ligands have attained more than one moiety to chelating to form complexes of Co (II), Ni (II), Cu (II), and Zn (II). The prepared ligand and its complexes have illustrated a good inhibitory ability towards the three varieties of bacteria (*Staphylococcus aureus*, *Pseudomonas aeruginosa*, and *Proteus mirabilis*) as shown in Figure (1-19) [55].

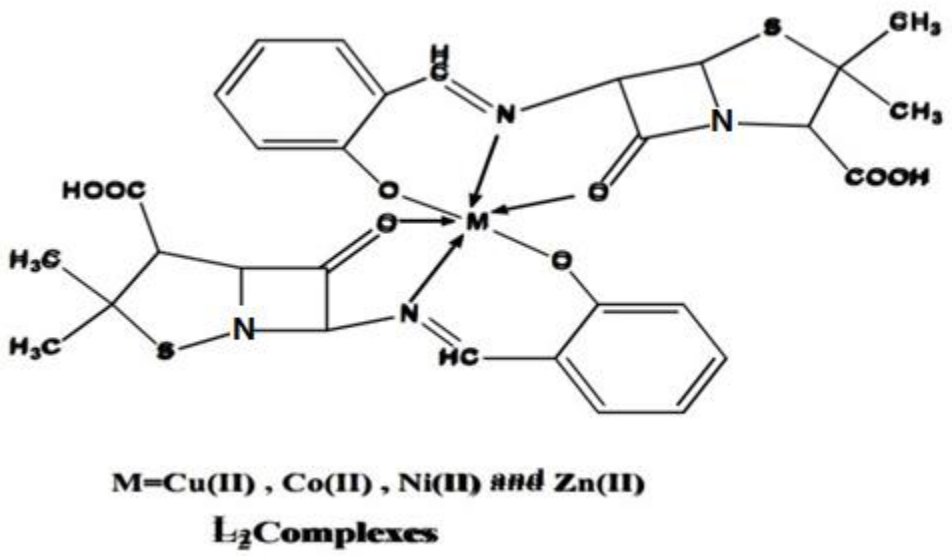

Figure (1-19) L_2 Complexes

1.5. Objectives of the Thesis:

In light of the previous introduction and the related literature review, the objectives of this thesis are:

1. Preparing a new ligand that includes a beta-lactam ring.
2. Preparing complexes from the reaction of prepared ligands with some transition metals ions.
3. Conducting analytical and diagnostic tests to propose the geometric form of the prepared complexes.
4. Isolate and Biological activity study of bacteria from deferent type of skin ulcers .

Chapter Two Experimental Part

This chapter gives insight into the chemicals used in the study the measurement and preparation process related to these chemicals.

2.1 The Chemicals

International chemicals were used and the purity of the chemicals was tested by measuring the melting point. The chemicals' purity and their suppliers are shown in Table (2-1)

Table (2-1). Purity of the Chemicals and their Suppliers

No	Substance	Formula	Company	Purity
1	6-Amino Penicillinic Acid	$C_8H_{12}O_3N_2S$	Sigma Aldrich	99.98%
2	3-amino phenol	$C_6H_4(NH_4)(OH)$	Sigma Aldrich	
3	4-amino phenol	$C_6H_4(NH_4)(OH)$	Sigma Aldrich	
4	M-hydroxy benzyldehyde	$C_7H_6O_2$	BDH	
5	P,N,N-dimethyl benzyldehyde	$C_7H_{11}NO$	BDH	
6	Absolute Ethanol	C_2H_5OH	CDH	98.99%
7	Sulphric acid	H_2SO_4	CDH	99.98%
8	Sodium nitrite	$NaNO_2$		
9	Acitic acid	$C_2H_4O_2$	CDH	
10	Copper Chloride	$CuCl_2.2H_2O$	BDH	97%
11	Nickel Chloride	$NiCl_2.6H_2O$	BDH	99%
12	Ferrous chloride	$Fecl_2.4H_2O$	BDH	98.98%
12	Dimethyl sulfoxide DMSO	C_2H_6OS	CDH	99.00%
13	Dimethylformamide DMF	C_3H_7NO	CHD	98%

2.2 Apparatus:

2.2.1 Measurement of the Melting Point:

The measurements of the melting point of the prepared ligands and complexes were made in the chemical precursors at the laboratory of the Department of Chemistry, College of Science for Woman, at the University of Babylon by using Stuart melting points SMP10.

2.2.2 FTIR Spectra

The FTIR spectra of ligands and their complexes were characterized at the laboratories of Science College / Karbala University within 4000-400 (cm^{-1}) spectrophotometers. KBr disks 400 cm^{-1} were measured using FT-IR Shimadzu FTIR 8400 S .

2.2.3 UV-Visible Spectra:

The electronic spectra of the synthesized ligand and complexes were obtained using Shimadzu1800-Uv Ultraviolet spectrophotometer using the quartz cell in the range (200-800) nm at College of Science for Woman, Department of Chemistry at the University of Babylon.

2.2.4 Magnetic Measurements:

Magnetic sensitivity of the complexes was tested for each sample at 298 k using a Susceptibility Balance Magnetic Sherwood scientific unit at the College of Science, Department of Chemistry at Al-Mustansiriya University.

2.2.5 Molar Conductivity Measurements:

Molar conductivity of the ligands and complexes were recorded at room temperature of 10^{-3}M solution for each sample using Digital Conductivity Series Ino.Lab.720 at the Department of Chemistry at Kerbala University.

2.2.6 Mass Spectroscopy:

The ligands' mass spectrum created by the system was reported as Agilent Technologies 5975C Mode with ionizing energy at the College of Science at Al-Mustansiriya University laboratories (5 to 20eV).

2.2.7 Elemental Analysis (C. H. N):

The element analysis technique was recorded in Thermo Finnigan Flash EA 1112 USA at The Isfahan University in the Islamic Republic of Iran.

2.2.8 Nuclear Magnetic Resonance Spectrum:

^{1}HNMR spectra were characterized by INOVA 500 MHz Varian, USA NMR spectrometer in DMSO-d^{6} as solvent and TMS as an internal standard at the University of Tehran in the Islamic Republic of Iran.

2.2.9 Metal Analysis:

The metal content of the complexes was measured using flame atomic absorption techniques by Agilent 30A at the Isfahan University in the Islamic Republic of Iran.

2.3.1 Preparation of the Ligand (HL_1):

Procedures:

a- Schiff base compound was prepared by dissolving (2 g, 0.0183mol) of 4-amino phenol in 10 mL absolute ethanol then mixing it with (2.6 g, 0.0176 moles,) of 4-N, N- dimethyl benzyldehyde. The reaction was refluxed for 1 hour with stirring and the proper pH was adjusted to ≈ 4 by adding several drops of glacial acetic acid where this process was followed up by a pH paper test. The color of the reaction mixture was changed to green –yellow color and precipitates were formed after cooling and evaporating the solvent. Ligand (L_1) was recrystallized by using absolute ethanol to give the titled compounds [56].

b- A solution was prepared from dissolving (2 g, $9.2x10^{-3}$mol) 6-amino pencillanic acid in 10% H_2SO_4 (1ml ,9 ml distilled water) in a baker 100mL), then a sodium nitrite solution which is concentrated 10% was prepared by dissolving (1 g, in 10 mL distilled water). Then, the two solutions were mixed with stirring and maintaining the temperature (0-5 ^{0}C). Then, the mixture was lifted for 15 minutes to complete the diazonium salt preparation [57].

A solution was also prepared from dissolving (2.2g - $9.2x10^{-3}$mol) of 4-((4-(dimethylamino)benzylidene)amino)phenol (Schiff base compound) prepared in the paragraph which was dissolved in (10% NaOH)). This solution was simultaneously mixed and stirred with the diazonium salt solution. The precipitate was filtered and washed several times with ethanol water and dried at room temperature as shown in the Scheme (2-1)

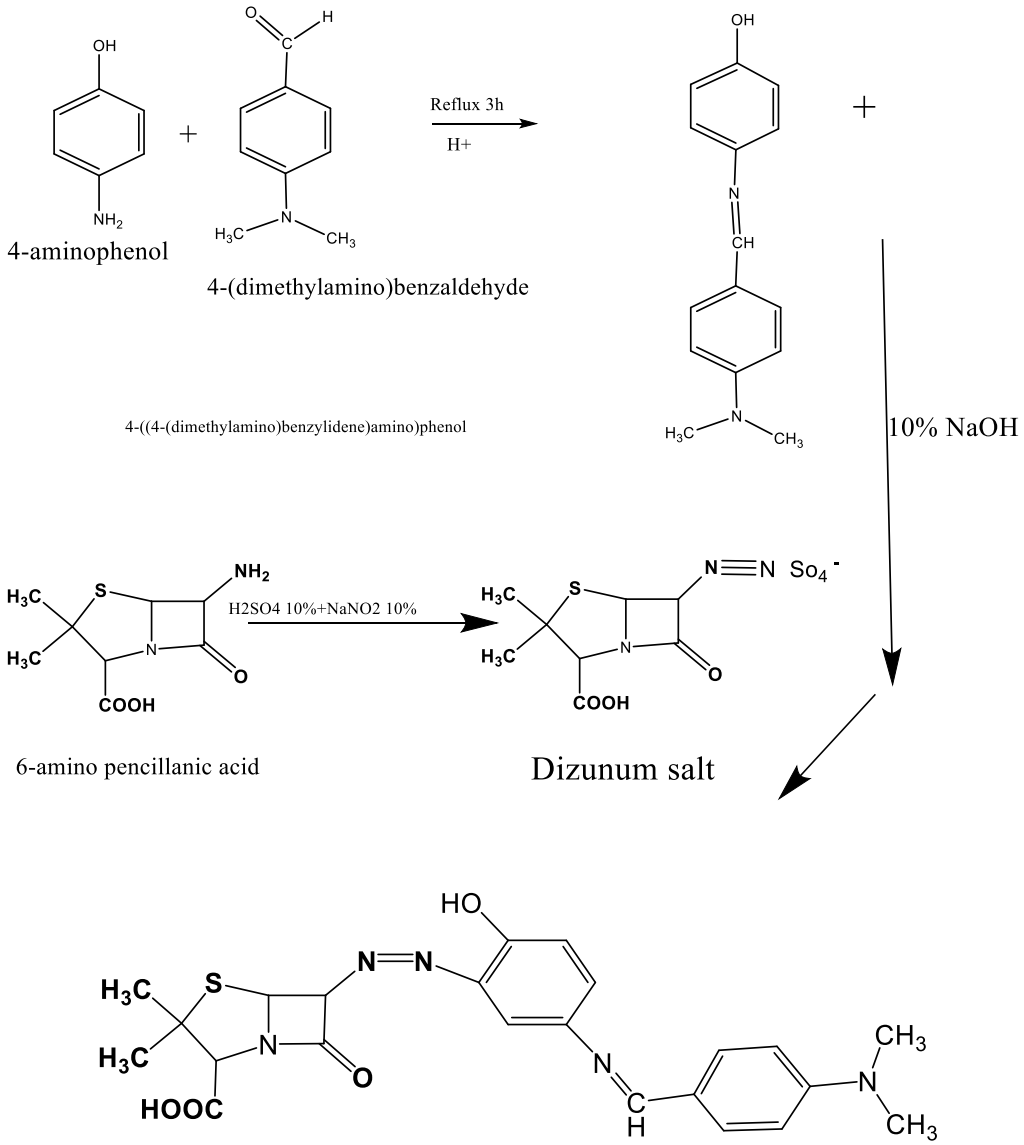

6-((1*Z*)-(5-((4-(dimethylamino)benzylidene)amino)-2-hydroxyphenyl)diazenyl)-3,3-dimethyl-7-oxo-4-thia-1-azabicyclo[3.2.0]heptane-2-carboxylic acid

HL1

Scheme (2-1) Preparation of (HL_1)

Preparation (HL_1) Complexes:

C- Complexes were prepared by dissolving (1g, $2.23x10^{-3}$mol) of (HL_1) in 10mL of absolute ethanol then mixing them with (0.76 g ,$4.47x10^{-3}$ mol) desired metal ion ($CuCl_2.2H_2O$), (1.06 g,4.47×10^{-3}mol) $NiCl_2.6\ H_2O$) and (0.88g,$4.47x10^{-3}$mol) ($FeCl_2.4H_2O$). The mixture was refluxed for 1 hour and the color was changed to Brown and Brown-orange. The resulting precipitates were formed after evaporating the solvent and recrystallized by two solvents, namely: acetone and absolute ethanol [58].

2.3.2 Preparation of Ligand (HL_2):

A-Schiff base compound was prepared by dissolving (2g, 0.0183mol) 3-amino phenol in 10 mL of absolute ethanol then mixing it with (2.15g 0.0176 mol) of 3-hydroxybenzyldehyde to prepare (Schiff base). The reaction was refluxed for 1 hour with stirring and the proper pH was adjusted to ≈ 4 by adding several drops of the glacial acetic acid where this process was followed up by a pH paper test. The color of the reaction mixture was changed and precipitates were formed after cooling and evaporating the solvent. Then, the Schiff base compound was recrystallized by using ethanol solvents to give the titled compounds as shown in Figure (2-2).

b- A solution was prepared from dissolving (2 g, $9.2x10^{-3}$mol) 6-amino pencillanic acid in 10%H_2SO_4 (1ml H_2SO_4 ,9ml distilled water) in a baker 100ml. A sodium nitrite solution which is concentrated 10% was prepared by dissolving 1 g, in 100 mL distilled water. Then, the two solutions were mixed with stirring and maintaining at the temperature (0-5 ^{0}C). Then, the mixture was lifted for 15 minutes to complete the diazonium process.

A solution was also prepared from dissolving (2.2g - 9.2×10^{-3}mol) of (Z)-3-((3-hydroxybenzylidene) amino) phenol (Schiff base compound) prepared in the (2.3.1) paragraph which was dissolved in (10% NaOH)). This solution was mixed and stirred with the diazonium salt solution. The precipitate was Brown color (104 ^{0}C m.p), filtered and washed several times with ethanol and dried at room temperature as shown in Figure (2-2).

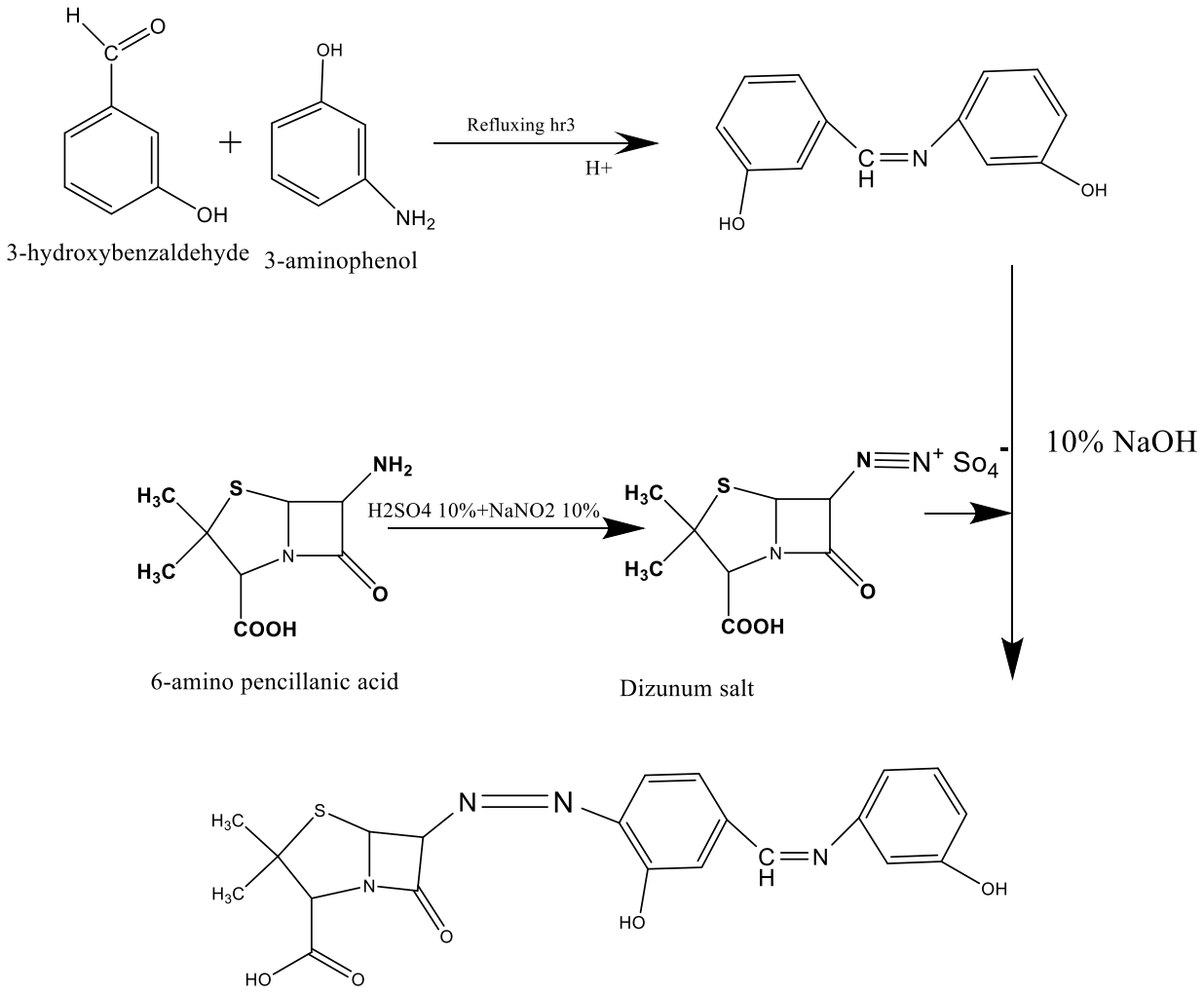

6-((*Z*)-(2-hydroxy-4-((*Z*)-((3-hydroxyphenyl)imino)methyl)phenyl)diazenyl)-3,3-dimethyl-7-oxo-4-thia-1-azabicyclo[3.2.0]heptane-2-carboxylic acid

HL2

Scheme (2-2) Preparation of Ligand (HL_2)

Complex Preparation of HL_2:

C- Complexes were prepared by dissolving (1g, 2.27 x 10^{-3} mol) of (HL) in 10mL of absolute ethanol then mixed them with (0.77g, 4.55 x 10^{-3} mol) desired metal ion ($CuCl_2.2H_2O$), (1.08 g, 4.55 x 10^{-3} mol) $NiCl_2.6\ H_2O$) and(0.90 g,4.55 x 10^{-3} mol) (FeCl2.4H2O). The mixture was refluxed for 1 hour and the color was changed to Brown –orange and Brown-yellow. The resulting precipitates were formed after evaporating the solvent and recrystallized by two solvents; acetone and absolute ethanol.

2.3.3 Preparation of the Ligand HL_3:

a- Schiff base compound was prepared by dissolving (2 g, 0.0183mol) 4-amino phenol in 10 mL of absolute ethanol then mixing it with (2.15g 0.0176 mol) of 3-hydroxybenzyldehyde to prepare (Schiff base). The reaction was refluxed for 1 hour with stirring and the proper a pH was adjusted to ≈ 4 by adding several drops of the glacial acetic acid where this process was followed up by pH paper test. The color of the reaction mixture was changed to light green_yellow and precipitates were formed after cooling and evaporating the solvent. Schiff base compound was also recrystallized by using ethanol solvents.

b- A solution was prepared by dissolving (2 g, 9.2 x 10^{-3}mol) in 10% H_2SO_4 (1 ml H_2SO_4 , 9ml distilled water)in a baker 100mL. A sodium nitrite solution which is concentrated 10% was prepared by dissolving 1 g, in 10 mL distilled water. Then, the two solutions were mixed with stirring and maintaining at the temperature (0-5 ^{0}C). The mixture was lifted for 15 minutes to complete the diazonium process.

A solution was prepared from dissolving (2.2g - 9.2 x 10^{-3}mol) of (Schiff base compound) prepared in the (a) 3-(((4-hydroxyphenyl) imino) methyl) phenol which was dissolved in (10% NaOH)). This solution was mixed and stirred with the diazonium salt solution. The precipitate was filtered and washed several times with ethanol and dried at room temperature as shown in Scheme (2-3).

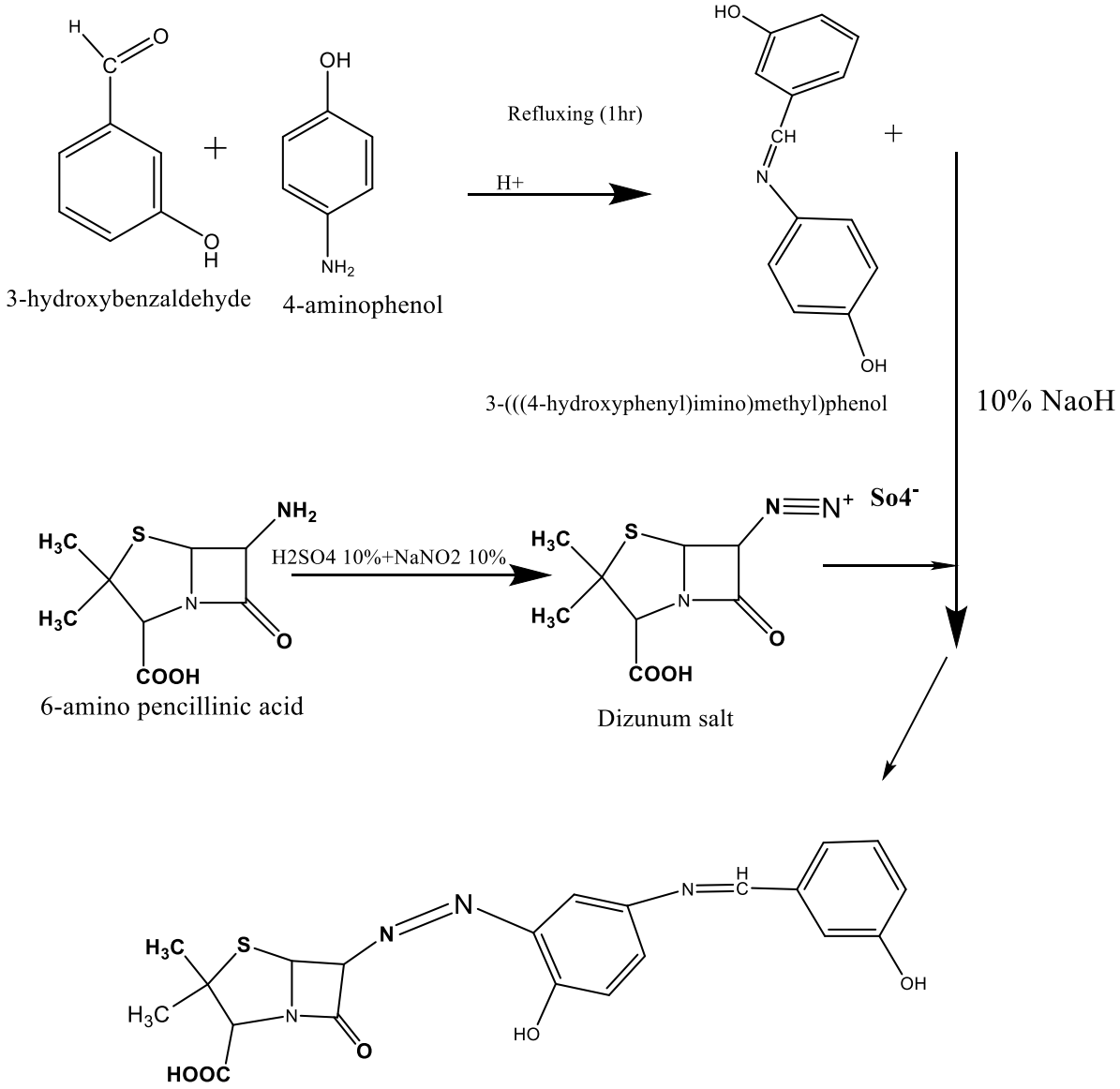

3-hydroxybenzaldehyde

4-aminophenol

3-(((4-hydroxyphenyl)imino)methyl)phenol

6-amino pencillinic acid

Dizunum salt

6-((1*E*)-(2-hydroxy-5-((3-hydroxybenzylidene)amino)phenyl)diazenyl)-3,3-dimethyl-7-oxo-4-thia-1-azabicyclo[3.2.0]heptane-2-carboxylic acid

HL3

Scheme (2-3) Preparation of Azo-azomethine (HL_3).

Complex Preparation of HL_3:

C- Complexes were prepared by dissolving (1 g, 2.27×10^{-3} mol) of (HL_3) in 10mL of absolute ethanol then mixing it with (0.77 g, 4.55×10^{-3} mol) desired metal ion($CuCl_2.2H_2O$), (1.08 g ,4.55×10^{-3} mol) $NiCl_2.6\ H_2O$)and (0.90 g, 4.55×10^{-3} mol) ($FeCl_2.4H_2O$). The mixture was refluxed for 1 hour and the color was changed to copper, Brown, Brown stone respectively . The resulting precipitates were formed after evaporating the solvent and recrystallized by two solvents: acetone and absolute.

2.3.4 Preparation of the Ligand HL_4:

a- Schiff base compound was prepared by dissolving (2 g, 0.0176 mol) 4-amino phenol in 10 mL of absolute ethanol then mixing it with (2.6 g, 0.0176 mol) of 4, N, N, and dimethylbenzyldehyde to prepare (Schiff base). The reaction was refluxed for 1 hour with stirring and the proper pH was adjusted to ≈ 4 by adding several drops of the glacial acetic acid where this process was followed up by a pH paper test. The color of the reaction mixture was changed and precipitates were formed after cooling and evaporating the solvent. Schiff base compound was recrystallized by using ethanol solvents to give the titled compounds as shown in the Scheme (2.4).

b- A solution was prepared by dissolving 2 g, 9.2×10^{-3}mol) 6-amino pencillanic acid in 10% H_2SO_4 (1 ml H_2SO_4 , ml distilled water)in a baker 100mL. A sodium nitrite solution which is concentrated 10% was prepared by dissolving 1 g, in 10 mL distilled water. Then, the two solutions were mixed with stirring and maintaining at the temperature (0-5 ^{0}C). The mixture was lifted for 15 minutes to complete the diazonium process.

A solution was prepared from dissolving (2.2g-9.2×10^{-3}mol) of 3-((4-(dimethylamino) benzylidene) amino) phenol (Schiff base compound) prepared in the (a) Paragraph which was dissolved in (10% NaOH). This solution was mixed and stirred with the diazonium salt solution. The precipitate was filtered and washed several times with ethanol and dried at room temperature as shown in (2-4).

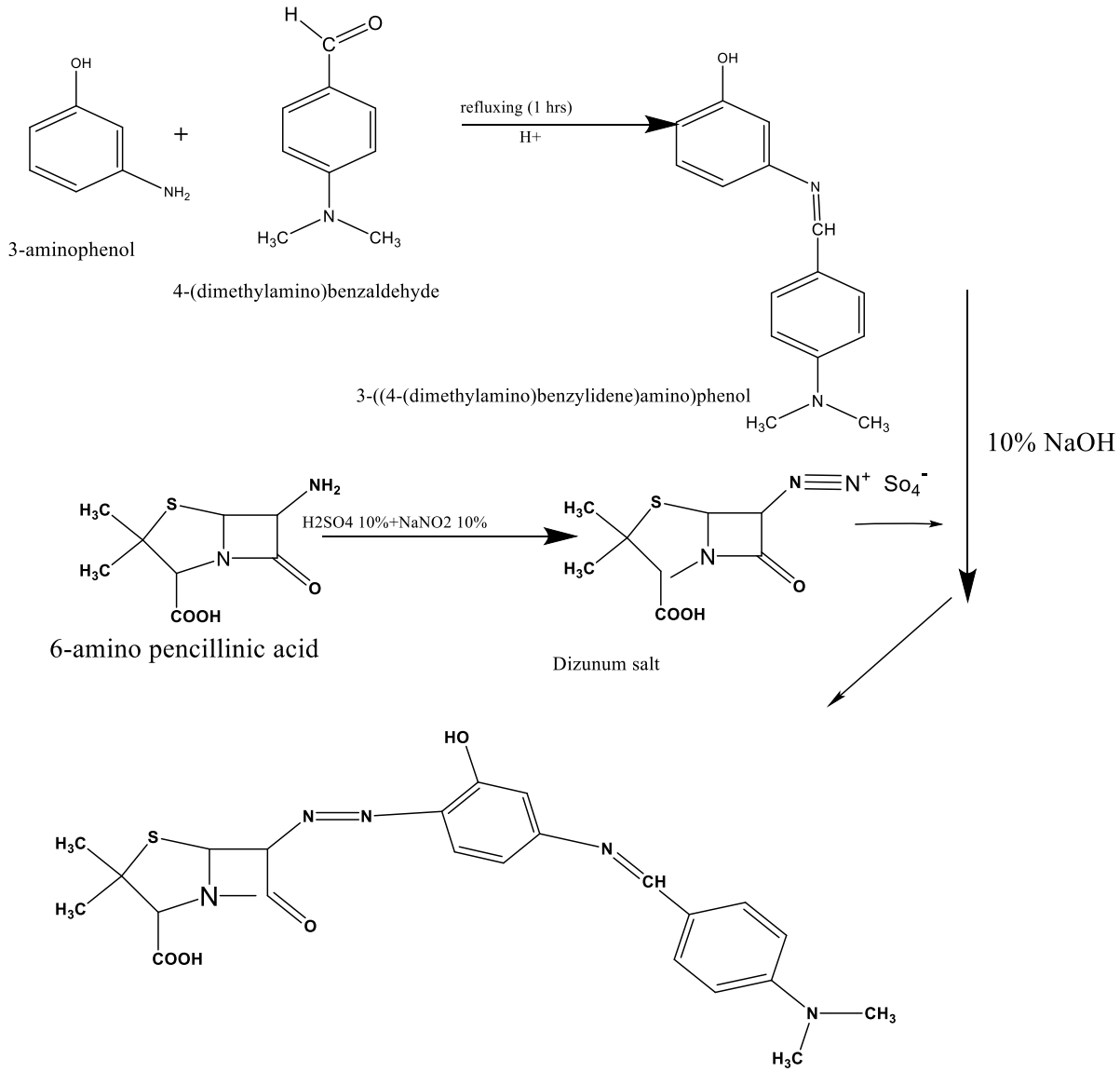

2-(1-((4-((4-(dimethylamino)benzylidene)amino)-2-hydroxyphenyl)diazenyl)-2-oxoethyl)-3,5,5-trimethylthiazolidine-4-carboxylic acid

HL4

Scheme (2-4) Preparation of Ligand HL_4

Preparation (HL_4) Complexes:

Complexes were prepared by dissolving (1g, 2.23 x 10^{-3}mol) of (HL_4) in 10mL of absolute ethanol then mixing it with (0.76 g, 4.47 x 10^{-3} mol) desired metal ion ($CuCl_2.2H_2O$), (1.06g, 4.47 x 10^{-3} mol) $NiCl_2.6\ H_2O$) and (0.88 g, 4.47 x 10^{-3}mol) ($FeCl_2$.4H2O). The mixture was refluxed for 1 hour and the color was changed to light Brown ,Brown orange . The resulting precipitates were formed after evaporating the solvent and recrystallized by two solvents; acetone and absolute ethanl , table (2-2)show the color, m.pt. And yield of Schiff base and Azo-Azomethine ligand

Table (2-2) Schiff base and Azo-Azomethine color m.pt. And yield%

No	Compound	M.wt	Color	M.P ^{0}C	Yield %
1	Schiff base Azo-Azomethine (HL_1)	240 467	Green-yellow orange	82 97	84 83
2	Schiff base Azo-Azomethine (HL_2)	213 440	Dark Brown Brown	101 104	69 64
3	Schiff base Azo-Azomethine (HL_3)	213 440	Brown Brown – Red	116 118	62 58
4	Schiff base Azo-Azomethine (HL_4)	240 467	Light yellow Golden-yellow	120 131	81 76

2.4. The Biological Activity of Ligand and its Complexes on (*Staphylococcus aureus*) Bacteria:

2.4.1 The Apparatus and Instruments Used in the Experiments of the Studies as shown in Table (2-3)

Table (2-3): Tools and instruments

No	**Instrument**	**Company**	**Origin**
1	Autoclave	Labtach	Korea
2	Balance	Sartorius	Germany
3	Incubator	Binder	Germany
4	PH- meter	Labtach	Korea
5	Centrifuge	Hettich	Germany
6	Micropipettes	Human	Germany
7	Refrigerator	LG	Korea
8	Spectrophotometer	Tuder	Korea

2.4.2 Methods

2.4.2.1 Culture Media:

The culture media used in this study are shown in Table (2-4)

Table (2-4) Culture Media

1	Brain Heart Infusion Broth	HIMIDIA/ India	Bacterial inocula
2	Nutrient Broth	HIMIDIA/ India	Bacterial inocula
3	Nutrient Agar	HIMIDIA/ India	Bacterial inocula
4	Muller Hinton Agar	HIMIDIA/ India	Antibiotic sensitivity
5	Blood Agar	Oxoid	Bacterial isolation and Hemolysin production
6	Plasma-coagulase EDTA (Rabbit	Mast / USA	/
7	N,N,N,N-Tetra methyl-P- Phenylene Diamine Dihydrochloride	Himedia /India	/

Sterilization of culture media and solutions were achieved by autoclaving at 121 0C of 15 lb/inch2 for1 h after adjusting PH for 7.2.

a- Nutrient Broth

It was prepared by dissolving 3.7g of the medium in 100 mL of distilled water, distributed into screw-capped test tubes, dispensed in 5 mL volume per tube, and autoclaved.

b-Nutrient Agar

It was prepared by dissolving 28 g of the medium in a 1liter of distilled water, autoclaved, and poured into Petri dishes. It was used as a selective and differential medium for *S. aureus* bacteria.

c- Muller-Hinton agar

It was prepared by dissolving 3.6g of the medium in 100 mL of distilled water, then boiled for complete dissolving, autoclaved, and poured into Petri dishes.

d- Brain Heart Infusion Broth:

The Brain Heart Infusion may be centered by dissolving 2.3g in 100 mL of distilled water and placing it in a conical flask, then transferring it into the sterilizer. Once the sterilization period ends and after cooling it using tap water, it is distributed in test tubes to be ready to transfer the bacterial culture into it.

e-Blood Agar Medium

It was prepared by dissolving 4 grams of the medium in 100 mL of distilled water, autoclaved and left to cool for 45-50 ^{0}C. Then, the whole human blood cells were added to the medium, thoroughly homogenized, and poured into Petri dishes. This medium was used to manage primary isolation and detect the ability of bacteria to hemolysis red blood corpuscles (RBCs).

2.4.2.2 Biochemical reagents

a.Oxidase reagent:

Freshly prepared from adding 0.1 g of N,N,N,N-Tetra methyl-P- Phenylene Diamine Dihydrochloride in 9 ml of distilled water , then the volume was completed to 10 ml in clean , dark and sterile container .[59]

b. Coagulase Reagent:

The tube coagulase test was conducted following the procedure reported by

C . Catalase reagent:

It was prepared as concentration of 3 % of hydrogen peroxide(H_2O_2) (3ml H_2O_2 in 90ml of distilled water then completed to 100ml). Reagent was used for detection the ability of bacterial isolates in production of catalase enzyme [59],[60].

Briefly, using a class tube, one drop of EDTA rabbit plasma was added and proper amount of fresh bacterial suspension, and mixed well by a wooden stick. Up on it, the presence of bound coagulase proteins (clumping factor) on the bacterial cells will lead to clot formation .

2.4.3 Collection of samples:

The blood samples and skin swabs were collected from 50 patients with atopic dermatitis , aged from 5 to 35 years , attending at Al- Hussein teaching hospital and some of private laboratory in Karbala Province, Iraq. Blood samples and skin swabs were also collected from 30 normal individuals with age range between 5-35 years, who were free from any infection depending on the physician identification and some clinical examination , according to [61]

Swab samples

One hundred skin swabs were taken from area of infection and surrounding area of each the patients and thirty from control group by using transport medium swabs for preservation from dryness until transport to laboratory. Samples then were cultured in different type of media after incubation period 24h of 37°C to isolate and determine the more frequent pathogenic bacteria[61].

2.4.4 Identification of Isolated Bacteria

Isolated bacteria were diagnosed depending in the literature [62]

2.4.5 Morphological and Culture Characteristic

The selected bacteria were initially identified according to the colony characteristics such as the, shape, size , color characteristic of the colonies on general and selective media .[63]

2.4.6 Biochemical Tests

It was done according to [64]as the flowing steps:

1. Catalase test

This test was performed by transferring part of the bacterial culture to a clean and dry glass slide using a carrier loop ring then a drop of hydrogen peroxide (H2O2) 3% was added. The appearance of air bubbles on the surface of the glass slide indicate of the positive result, This test is used to detect the ability of bacterial species for the production of catalase enzyme which convert hydrogen peroxide into oxygen and water.

2. Oxidase test

Drops of the oxidase enzyme reagent were prepared, and placed on a clean and dry filter paper. Then part of the colony was transferred by wooden sticks on the filter paper for 10-15 sec, the appearance of the dark violet color is sign of positive result.

3.Coagulase test (Free Coagulase test)

The bacteria grew on Nutrient broth and incubated in 37 degree for 18-24 hours, then transfer 0.1ml of bacterial culture to sterile glass tube containing o.5 ml from rabbit plasma and tubes were incubated in 37 ° C for 4hours and check the tube every hour because it may degrade again when formed, and negative tube should be left at room temperature for the overnight to notice the thrombus – producing bacteria slowly, plasma clotting is a sign of plasma clotting enzyme.

2.4.7 Vitek Diagnosis System

This system was used for biochemical diagnosis of bacterial species to determine the type of isolated bacteria through the color detection cards GP color–coded diagnostic. Cards were used to diagnose the Gram positive bacteria and the card marked with GN to diagnose bacterial samples , according to the following

steps:

1. Samples were cultivated on culture media (nutrient agar) for bacterial growth in the laboratory and then placed in the incubator for 24 hours at 37°C .

2.Then bacterial suspension (pure culture) was prepared by transporting a sufficient number of pure colonies using a loop to a special test tube (made of polystyrene in 12× 75 ml sizes) .This tube contains 3.0 ml of salt solution with adjusting the turbidity according to special measurements by type of colonies ,

3.The test tubes were transferred to the Cassette of the Vitek device and it was transferred to Vitek 2 compact device in the designated area and the machine was turned on.

4.The inoculated cards were passed through a mechanism whereby the transfer tube was cut and the card was pasted before being loaded into the circular incubator. The circular incubator can hold up to 30 or even 60 cards, cards were incubated at 35.5 °C.

2.4.8 Minimum Inhibitory Concentration (MIC)

The Agar dilution method was used to detect MIC of the ligand and complexes according to [65]. The dilutions of the compounds ranging from (0.01-0.1) g/ml were prepared by mixing each one of the concentrations of the compound with 100 mL of sterile and cooling Muller Hinton medium. The Petri dishes were cultured as the spot with 100 µL of the bacterial suspension. Then, the Petri dishes were incubated at 37 ^{0}C for 18-24 h. Final results were recorded as positive ones when growth was presented and negative results if there was no growth. The MIC represented by the last concentration is with little or no visible growth.

2.4.9 Antibacterial Activity of the Ligand and Complexes

Agar well diffusion method which was used included making 5 holes with 6 mm diameter done by corky bore. Then, 100 µL from each concentration of the compounds was put in each hole by using a micropipette, where distilled water was added to one hole in the cultured media to be as control, and then the Petri dishes were incubated at 37^0C for 24h. The inhibitions zone was measured by ruler twice to ensure the process is done as required [66].

2.4.10 Effects of the Ligands and Complexes on inhibition Bacteria to Procedure Virulence Factors

a. Tube Method (TM)

A qualitative assessment of biofilm formation was determined as previously described in the following steps [67].

1. 10 mL of brain heart infusion broth (BHI) prepared as in step 2.4.3-a) with 2% sucrose (BHISuc) (10mL) was inoculated with loopful of microorganism from overnight culture plates and incubated for 24 hours at 37°C.

2. The tubes were decanted, washed with PBS (pH 7.2), and duly dried.

3. Dried tubes were stained with crystal violet stain (0.1%) prepared as in step 2.4.3-b) for 10 min. Then, the excess stain was removed and tubes were washed with deionized water.

4. Tubes were dried in the inverted position and observed for biofilm formation.

5. Biofilm formation was considered positive when a visible film lined the wall and bottom of the tube. Ring formation at the liquid interface was not indicative of biofilm formation. The results have reported dependence on the degree of the stained tubes and the amount of biofilm formation was scored as 0- absent, 1- moderate, or 2- strong (experiments were performed in triplicate and repeated three times).

b. **Hemolysin Production**

Blood agar plates were inoculated with the tested organism, where the plates were incubated at 37^0C for 48 hours. Then the plates were examined for observing the type of hemolysis.

Chapter Three Results and Discussion

This section provides an overview related to the chemical tests conducted to attain the new type of azo-Schiff base ligands. Ligands comprising nitrogen and oxygen as donor atoms have a vital role in biological systems. There are multiple ways to prepare the ligands, which vary depending on the raw materials, solvents, and temperature needed for its preparation [68]. One of the most common methods to prepare the azo-Schiff base ligands is the The condensation of primary amines with carbonyl compounds to form Schiff-base compounds and then bonding them with the 6-aminopenicillinic acid compound by the azo bond To form the compound azo-azomethine and use it as a ligand is known topics in incoordination chemistry. Azo-azomethine ligands and their complexes are the most well-known chemical compounds and an important class in chemistry due to their various uses and benefits in various fields [69]. However, in this research, four ligands derived from 6-aminopencellanic acid have been prepared by a well-known method for preparing azo-azomethine compound and have been treated with some metal ions of the first row to form the required new complexes.

3.1. Solubility Tests:

The solubility of the prepared ligands as derivatives of 6-aminopencillanic acid and its complexes prepared by several transitional metal ions (Cu II), (Ni II), (Fe II) were studied by using various solvents. The results involved in Table (3-1) showed that the ligands and all their complexes are non-soluble in water. They are also poorly soluble in many organic solvents such as Methanol, Ethanol, acetone, and $CHCl_3$ except the solvents of DMSO and DMF.

Table (3-1): Solubility of organic ligands and their complexes in different solvents:

No	Comp	D. water	Methanol	Ethanol	Acetone	$CHCl_3$	DMf	DMSO
1	L_1	-	++	++	++	+++	+++	+++
2	$[Cu(L_1)_2]$	-	-	_	_	_	+++	+++
3	$[Ni(L_1)_2]$	_	_	_	_	_	+++	+++
4	$[Fe(L_1)_2]$	_	_	_	_	_	+++	+++
5	L_2	_	_	_	_	_	+++	+++
6	$[Cu(L_2)_2]$	_	_	_	_	_	+++	+++
7	$[Ni(L_2)_2]$	_	_	_	_	_	+++	+++
8	$[Fe(L_2)_2]$	_	_	_	_	_	+++	++
9	L_3	_	_	_	_	_	++	+++
10	$[Cu(L_3)_2]$	_	_	_	_	_	+++	+++
11	$[Ni(L_3)_2]$	_	_	_	_	_	+++	+++
12	$[Fe(L_3)_2]$	_	_	_	_	_	+++	+++
13	L_4	_	_	_	_	_	+++	+++
14	$[Cu(L_4)_2]$	_	_	_	_	_	+++	+++
15	$[Ni(L_4)_2]$	_	_	_	_	_	+++	+++
16	$[Fe(L_4)_2]$	_	_	_	_	_	+++	+++

(-) Non-soluble (++) Partial soluble (+++) Soluble

3.2 Infrared Spectra:

The infrared spectrum is one of the important techniques that can be relied on to find and detect the frequencies of the function group of compounds and identify the changes that may occur when treating the ligands with metal ion[70], By comparing the FTIR of ligands and the prepared complexes, the changes in the frequency sites of the function groups are defined accompanied by the appearance of new frequencies due to the coordination bonds between the metal and the ligand,[71] that are not found in the free ligand. This is the easiest way to identify the different types of various bonds and structural forms of ligands and prepared complexes.

The infrared spectrum plays a key role in providing us with information about the nature and the structure of the functional groups because each group has its frequency and through it and can offer the initial information of the spatial shapes of the particles, as the absorption of each type of these bonds regularly certainly give the infrared frequency sites [72].

The stretching band sites were determined for the selection of their function groups of ligands that may be included in the coordination process with the metal ions, trying to explain it by relying on the literature with observing the changes in the shape of these bands, their intensity, and their position when the coordination process of the ligand with metal ions is conducted to form complexes. As for the hydroxyl group which has an electron pair, it can coordinate through it and has its frequency in the region of (3200-3600) cm^{-1} .The azo bond group of (N = N) sp^2 hybrid bonds includes a frequency within the range (1450-1550) cm^{-1}[73].

The azomethine bond group of the sp^2 hybridization has wavelengths close to the ν(C = C). Also, azomethine absorption can be observed within the range cm^{-1} (1580-1650) at higher or lower frequencies [74]. (M-N st) is considered one of the types of bonds that appear within a low range of frequencies. Their presence informed and guided us about the process of coordination between the metal and the ligand. The ligand-metal band coordination in the range (325-700) were coordination process occurred [75].

3.2. 1 Infrared Spectrum Ligand (HL_1):

The FT-IR spectra of the synthesized ligands (HL_1) exhibit broadband at site (3169) cm^{-1} attributed to the Hydroxyl group (OH), and strong bands at 1695cm^{-1} due to the presence of carboxylic carbonyl group (C=O) that usually appears around 1700 cm^{-1}[76]. The band at 1595cm^{-1} was assigned to the imine group (C=N), where azomethine (imine group) absorption band generally appears in the region (1600-1680) cm^{-1} [77]. The appearance of the imine group in the ligand spectrum confirms the formation of Schiff base ligand, as it is noticed that a sharp and strong band at the site (1537 cm^{-1}) returns to the (N = N) bond [78]. There is evidence of the formation of the Azo group, β-lactam carbonyl group (C=O) for the synthesized ligand that occurred at a significant value of 1660 cm^{-1}[79]. The other important characteristic peaks in the FT-IR spectra were assigned in Table (3-3) and shown in Figure (3-1).

3.2.2. Infrared Spectrum Ligand (HL_2):

The FTIR spectra of ligand (HL_2) showed a broad beam at the site (3348 cm^{-1}) belongs to a band (O - H) that returns to 3-Hydroxy Benzaldehyde [80]. There was also a carbonyl of lactam group(C=O) at position (1643cm^{-1}) [81]. As put by [82], the elastic Frequency of the Azomethine Group (C = N) appeared on the site (1606 cm^{-1}) while the absorption frequency of the azo group (N=N) appeared at the position (1525 cm^{-1}) comparisons of the infrared spectrum frequencies of the basic material with the prepared ligand [83]. A second weak beam (1109 cm^{-1}) of the association (C-N) was also observed in the following Figure (3-2).

3.2.3. Infrared Spectrum Ligand (HL_3):

When studying the FTIR spectrum of ligand (HL_3), it was observed that there was broadband belonging to the hydroxyl group at (3350 cm^{-1}) [84]. There were also strong bands at (1631cm^{-1}) due to the presence of lactam carbonyl (C=O) that usually appeared around (1700cm^{-1}) [85]. The azomethine (imine group) absorption band appeared in the region (1610cm^{-1}) that is in agreement with the literature [86], [87]. The bands at (1508cm-1) of ligand (HL_3) were assigned to the

azo group (N=N), as the appearance of the azo group in the ligand spectrum confirmed the formation of the azo ligand as shown in figure (3-3) [88].

3.2.4. Infrared Spectrum Ligand (HL_4):

The Infrared spectrum of ligand (HL_4) showed an absorption band at ($3352cm^{-1}$) which was attributed to (OH) [89]. The absorption band that appeared at ($1687cm^{-1}$) was assigned to the carboxylic group (COOH). There was also a band at the site ($1651cm^{-1}$) for the carbonyl group [90]. The Azomethine Group (C = N) appeared on the site (1585 cm^{-1}) [91]. This is in agreement with the literature [92], as the azo group appeared at the site ($1533cm^{-1}$), as shown in Figure (3-4).

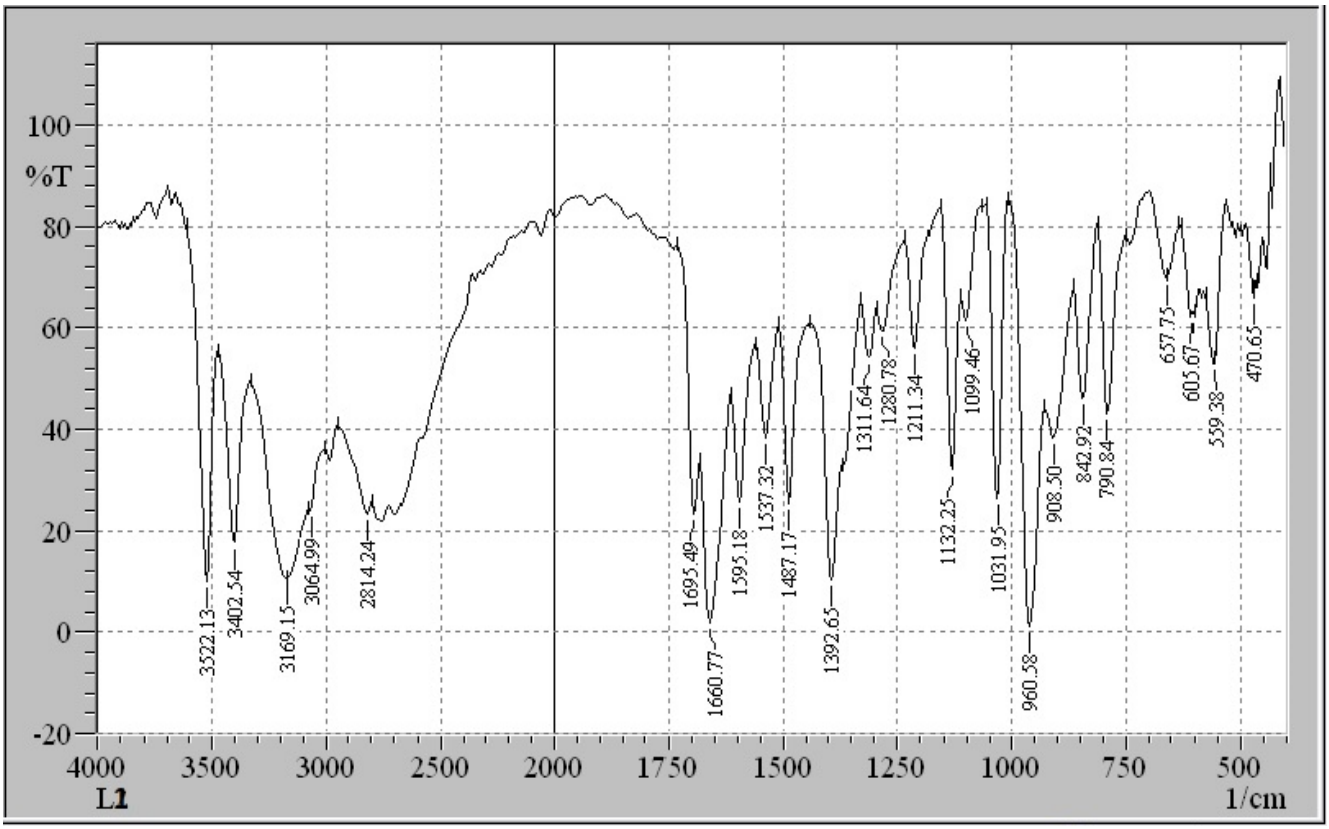

Figure (3-1) FTIR Ligand (HL_1)

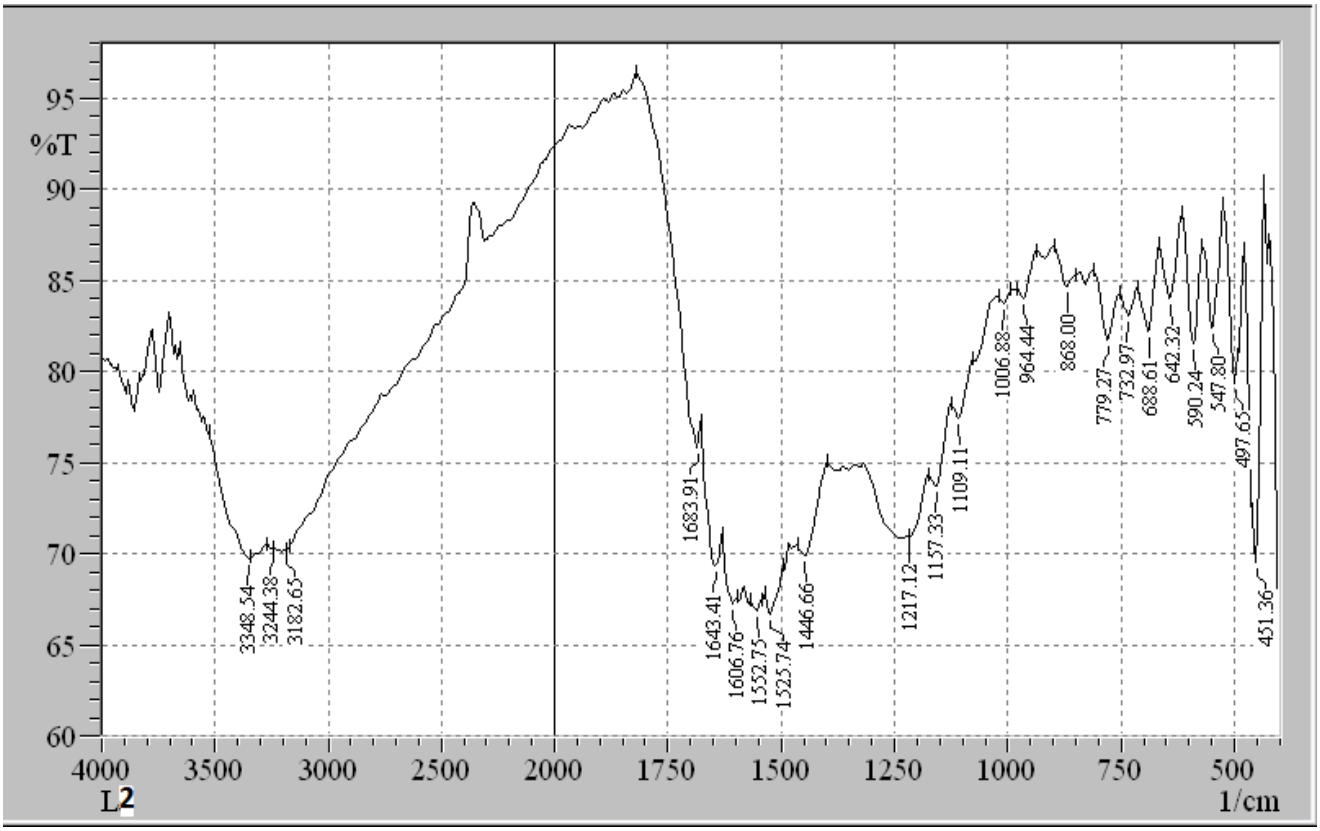

Figure (3-2) FTIR Ligand (HL_2)

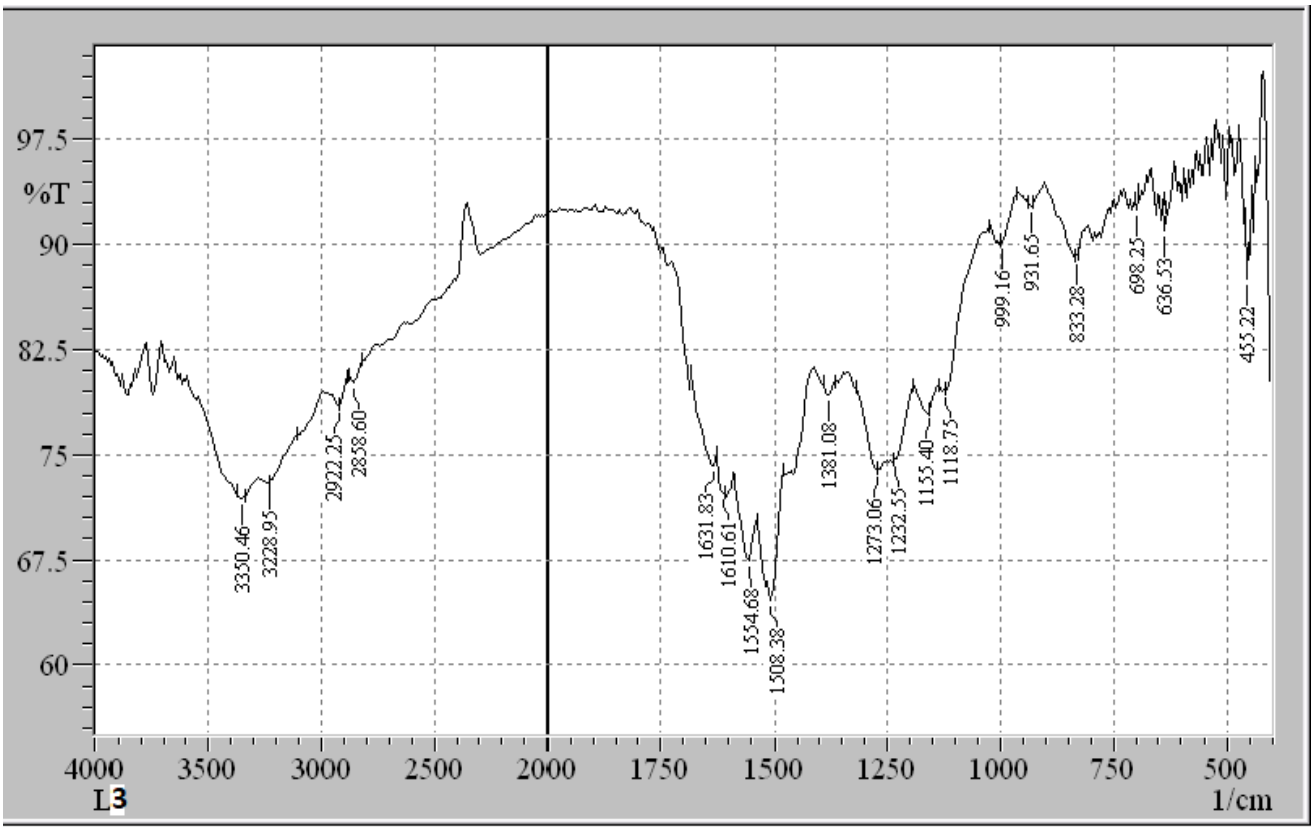

Figure (3-3) FTIR Ligand (HL3)

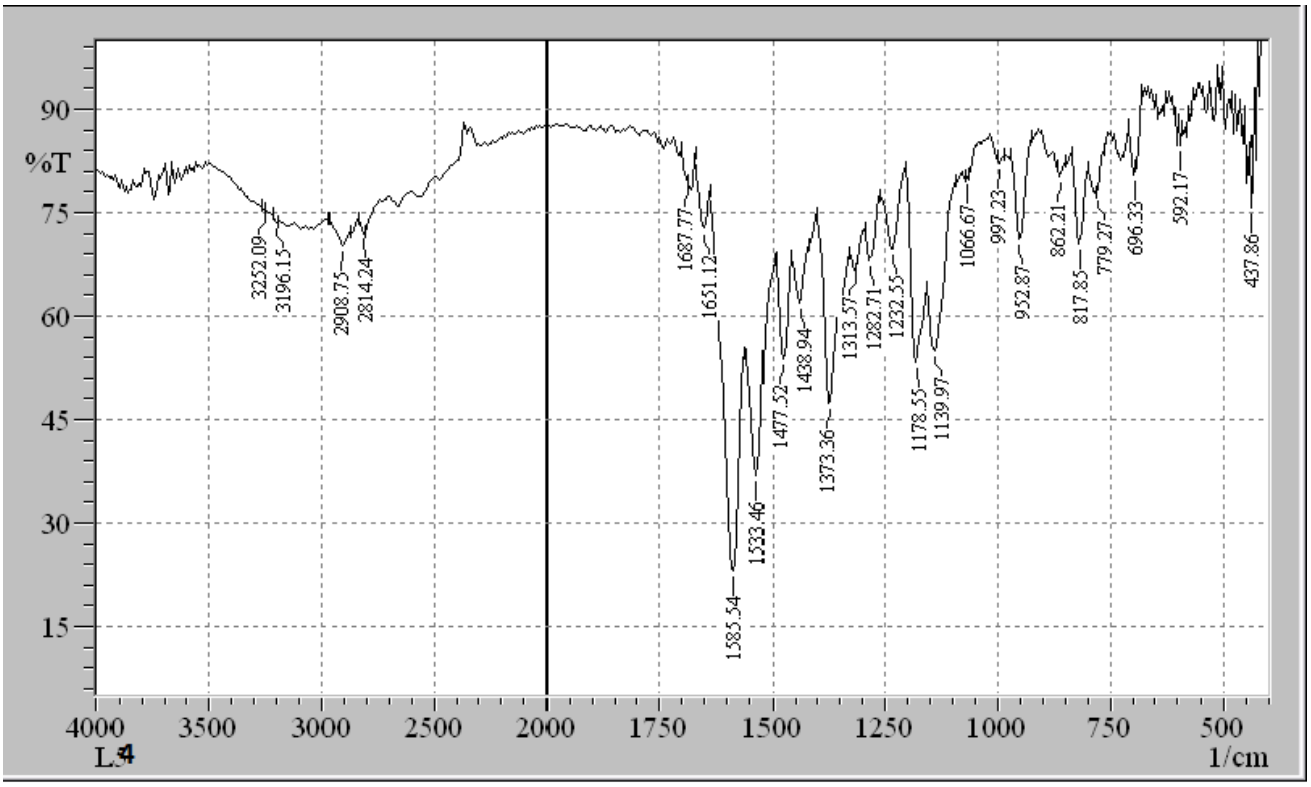

Figure (3-4) FTIR Ligand (HL4)

3.2.5 Infrared Spectrum of Complexes with (HL_1)

When studying the spectra of[Cu $(L_1)_2$],[Ni $(L_1)_2$],] Fe $(L_1)_2$] complexes, it is noticed that the bands attributed to the carboxylic hydroxyl groups (OH) of the HL_1 were disappeared in all complexes, indicating that hydroxyl group was involved in complex formation, i.e. (3144, 3153, and 3140) cm^{-1}. As for the phenolic hydroxyl group, it overlapped with the hydroxyl group belonging to the carboxyl group. The bands of β-Lactam carbonyl groups (C=O) were shifted towards the lower frequencies at the sit at (1649, 1645, 1651) cm^{-1} in all complexes, while the bands at the sites (1508, 1514, and 1514) cm^{-1} attributed to azo groups had changes in shape, intensity, and shifts towards the lower frequencies situated in a favorable position to form a 6-membered ring. The coordination through an oxygen atom of C=O of β-lactam, hydroxyl group, and nitrogen atom azo group was further supported by the occurrence of M-O and M-N bands in the spectra of the complexes at the range mentioned in the pieces of literature [93], [94] and [95] as shown in Table (3-3) and Figures (3-5), (3-6), and (3-7).

3.2.6 Infrared Spectrum of Complexes with (HL_2):

The bands attributed to the hydroxyl groups (OH) previously mentioned were disappeared in all complexes [$Cu(L_2)_2$] [$Ni(L_2)_2$] and [$Fe(L_2)_2$] and the aother hydroxyl group had shifted to the lower wave length in the (3323, 3277, 3356) cm-1 [96]. It can be seen that the carbonyl of lactam group(C=O) band is shifted to lower frequencies at the sites (1640, 1637, 1637) cm^{-1} with the occurrence of a change in shape and the sites of absorption. This indicates that the coordination process is in agreement with what was mentioned in the literature [97].

The ν (N=N) group observed at the range of (1512, 1512, 1485) cm^{-1} showed a shift to lower frequencies in all complexes [98]. The band of the azomethine group (C=N) did not participate in the coordination process in all complexes because it is not situated in a favorable position to form a 4 or 5-membered ring to support the coordinate process. The important characteristic peaks in the FT-IR spectra were assigned in Table (3-3) and Figures (3-8), (3-9), and (3-10).

3.2.7 Infrared Spectrum of Complexes with (HL_3):

The FTIR spectrum of complexes [Cu $(L_3)_2$] [$Ni(L_3)_2$], and[$Fe(L_3)_2$] showed the carboxylic hydroxyl groups (OH) of the HL_3 previously disappeared in all complexes and the another hydroxyl group were shifted to higher wavenumber (3369, 3369, and 3377)cm^{-1} [98]. The band of carbonyl groups (C=O) was also shifted towards the higher frequencies [99], along with binged shoulder at the sit at (1645, 1645, and1668) cm^{-1} in all complexes. The azo group ν (N = N) had changes in shape, intensity, and shifts towards the higher frequencies at the sites (1514, 1514, and 1510cm^{-1}) as a result of participation in the coordination process. This result is supported by the formation of a 6-member ring and the appearance of M-O, M-N peaks as shown in Figures (3-11), (3-12), (3-13), and table (3-3).

3.2.8 Infrared Spectrum of Complexes with (HL_4):

The FTIR spectra of [Cu $(L_4)_2$] [$Ni(L_4)_2$], and [$Fe(L_4)_2$] were assigned to the hydroxyl groups (OH) of the [HL_4]previously disappeared and the aother hydroxyl group had shifted to (3257, 3254, and 3275) cm^{-1}. The azo group ν (N = N) had changes in shape, intensity, and shifts towards the higher frequencies at the sites (1541, 1546, and1546) cm^{-1}, while the azomethine group was shifted to the (1595, 1604, and1604) cm^{-1} in all complexes due to participation in the coordination process. This result is supported by the formation of a 6-member ring and the appearance of M-O, M-N bands,The band of the carbonyl group of β-Lactam (C=O) did not participate in the coordination process in all complexes as shown in Figures (3-14), (3-15), (3-16), and Table (3-3).

the investigative results of infrared spectroscopy show the prepared ligands act as tridentate ligand and the active groups in the ligands were coordinated to the metal ions in show that the active groups in the azo_azomethine ligands were the Hydroxyl ,carbonyl of lactam, azo ,Schiff base and carboxyl group .

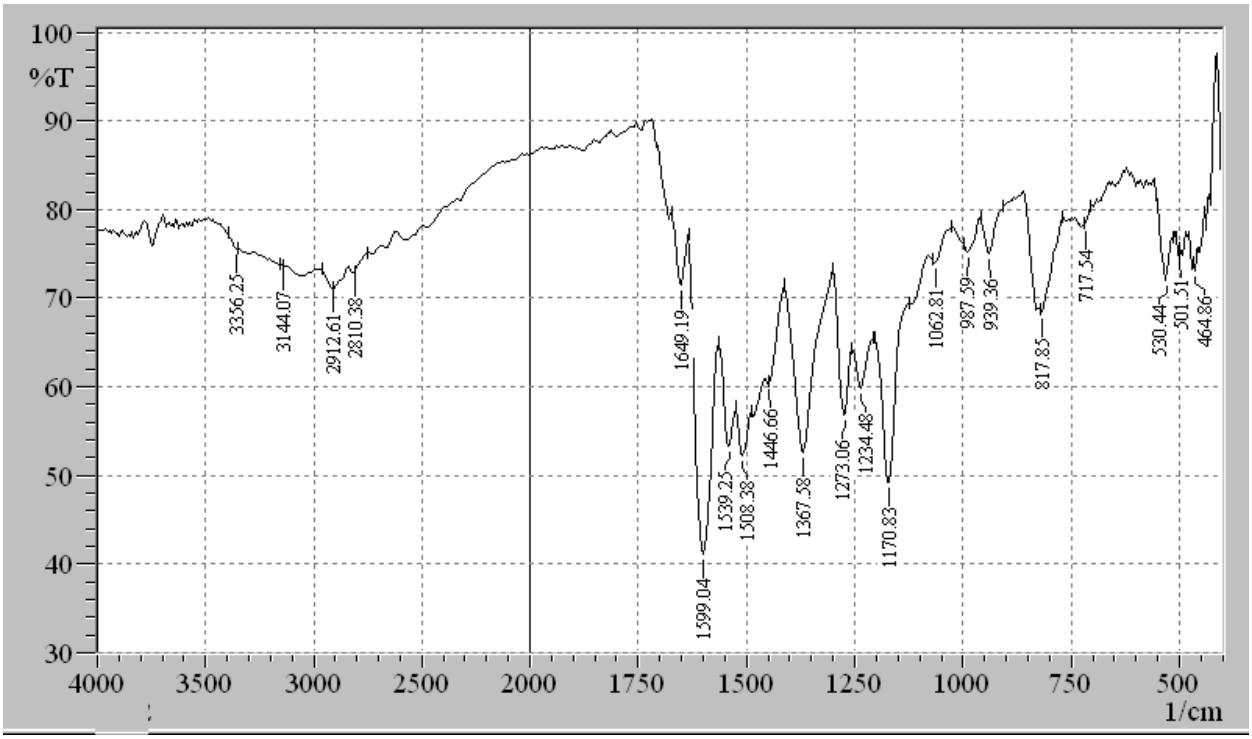

Figure (3-5) FTIR Spectra of the Copper complex[Cu $(L_1)_2$]

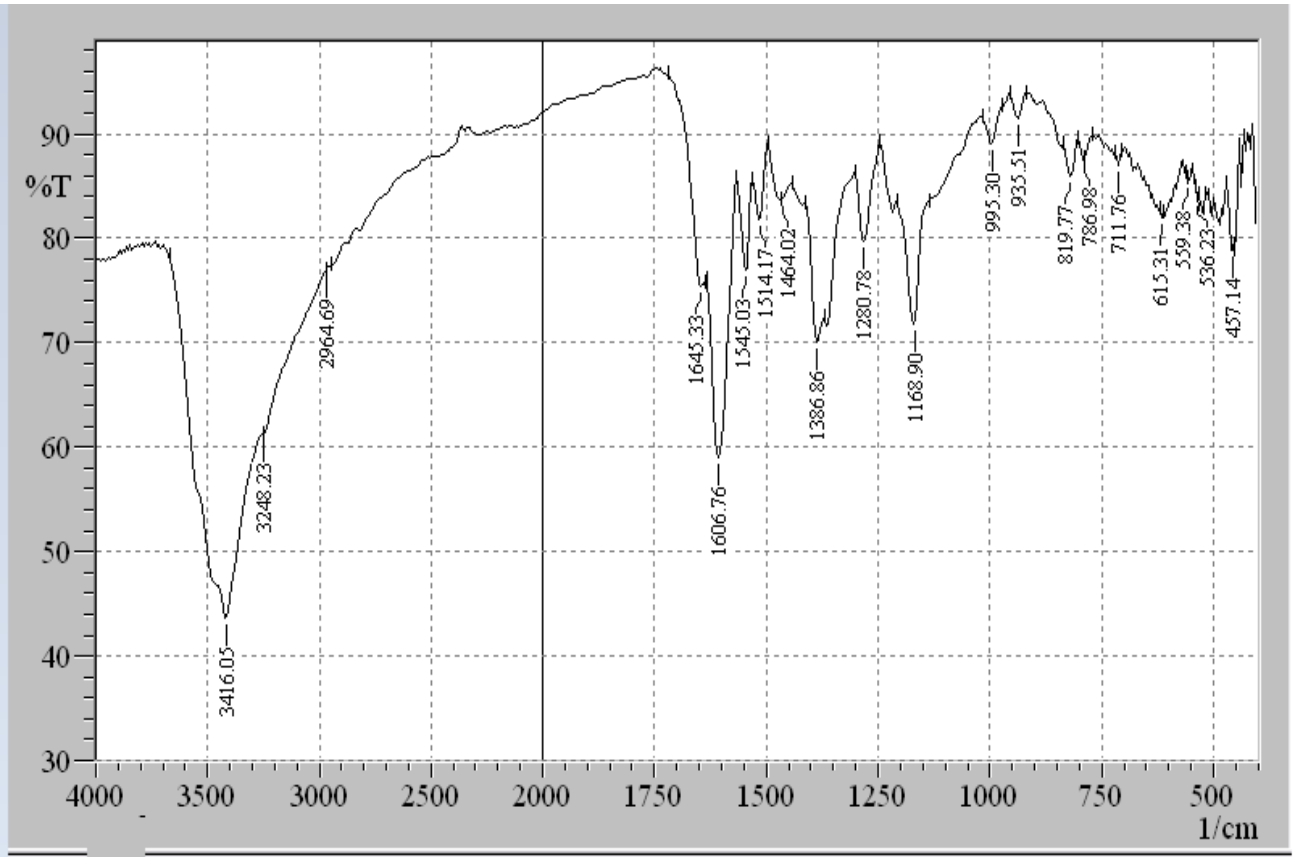

Figure (3-6) Nickel Complex [Ni $(L_1)_2$]

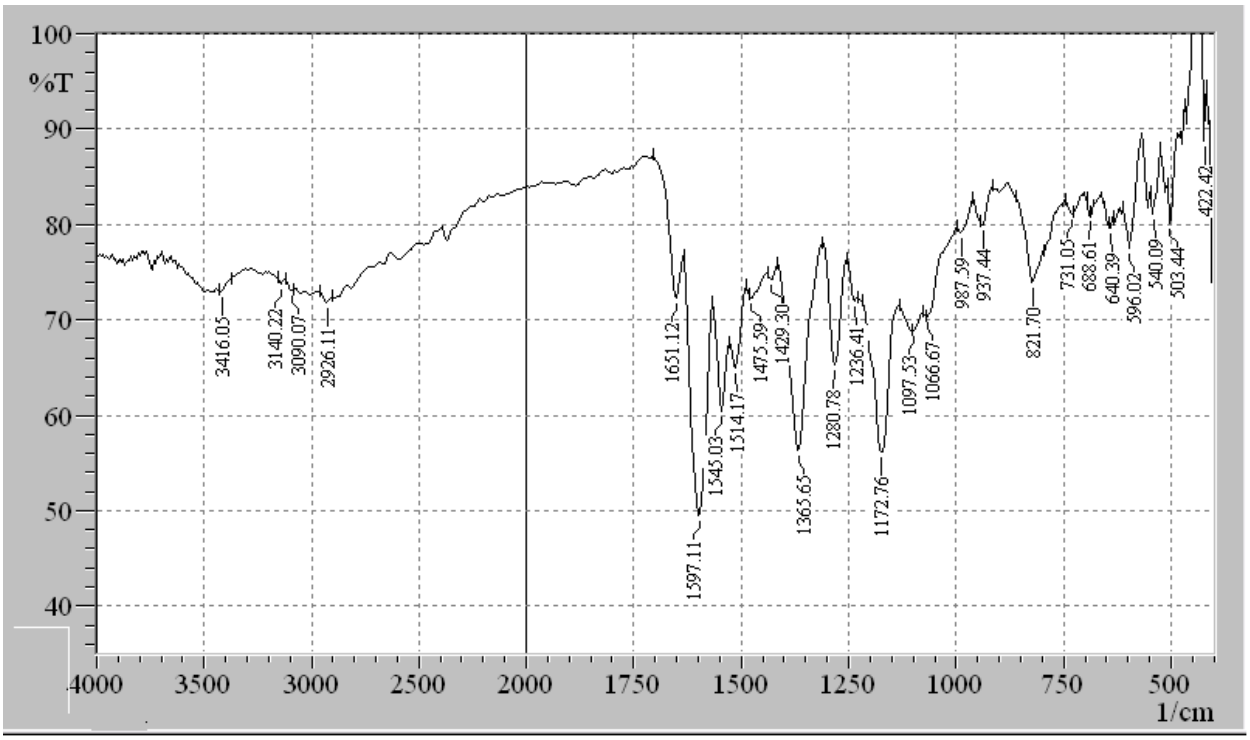

Figure (3-7) Iron Complex [Fe $(L_1)_2$]

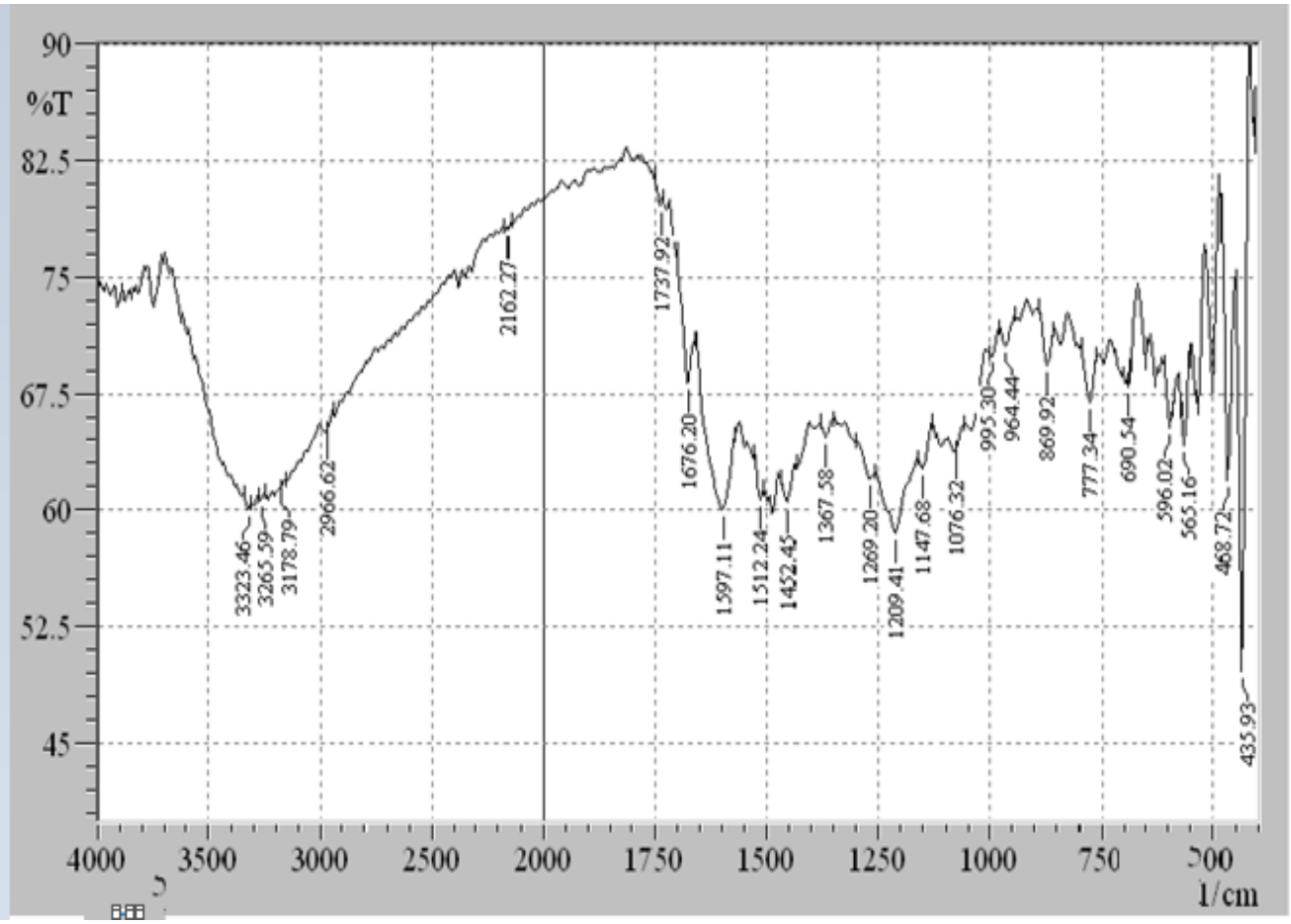

Figure (3-8) Copper Complex[Cu $(L_2)_2$]

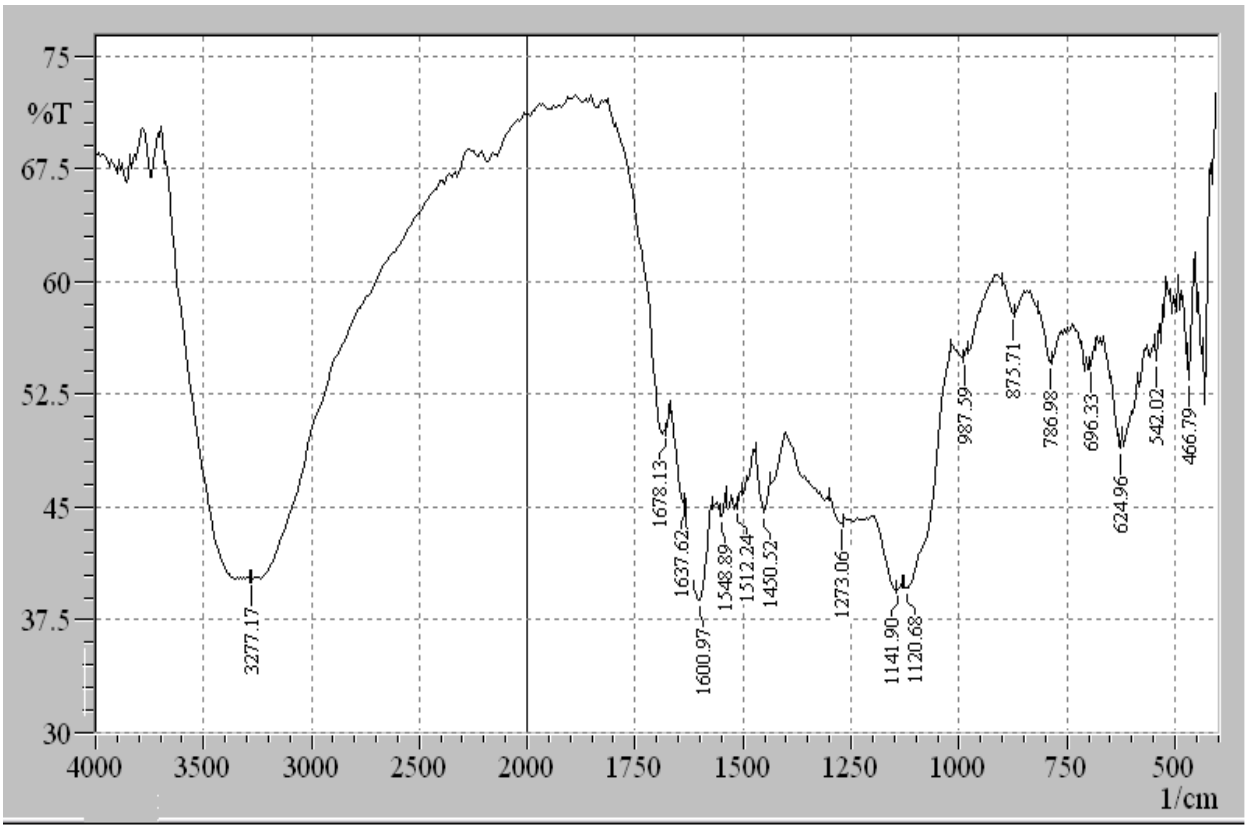

Figure (3-9) FTIR of Nickel Complex [Ni $(L_2)_2$]

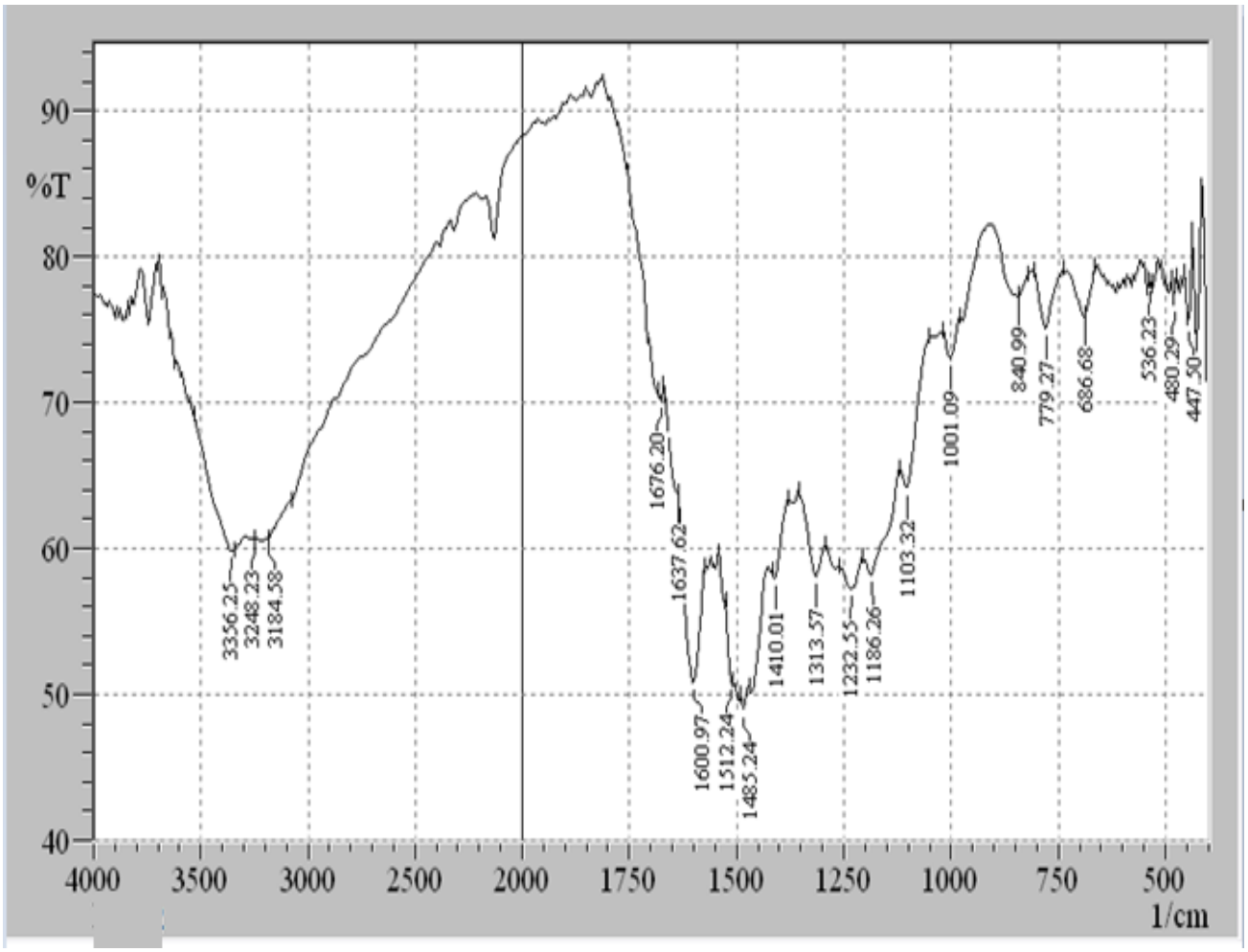

Figure (3-10) FTIR Spectra of Iron Complex[Fe $(L_2)_2$]

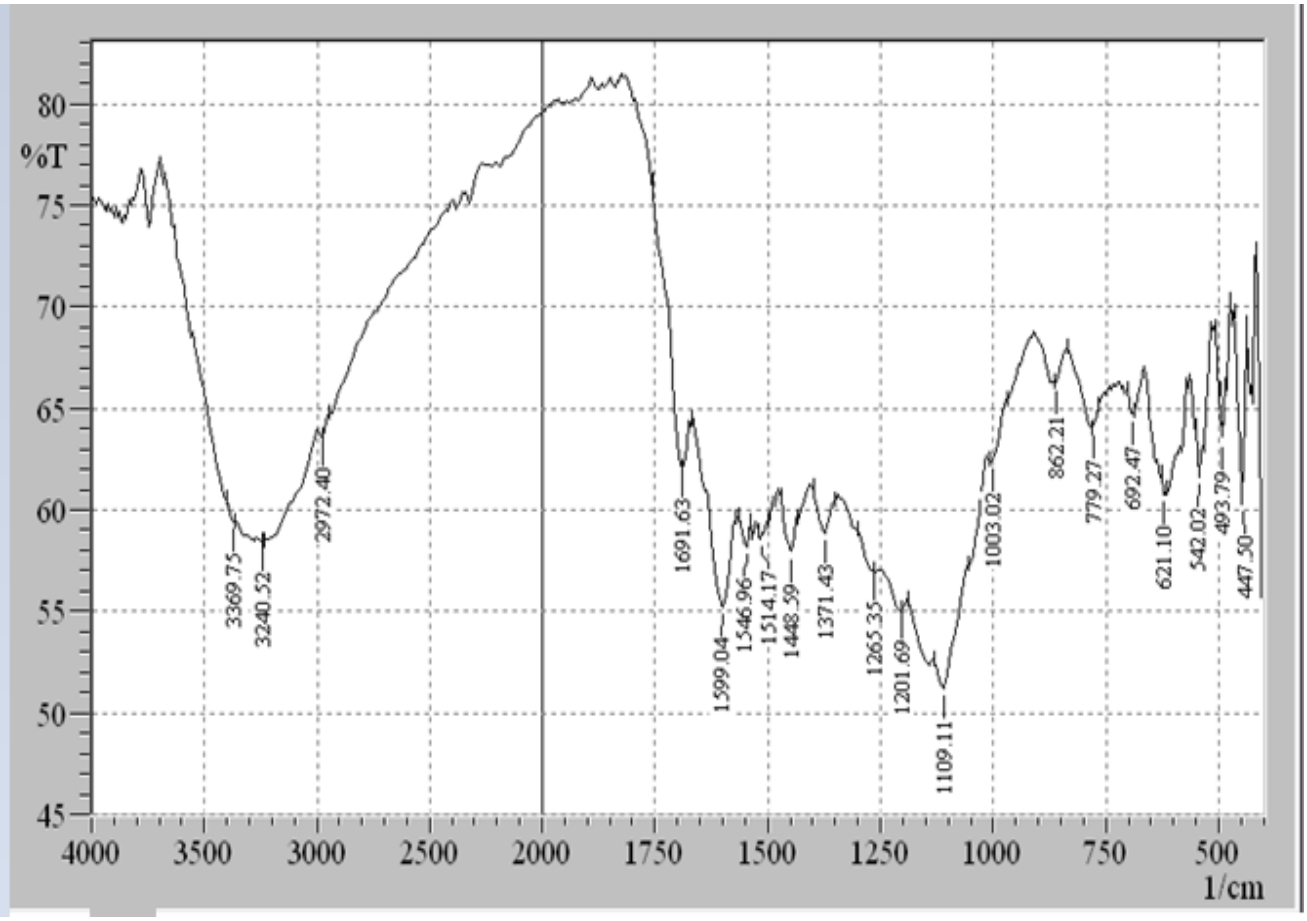

Figure (3-11) Copper Complex[Cu $(L_3)_2$]

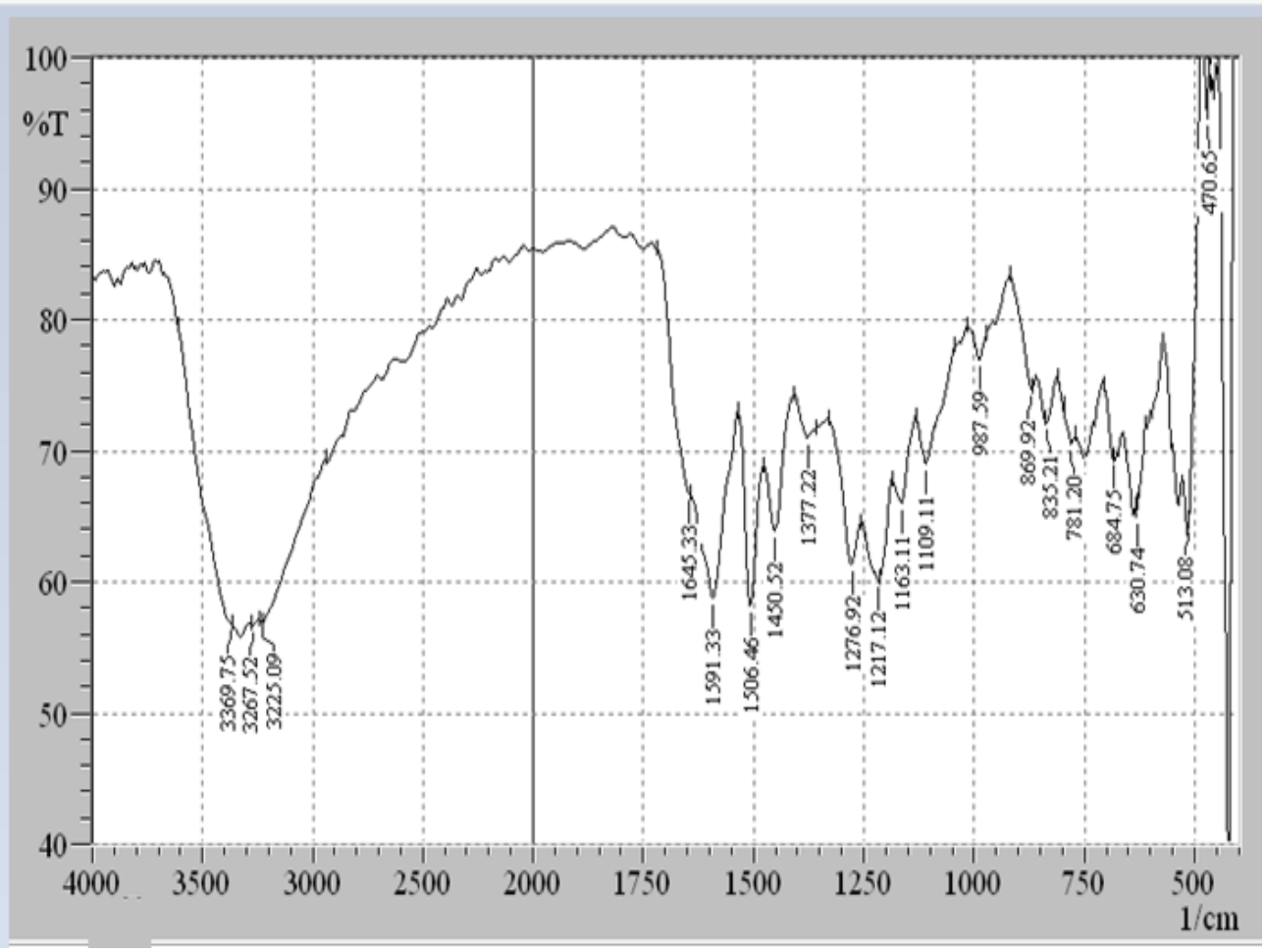

Figure (3-12) Nickel Complex [Ni $(L_3)_2$]

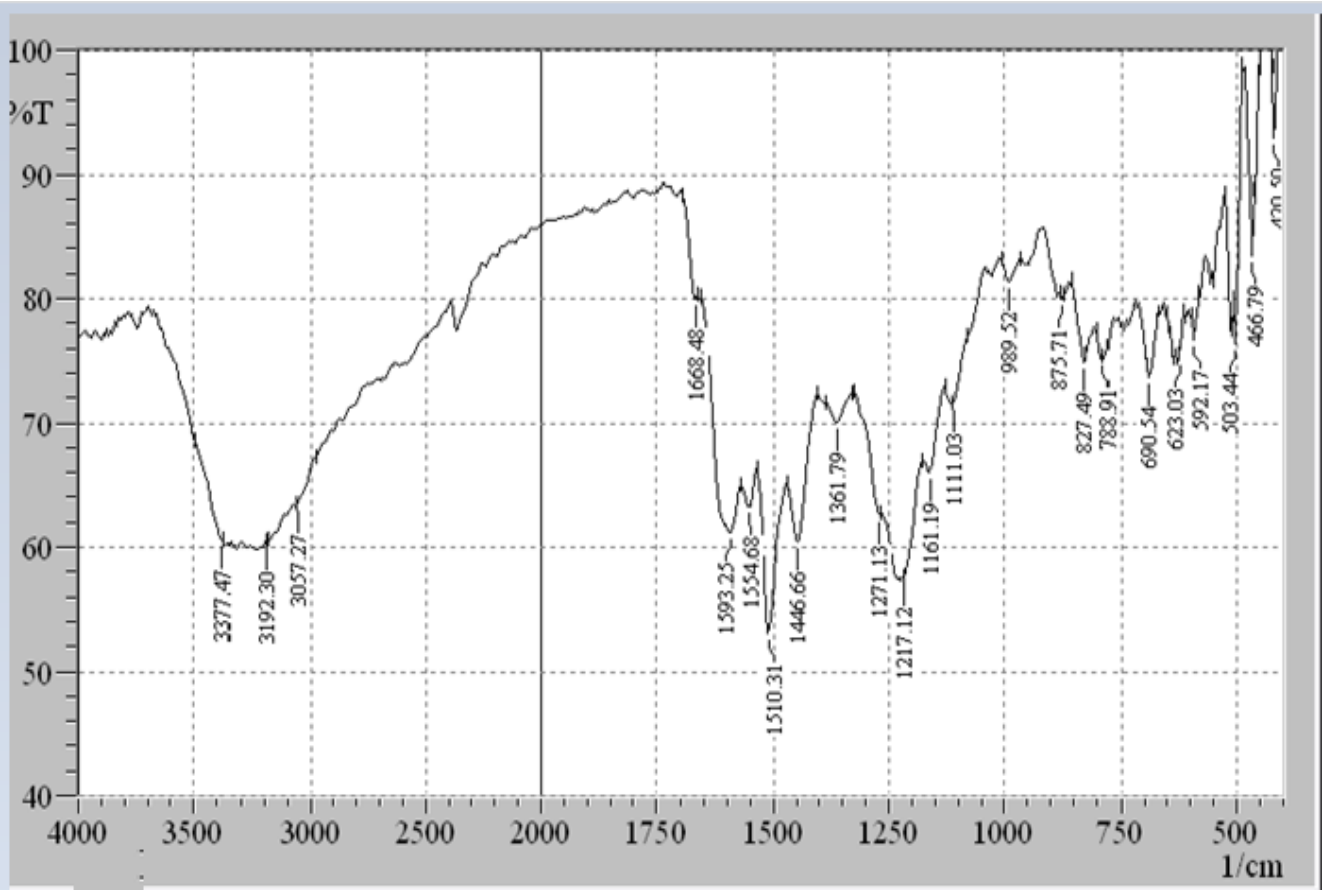

Figure (3-13) iron Complex[Fe $(L_3)_2$]

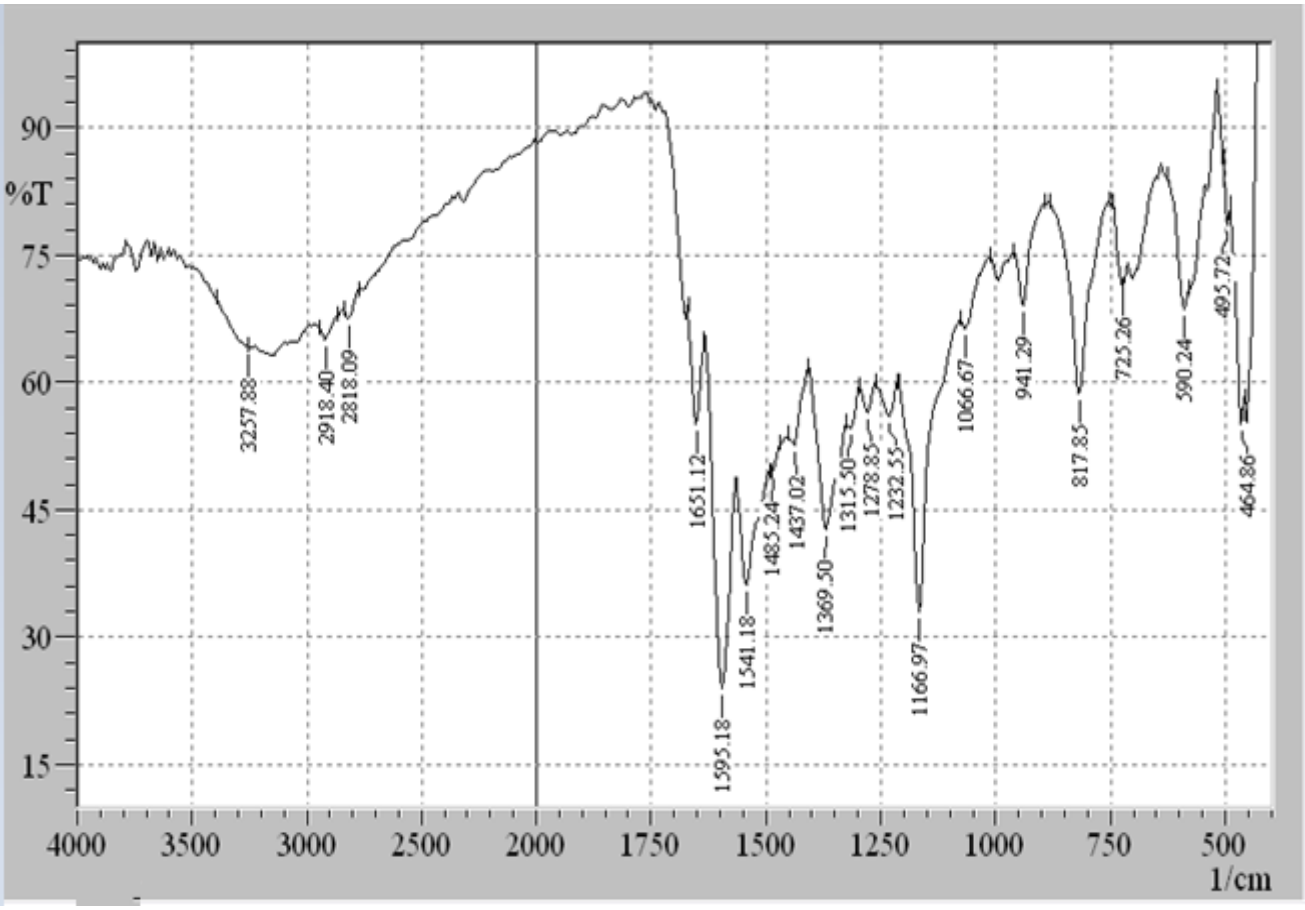

Figure (3-14) Copper Complex[Cu $(L_4)_2$]

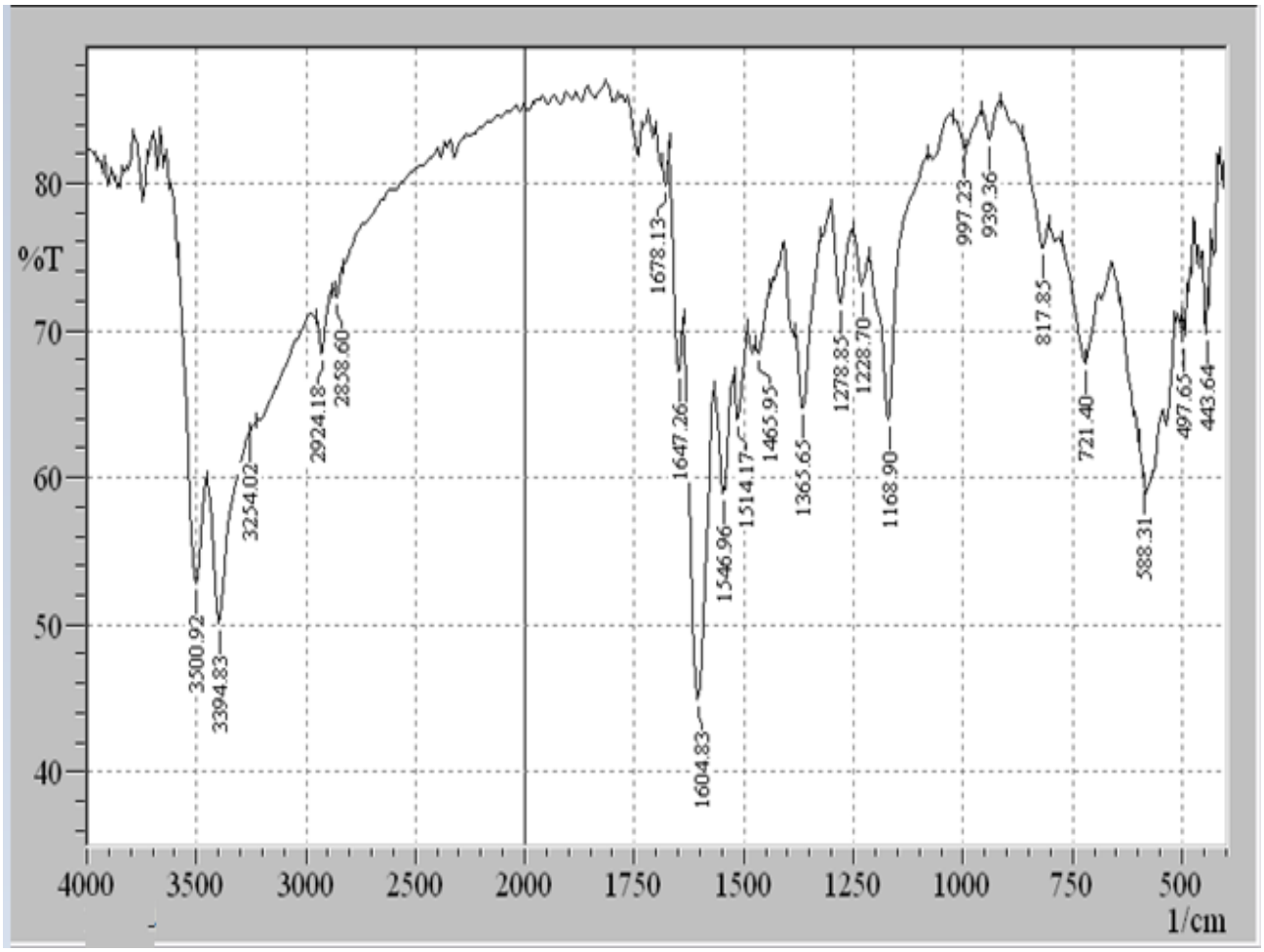

Figure (3-15) Nickel Complex [Ni $(L_4)_2$]

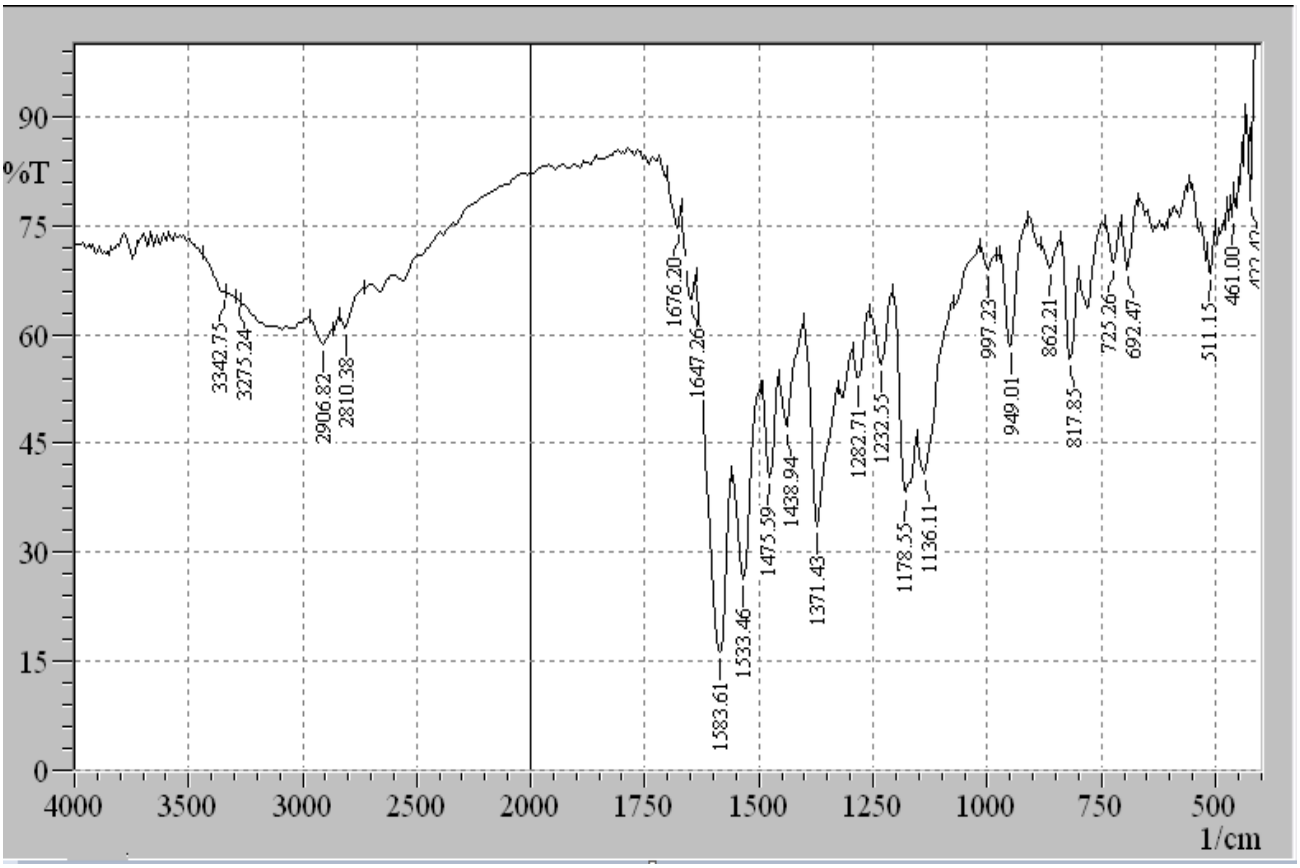

Figure (3-16) Iron Complex[Fe $(L_4)_2$]

Table (3-2) FT-IR Spectra Bands of the Synthesized Ligands and Complexes

comp	O-H 6-amino	O-H m-hydroxy	OH Phenol	COOH 6-amino	C=O lactam	C=N	N=N	S-C	C-N	M-O	M-N
Started mterial	3134	3311	3269	1680	1645	_	_	2152	1107		
L1	3169	_	_	1695	1660	1595	1537		1132	_	_
$[Cu(L_1)_2]$	3144	_	_	_	1649	1599	1508	_	_	464 501	530
$[Ni(L_1)_2]$	3153	_	_	_	1645	1606	1514	_	_	457 536	540
$[Fe(L_1)_2]$	3140	_	_	_	1651	1597	1514	_	_	422 503	540
L_2	3182	3348	3244	1676	1643	1606	1525	_	_	_	_
$[Cu(L_2)_2]$	_	3323	_	1676	1640	1597	1512	2162	_	435 468	556
$[Ni(L_2)_2]$	_	3277	_	1678	1637	1600	1512	_	_	436 466	542
$[Fe(L_2)_2]$	3184	3356	3248	1676	1637	1600	1485	_	-	447 480	536
L_3	_	_	3350	_	1631	1610	1508	_	1118	_	_
$[Cu(L_3)_2]$	_	_	3369	1691	1645	1595	1514	_	1109	447 493	542
$[Ni(L_3)_2]$	_	_	3369	_	1645	1591	1506	_	_	427 470	513
$[Fe(L_3)_2]$	_	_	3377	1668	1668	1593	1510	_	_	420 466	503

comp	O-H 6-amino	O-H m-hydroxy	OH Phenol	COOH 6-amino	C=O lactam	C=N	N=N	S-C	C-N	M-O	M-N
L_4	_	3352	_	1687	1651	1585	1533	_	_	_	_
$[Cu(L_4)_2]$	_	3257	_	1670	1651	1595	1541	_	_	464	496 590
$[Ni(L_4)_2]$	_	3254	_	1678	1647	1604	1546	_	_	443	497 588
$[Fe(L_4)_2]$	_	3275	_	1676	1647	1604	1546	_	_	443	497 588

3.3 Micro-elemental Analysis:

Micro elemental analysis (C.H.N) of the synthesized ligands played an important role in predicting the final structure and formula accompanied by metal analysis by using atomic absorption spectroscopy, where the ratio of the elements of carbon, hydrogen, nitrogen, and sulfur are calculated[100]. In this study, the use of (C.H.N) helped in calculating the proportion of the above-mentioned elements for the following four ligands (HL_1, HL_2, HL_3, and HL_4).

The proportions of metal elements were calculated by using atomic absorption spectroscopy. The results are estimated in Table (3-3), (3-4)These results illustrated the calculated theoretical value which is in good agreement and found experimental.

Table (3-3) shows the results of the element analysis (CHN) of the ligands (HL_1), (HL_2), (HL_3), (HL_4).

Chemical Formula	M.Wt	C Found% (cal).	H Found% (cal)	N Found% (cal).	S Found% (cal).	Metal Found% (cal).
$C_{23}H_{25}N_5O_4S$	467.5	58.7 (59.1)	4.9 (5.3)	11.01 (14.9)	5.12 (6.8)	
$C_{21}H_{20}N_4O_5S$	440.5	59.4 (57.2)	4.2 (4.5)	9.6 (12.7)	7.15 (7.2)	
$C_{21}H_{20}N_4O_5S$	440.5	57.4 (57.2)	4.6 (4.5)	8.5 (12.7)	5.6 (7.2)	
$C_{23}H_{25}N_5O_4S$	467.5	64.1 59.03	5.1 (5.3)	11.0 (14.9)	6.8 (6.8)	

Table (3-4) the atomic absorption of the metal in their complexes

Chemical Formula	M.Wt	Metal Found% (cal).
$[Cu(C_{23}H_{23}N_5O_4S)_2]$	996.5	6.0 (6.37)
$[Ni(C_{23}H_{23}N_5O_4S)_2]$	991.6	4.82 (5.90)
$[Fe(C_{23}H_{23}N_5O_4S)_2]$	988.8	5.51 (5.64)
$[Cu(C_{21}H_{18}N_4O_5S)_2]$	942.5	6.24 (6.73)
$[Ni(C_{21}H_{18}N_4O_5S)_2]$	937.6	5.3 (6.25)
$[Fe(C_{21}H_{18}N_4O_5S)_2]$	934.8	5.1 (5.96)
$[Cu(C_{21}H_{18}N_4O_5S)_{2]}$	942.5	5.8 (6.73)
$[Ni(C_{21}H_{18}N_4O_5S)_2]$	937.6	4.98 (6.25)
$[Fe(C_{21}H_{18}N_4O_5S)_2]$	934.8	5.1 (5.96)
$[Cu(C_{23}H_{23}N_5O_4S)_2]$	996.5	5.7 (6.37)
$[Ni(C_{23}H_{23}N_5O_4S)_2]$	991.6	5.4 (5.90)
$[Fe(C_{23}H_{23}N_5O_4S)_2]$	988.8	5.2 (5.64)

(cal) calculated found % experimental

3.4 Molar Conductivity Measurements:

The conductivity measurement of a compound is used to determine the conductance property (electrolyte or non-electrolyte natur) [101] The increase in the charged particles led to an increase in the electrical conductivity. It is not recommended to use water as a solvent in coordination compounds due to the difficulty of dissolving these compounds in water. Therefore, organic solvents were often used because the solvent had a high dielectric constant and a low viscosity such as Dimethyl Sulfoxides (DMSO) and Dimethyl Formamide (DMF). This was found based on the measured values in Table (3-5).

Table (3-5) the molar conductivity values of some of the electrolytes in solvents with ($1x10^{-3}$) concentration

Solvent	Non-Electrolyte	Electroyte Type			
		1:1	1:2	1:3	1:4
Water	0.0	120	240	360	480
Ethanol	0-20	35-45	70-90	120	160
Nitro Methane	0-20	75-95	150-180	220-260	290-330
Methyl Cyanide	0-30	120-160	220-300	340-420	500
DMF	0-30	65-90	130-170	200-240	300
DMSO	0-20	30-40	70-80	-	-

The ligands and their complexes were used to measure the molar conductivity. The results of the obtained values were shown at a concentration of ($1x10^{-3}$) molar at laboratory temperature using the solvent DMSO. Table (3-6) showed the molar conductivity of the complexes. Ligands' molar conductivity was measured in units (mol^{-1} ohm^{-1} cm^2) and showed the value (2.24, 4.43, 2.21, and 2.17). The complexes showed the non-electrolytic property in DMSO solvent [102]. Molar conductivity of complex was measured in units of (mol^{-1} ohm^{-1} cm^2). The electrical conductivity of the copper complex of the ligands was equal to (6.84, 11.1, 12.4, and 6.5) while the Nickel complexes had reached (15.4, 16, 15.3, and 15.2)). The

value of the molar conductivity of the ferrous complex was (14.8, 24.8, 19.6, and 14.6). This confirmed that the non-electrolyte solutions had a molar ratio of 1:2 and This confirms that there is no chlorine ion outside the coordination sphere [103].

Table (3-6) Values of molar conductivity (mol^{-1} ohm^{-1} cm^2) for ligands and their complexes in DMSO solvent at ($1x10^{-3}$) molar concentration at laboratory temperature

No	Comp	Λm $S.cm^2$ $.mole^{-1}$
1	HL_1	2.24
2	$[Cu(L_1)_2]$	6.84
3	$[Ni(L_1)_2]$	15.4
4	$[Fe(L_1)_2]$	14.8
5	HL_2	4.43
6	$[Cu(L_2)_2]$	11.1
7	$[Ni(L_2)_2]$	16
8	$[Fe(L_2)_2]$	24.8
9	HL_3	2.23
10	$[Cu(L_3)_2]$	12.4
11	$[Ni(L_3)_2]$	15.3
12	$[Fe(L_3)_2]$	19.6
13	HL_4	2.17
14	$[Cu(L_4)_2]$	6.82
15	$[Ni(L_4)_2]$	15.2
16	$[Fe(L_4)_2]$	14.6

3.5 Magnetic Susceptibility Measurements:

Magnetic Susceptibility Measurements are one of the most important techniques, as they provide us with important information about oxidation state, electronic arrangement, and hybridization of the central atom along with the number of unpaired electrons of the metal ion. Therefore, there is an increase in the use of this measurement to employ it with other technologies to predict the complex configuration [104] and [105]. Accordingly, magnetic materials can be classified as Paramagnetic materials and Diamagnetic materials.

Paramagnetic materials referred to the magnetic state of an atom with one or more unpaired electrons, while diamagnetic complexes referred to the state of an atom characterized by paired electrons. The paramagnetic characteristics were not affected by the atoms or molecules that possess the magnetic properties such as solvent particles or the complexes surrounding their central ions. Conversely, the diamagnetic resulted from the inductive effect of the external magnetic field on the electronic cloud. Therefore, when dealing with paramagnetic materials, correction shall be made due to the presence of diamagnetic properties within the molecule [106]. Magnetic properties arise from electron spin and orbital angular momentum. The magnetic moment of metal ions can be calculated from the following equations.

$\mu S+L=\sqrt{(4S(S+1)+L(L+1))}$ B.M ……(1)

S= spin quantum number

L=angular momentum operator

When the atom or ion is a part of a complex, this relationship reduces to include spin quantum when the angular momentum quenching

$\mu S=\sqrt{(4S(S+1))}$ B.M……..(2)

When (S = n / 2): n = number of unpaired electrons

$\mu S=\sqrt{(n(n+2))}$ B.M……(3)

The magnetic susceptibility of the complexes was measured at (298k). The diamagnetic value (μeff) of the atoms in organic molecules, inorganic radicals, and metal ions was corrected by using (Pascal constant) of the magnetic moment (μeff) which can be calculated according to these equations:

$\mu eff = 2.828\ \sqrt{XAT}$ B.M ……(4)

$X_A=X_M-D$ …….. (5)

$X_M = X_g \times$ M.wt……. (6)

T= Absolute temperature =298K

XA=Magnetic susceptibility

Xm=Molar susceptibility

Xg= general mass magnetic susceptibility

D=Diamagnetic correction

ueff =effective magnetic moment

M.wt =molecular weight of complex

B.M = magnetic susceptibility unite

The results of the measurements were estimated in Table (3-7)

The magnetic moment of the copper (Cu II) complexes[Cu $(L_1)_2$],[Cu $(L_2)_2$][Cu $(L_3)_2$] and [Cu $(L_4)_2$]was equal to (1.83, 1.8, 1.7, and 1.7) respectively, where the magnetic moment of octahedral copper complexes was (1.8-2.1) and this is in agreement with the literature [107]. This indicated that copper complexes had an 'octahedral' configuration. The complexes,[Ni $(L_1)_2$] ,[Ni $(L_2)_2$] ,[Ni $(L_3)_2$], [Ni $(L_4)_2$] indicated that the paramagnetic properties were equal to (2.9, 3.2, 2.7, and 3.0) and this is consistent with the literature [108] related to the octahedral Nickel complexes (2.9, 3.3). The results of measuring magnetic susceptibility of iron complexes[Fe $(L_1)_2$] , [Fe $(L_2)_2$], [Fe $(L_3)_2$] , [Fe $(L_3)_2$], showed magnetic moment equal to (5.7, 5.4, 5.4, and 5.6) complexes, respectively, and this is in harmony with what is mentioned in the literature [109]. The obtained values indicated the presence of the magnetic susceptibility of Fe^{+2} ion (5.1 and 5.7) resulting from the complexes that had an octahedral shape.

3.6 Study of the electronic spectra of ligands and metal complexes:

Electronic absorption spectra of transition metal complexes are usually attributed to the electronic transitions of metal d-orbital. The energy required for such transitions is within the UV and visible regions. The spectra helped us to predict the suggested geometry according to the shape and number of observed peaks. The calculated ones depend on the information of the Racah parameter [110].

The interest and focus on the chemistry of transitional elements is due to the huge development of the successful theories in explaining these properties associated with metal ion-containing incompletely occupied orbitals (d) [111]. The colors of the complexes and their magnetic properties can be explained based on these theories. At present, the measurement of the UV& Visible spectrum has become an important part of the explanation and characterization of complex types [112]. The transitions in the electronic spectra of the complexes can be divided into the following:

3.6.1 Ligand Spectra:

The organic and inorganic molecules often behave as ligands in the transition metal complexes, especially when these particles contain π electron systems. These particles possess distinct absorption peaks that usually appear in the UV region. Therefore, they take the form of strong peaks because they have allowed transitions ($\pi \rightarrow \pi^*$) or ($n \rightarrow \pi^*$).

3.6.1 Charge-transfer Spectra:

The source of this type of spectra is the electron transitions between the metal and the ligand as a result of the closeness of the ligand and the metal orbitals and the interaction between them. If this bond is achieved by transferring the charge from the ligand to the metal ion, the electronic transmission will be (L → M). This charge transfer increases with the increase of both the oxidation state of the metal ion and the stability of their empty orbitals that led to the (metal reduction). Importantly, when the electron transfers from the metal with a low oxidation state to the ligand, the electronic transmission will be (M → L), which leads to the (oxidation of the metal). Likewise, when the composition of the inorganic compound contains two metallic ions differing in the oxidation state, the charge transfer occurs between these two ions of the type (M → M) [113].

3.6.2 Transition Spectra (d-d):

It is one of the spectra of the metal ions and is affected by the presence of a ligand. This spectrum occurs as a result of the electron excitation o between two energy levels represented by the d-orbital transitions. It was found that the spectra of the charge transfer and the free ligand transfer provide strong peaks.

However, it was found that the spectra of d-d electron transitions are not allowed according to the Laporte Rule. Thus, the transmission peaks are very weak and appear in the visible region of the spectrum. The number and sites of the absorption peaks depend on the energy of the secondary level (d) degeneration, the number of electrons included in the level orbitals (d), the oxidation state of the metal ion, and the number and type of ligands involved in the formation of the complex and its steric shape. This clearly appears when comparing the spectra of the octahedral and tetrahedral complexes [114]. The British chemist, Leslie Orgel developed a scheme called (Orgel Diagram) for both electronic transfers of systems (d^2, d^3, d^7, and d^8) [115].

These peaks are characterized by their wide shape due to the short time required for the absorption of a photon from the particle, which occurs in a time of (10^{-8}) seconds compared to the period required for the occurrence of the vibrational or rotational movements of the relatively slow molecule [116].

3.6.3 Counter-ion Spectra:

It is a type of absorption spectra associated with the formation of the ion complex, and this nucleus is present in the spectra of many complexes. It also interferes with the spectra, so it is preferable to remove them by changing the associated ion, so the metal nitrates were excluded and chlorides were used instead. Electron spectra for solutions of ligands (HL_1, HL_2, HL_3, and HL_4) were recorded. Complexes were prepared in the current study by using a solvent of dimethyl sulfur oxide (DMSO) and (d → d) electron transitions characterized in some of these complexes. Other complexes showed the peaks of charge transfer at different wavelengths higher or lower than what is apparent in the free ligand spectra.

3.6.4 Ligand Spectra:

a- Ligand (HL_1)

The electronic spectrum of ligand (HL_1) exhibits two bands; one at 305 nm which was assigned to $\pi \rightarrow \pi^*$ of the aromatic rings present in the ligand and the other was assigned at 362 nm $n \rightarrow \pi^*$ transitions which was retained to azo and azomethine groups [117].

b- Ligand (HL_2)

The electronic spectra of the prepared ligand (HL_2) showed two peaks at 272nm and 380nm which were assigned to $\pi \rightarrow \pi^*$ and $n \rightarrow \pi^*$ transitions. This belongs to the aromatic rings present in the ligand, azo, and azomethine groups, respectively [118].

c- Ligand (HL_3)

The ligand (HL_3) electronic spectra showed two absorption peaks at 272.3 nm that returns to ($\pi \rightarrow \pi^*$) electronic transmission of the benzene ring, and at 311 nm $n \rightarrow \pi^*$ electronic transmission for azo and azomethine groups [119].

d- Ligand (HL_4)

The Ligand spectrum (HL_4) showed two absorption peaks at (277.5, 303) nm the band at 277.5 nm which was assigned to π–π^* transitions of the aromatic rings present in the ligand and the band at 303 nm which was assigned to n–π^* transitions of azomethine and Azo groups present in (L_4) [120] as shown in Table (3-8) and Figures (3-18), (3-19), (3-20), and (3-21).

3.6.4 Complexes Spectrum:

a- Copper (II) Complexes

Electronic spectra of [Cu $(L_1)_2$] complex showed a single band As a result of the fusion of the spectra of the d-d transitions with the spectra of the ligand, they appeared in the form of a single peak in the site,(466.6) nm which was attributed to $^2Eg \rightarrow ^2T_2g$. This transition supported the octahedral shape of the complexes.

The spectrum of the complex [$Cu(L_2)_2$] derived of the(HL_2) ligand showed three absorption peaks at the wavelength (475,268, and 293)nm assigned to $^2Eg \rightarrow ^2T_2g$ electronic transition due to coordination of octahedral of copper complex and the peaks at (268,293) assigned to π–π* and n–π* It is shown that there was a redshift to the ligand absorption peaks.

Besides, the UV-visible spectrum of the Cu (II) complex derived from ligand (HL_3) [Cu $(L_3)_2$] complex showed broadband at the site (499) nm. It may return to electronic transmission $^2Eg \rightarrow ^2T_2g$, as the charge transfer (C.T) peak appeared at (300) nm. The resulting information can be relied on other technologies to suggest the octahedral shape.

As for the spectrum of the copper complex[Cu $(L_4)_2$], this showed an absorption peak at the wavelength (456.5) nm which was attributed to$^2Eg \rightarrow ^2T_2g$. The charge transfer C.T peak appeared at (362.5) nm while the peak at (310) was assigned to π–π* transition . It can rely on the information of other techniques to suggest the octahedral shape of complexes [121], [122], and [123].

b- Nickel (II) Complexes

The electronic spectra of nickel complex, derived from ligand (HL_1), showed three peaks at (450) nm assigned to $^3A_2g_{(F)} \_ ^3T_1g_{(p)}$, (318) to C.T peak and the peak at the site (312)nm was attributed to π–π*. This is consistent with the spectra of octahedral nickel (II) complexes.

Nickel complex, derived from ligand (HL_2), also showed three peaks as follows: the first was attributed to $^3A_2g_{(F)} \_ ^3T_1g_{(p)}$ at (536) nm and peak at (356)nm assigned to π–π*. . The appearance of this electronic transition in these locations supported the octahedral shape of the complex, where the electronic transition at (288) nm was assigned to C.T electron transition, showing redshift due to the coordination process.

Besides, the electronic spectra of nickel complex, derived from ligand (HL_3), showed two peaks; (410) nm which was assigned to $^3A_2g_{(F)} \_ ^3T_1g_{(p)}$ electronic transition. This is consistent with the spectra of octahedral nickel (II) complexes, where the electronic transition at (266.5) nm was assigned to C.T electron transition, showing redshift due to the coordination process.

The electronic spectra of the nickel complex, derived from ligand (HL_4), showed four peaks at (512) nm assigned to ^3A_2g (F) _ ^3T_1g (p). This is also consistent with the spectra of octahedral nickel (II) complexes. The charge transfer peak C.T appeared at (270) nm while the (264) and (258) nm represented the π–π* , n–π*.. [124], [125], and [126].

c- Iron Complexes

The UV-visible spectrum of iron (II) complex of ligand (HL_1) showed a single band appeared As a result of the fusion of the spectra of the d-d transitions with the spectra of the ligand, in the site in the site (448) nm which was attributed to $^5T_2g \rightarrow {}^5Eg$ electron transition. This transition supported the octahedral shape of the complexes.

The spectrum of the complex [Fe $(L_1)_2$] derived of the (HL_2) ligand also showed two absorption peaks at the wavelength (410, 291) nm which was assigned to ^5T_2g (P) → ^5Eg (F) electronic transition due to coordination of octahedral and charge transition C. T, showing a redshift.

The electronic spectra of iron complex[Fe_3] a derived from ligand (HL_3) showed two peaks (436) nm which was assigned to $^5T_2g \rightarrow {}^5Eg$ electronic transition. This is consistent with the spectra of octahedral iron (II) complexes, the electronic transition at (305) nm is assigned to C.T electron transition, showing a redshift due to the coordination process.

The electronic spectra of iron complex [Fe $(L_4)_2$] derived from ligand (HL_4) showed three peaks at (365.5) nm assigned to $^5T_2g \rightarrow {}^5Eg$,As a result of the fusion of the spectra of the d-d transitions with the spectra of the ligand, where the peak at (306) was attributed to n–π* electronic transition and (255) nm was assigned to π–π*.. This is consistent with the spectra of octahedral iron (II) complexes [127], [128], and [129] as the important peaks are shown in Table (3-7) and Figures (3-22), (3-23), (3-24), (3-25), (3-26), (3-27), (3-28),(3-29),(3-30),(3-31),(3-32), and (3-33), respectively.

From the knowledge of the electronic transitions in the visible region, can know the spatial geometry of complexes because the number of transitions in the visible region depends on the Geometry complex.

Table (3-7) Electronic Spectra and Magnetic Susceptibility of Ligands and Complexes in DMSO Solvent at Laboratory Temperature

Complexes	**Absorption band(nm)**	**Absorption band(cm^{-1})**	**Assignment**	**μeff (B.M)**	**Proposed Structural**
$C_{24}H_{26}N_4O_4S$ HL_1	305 362	32786 27624	π →π* n →π*	_	_
$[Cu(C_{25}H_{25}N_4O_4S)_2]$	466.6	21431	$^2Eg \rightarrow {}^2T_2g$	1.83	O.h
$[Ni(C_{25}H_{25}N_4O_4S)_2]$	450 318 312	22222 31446 32051	$^3A_2g_{(F)} \_ {}^3T_1g_{(p)}$ C.T π →π*	2.9	O.h
$[Fe(C_{25}H_{25}N_4O_4S)_2]$	448	22321	$^5T_2g \rightarrow {}^5Eg$	5.7	O.h
$C_{22}H_{21}N_3O_5S$ L_2	272 380	36764 26315	π →π* n →π*		
$[Cu(C_{22}H_{20}N_3O_5S)_2]$	475 269 293	21052 37174 34129	$^2Eg \rightarrow {}^2T_2g$ π →π* n→π*	1.8	O.h

Complexes	**Absorption band(nm)**	**Absorption band(cm^{-1})**	**Assignment**	**μeff (B.M)**	**Proposed Structural**
$[Ni(C_{22}H_{20}N_3O_5S)_2]$	536 356 288	18656 28089 34722	$^3A_2g_{(F)} \_ ^3T_1g_{(p)}$ π→π* C.T	3.2	O.h
$[Fe(C_{22}H_{20}N_3O_5S]$	410 291	24390 34364	$^5T_2g \rightarrow {}^5Eg$ C.T	5.4	O.h
$C_{22}H_{21}N_3O_5S$ L_3	272.3 311	36724 32154	π →π* n →π*		
$[Cu(C_{22}H_{20}N_3O_5S)_2]$	499 300	20040 33333	$^2Eg \rightarrow {}^2T_2g$ C.T	1.7	O.h
$[Ni(C_{22}H_{20}N_3O_5S)_2]$	410 266.5	24390 37523	$^3A_2g_{(F)} \_ ^3T_1g_{(p)}$ C.T	2.7	O.h
$[Fe(C_{22}H_{20}N_3O_5S)_2]$	436 305	22935 32786	$^5T_2g \rightarrow {}^5Eg$ C.T	5.4	O.h
$C_{24}H_{26}N_4O_4S$ L_4	277.5 303	36036 33003	π →π* n→π		
$[Cu(C_{24}H_{25}N_4O_4S)_2]$	456.5 362.5 310	21905 27586 32258	$^2Eg \rightarrow {}^2T_2g$ C.T π →π*	1.9	O.h
$[Ni(C_{24}H_{25}N_4O_4S)_2]$	512 270 264,258	19531 37037 37878 ,38759	$^3A_2g_{(F)} \_ ^3T_1g_{(p)}$ C.T π →π*, n→π	3.0	O.h
$[Fe(C_{24}H_{25}N_4O_4S)_2]$	365.5 306 255	27397 32679 39215	$^5T_2g \rightarrow {}^5Eg$ π →π* n→π	5.6	O.h

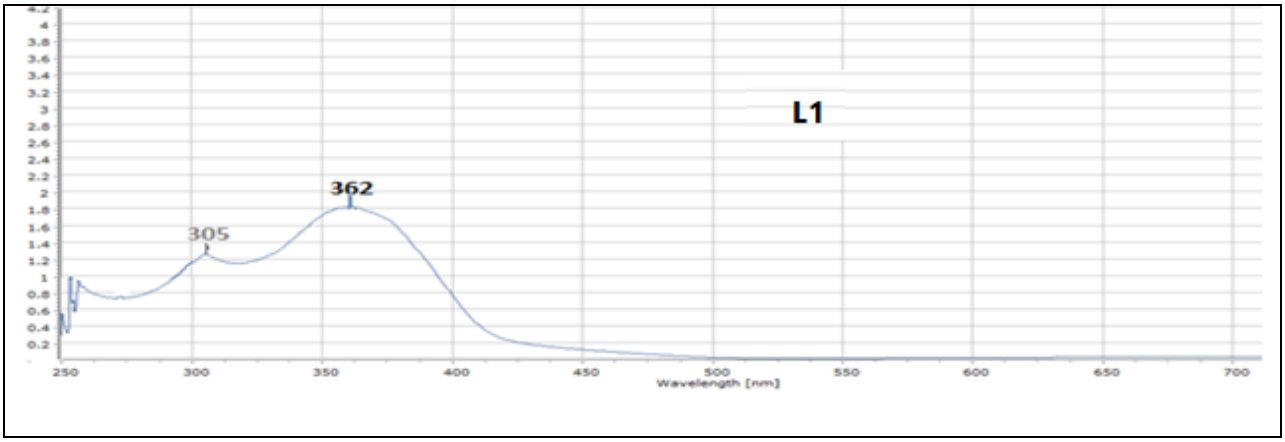

Figure (3-18) Electronic Spectra of HL_1 ($C_{24}H_{26}N_4O_4S$)

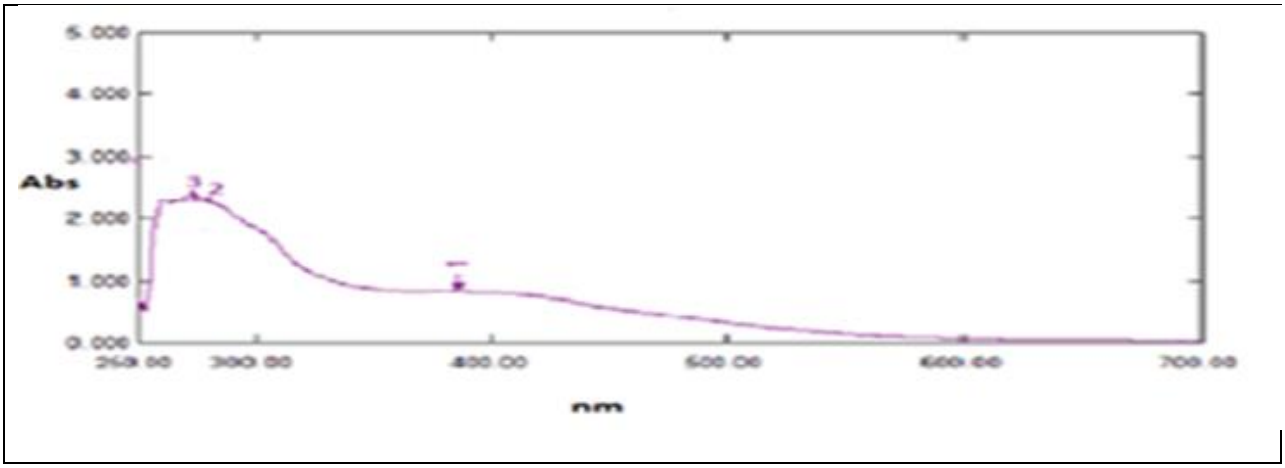

Figure (3-19) Electronic Spectra of ($C_{22}H_{21}N_3O_5S$) HL_2

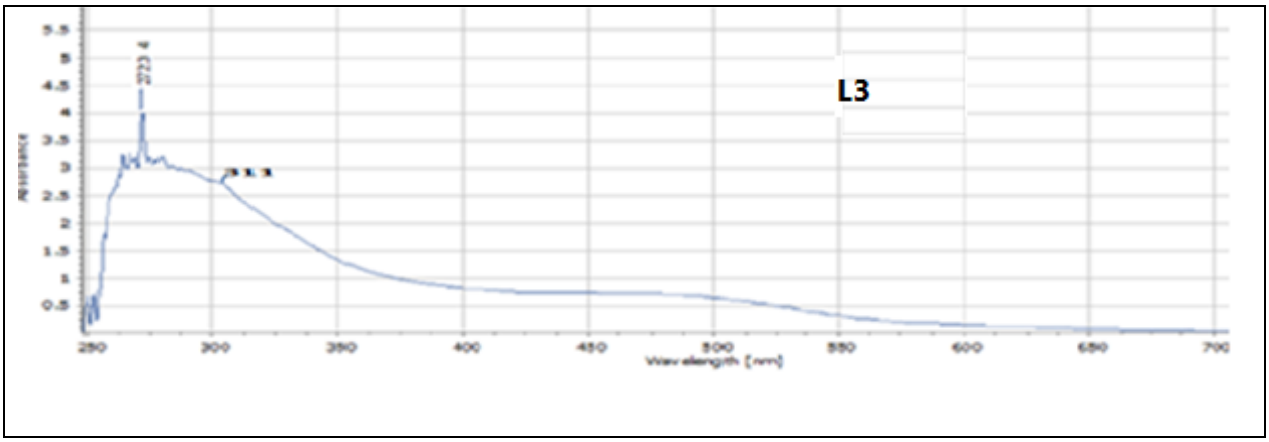

Figure (3-20) Electronic Spectra of ($C_{22}H_{21}N_3O_5S$) HL_3

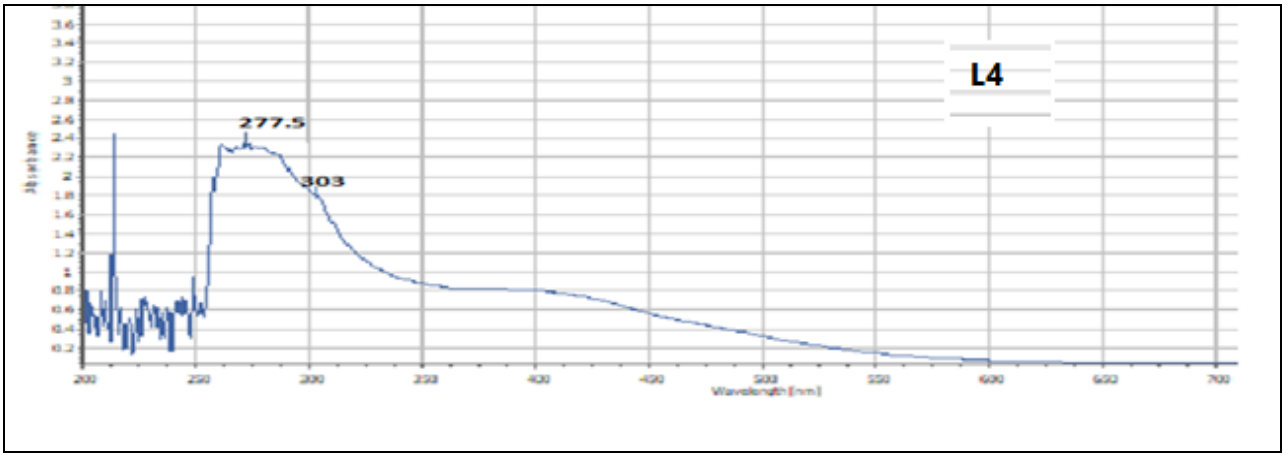

Figure (3-21) Electronic Spectra of ($C_{22}H_{21}N_3O_5S$) HL_4

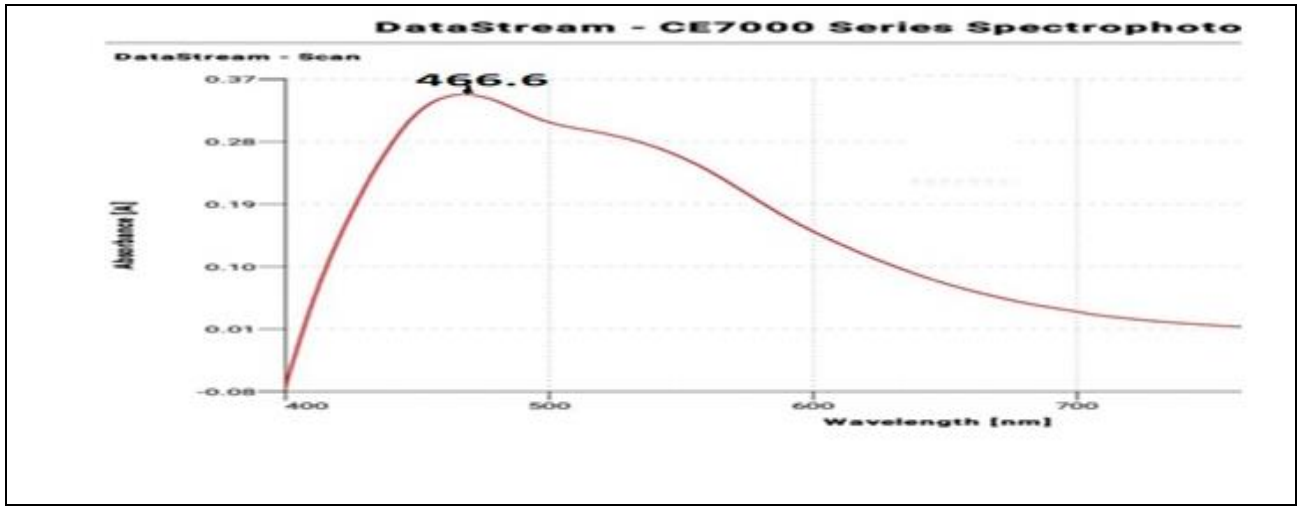

Figure (3-22) Electronic Spectra of Copper Complex [Cu $(HL_1)_2$]

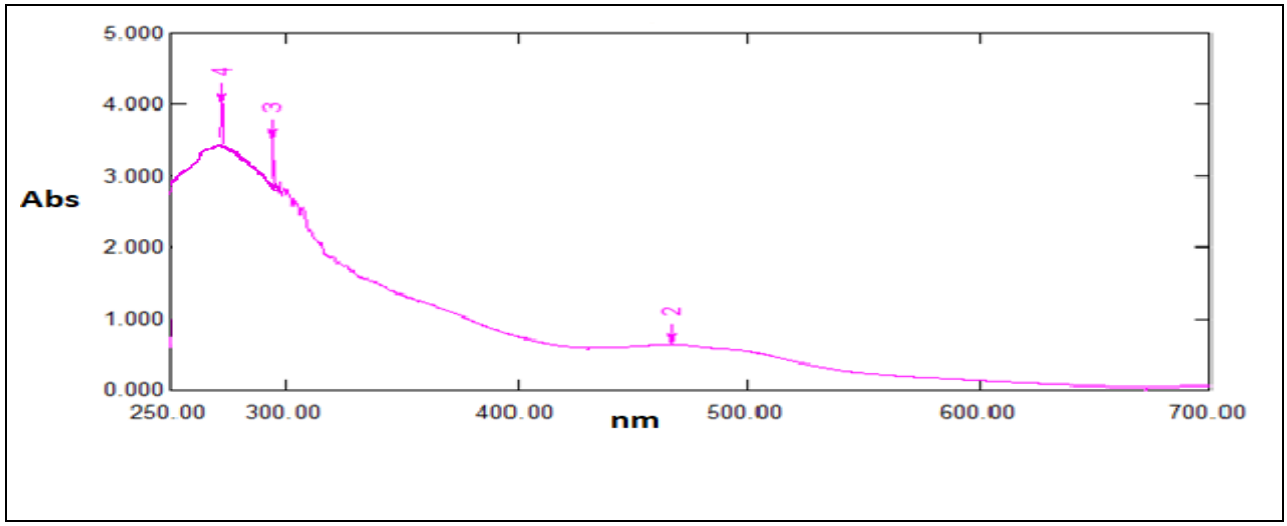

Figure (3-23) Electronic Spectra of Copper Complex [Cu $(HL_2)_2$]

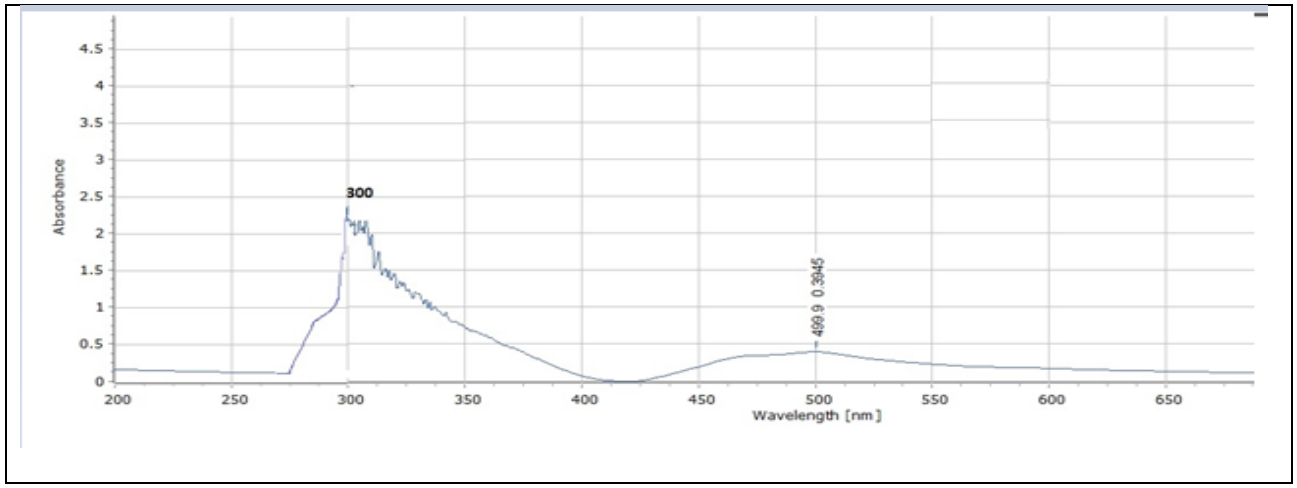

Figure (3-24) Electronic Spectra of Copper Complex [Cu $(HL_3)_2$]

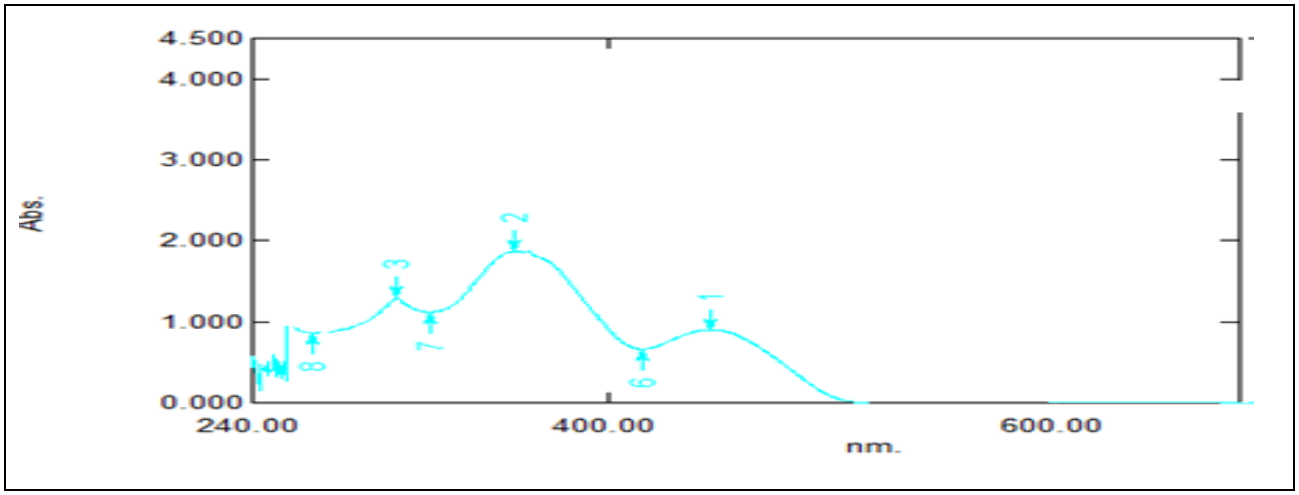

Figure (3-25) Electronic Spectra of Copper Complex [Cu $(HL_4)_2$]

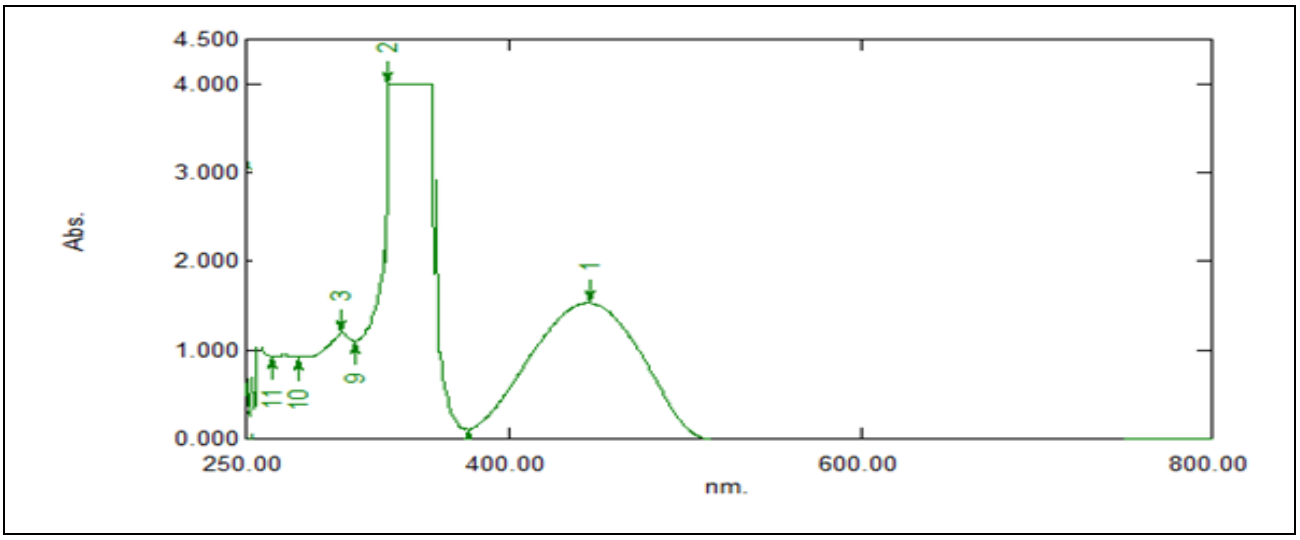

Figure (3-26) Electronic Spectra of Nickel Complex [Ni $(HL_1)_2$]

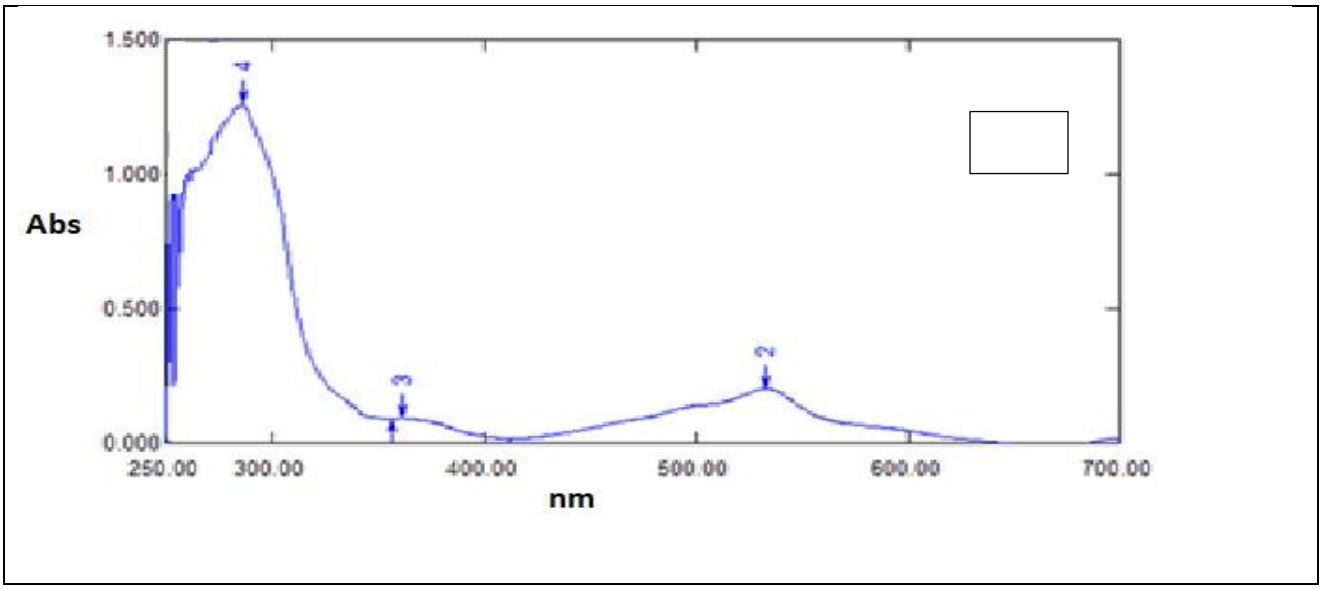

Figure (3-27) Electronic Spectra of Nickel Complex [Ni $(HL_2)_2$]

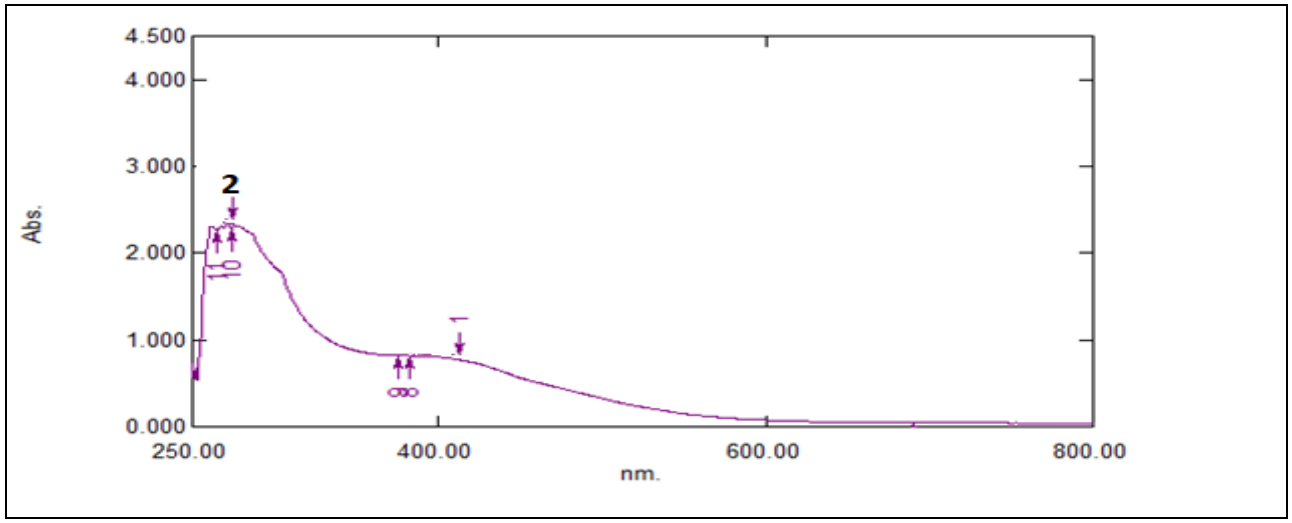

Figure (3-28) Electronic Spectra of Nickel Complex [Ni $(HL_3)_2$]

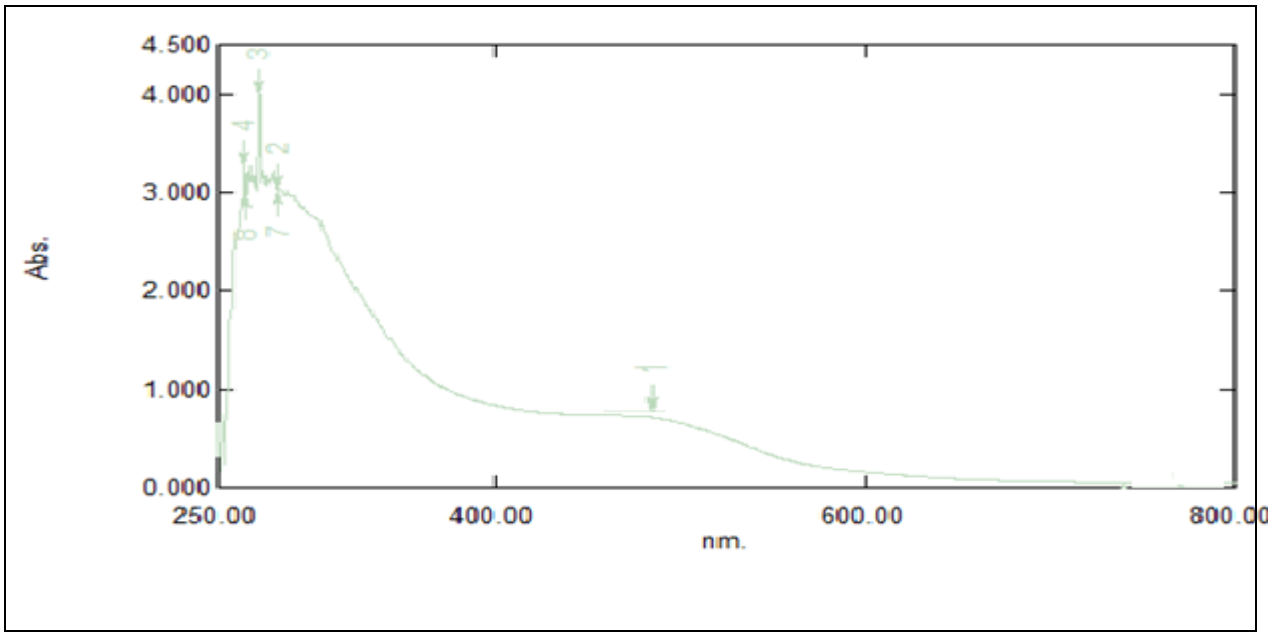

Figure (2-29) Electronic Spectra of Nickel Complex [Ni $(HL_4)_2$]

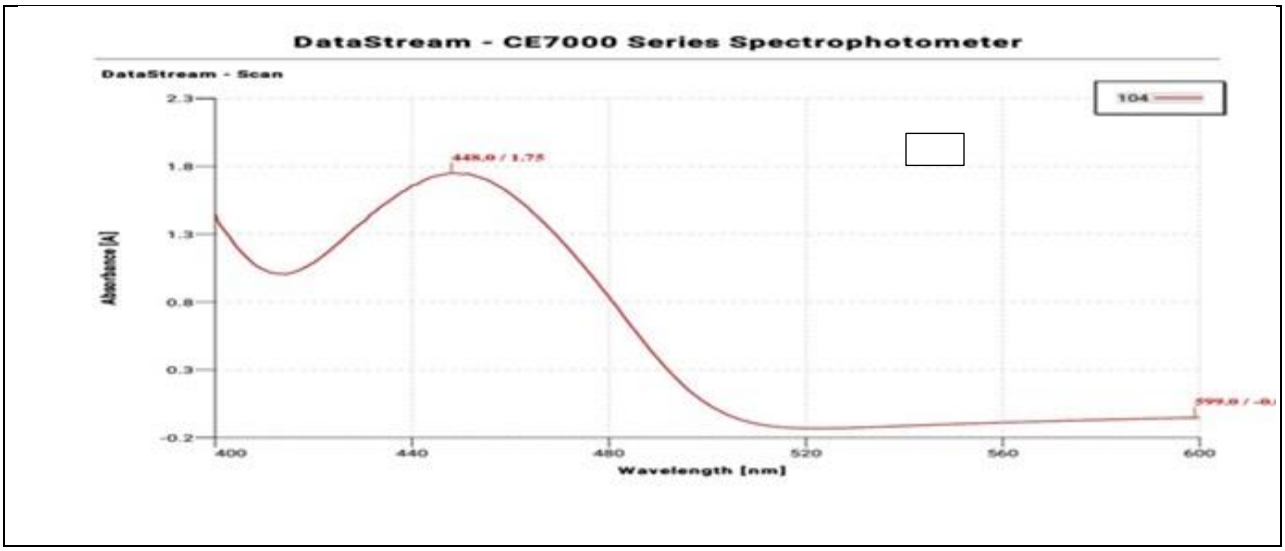

Figure (3-30) Electronic Spectra of [Fe $(HL_1)_2$]

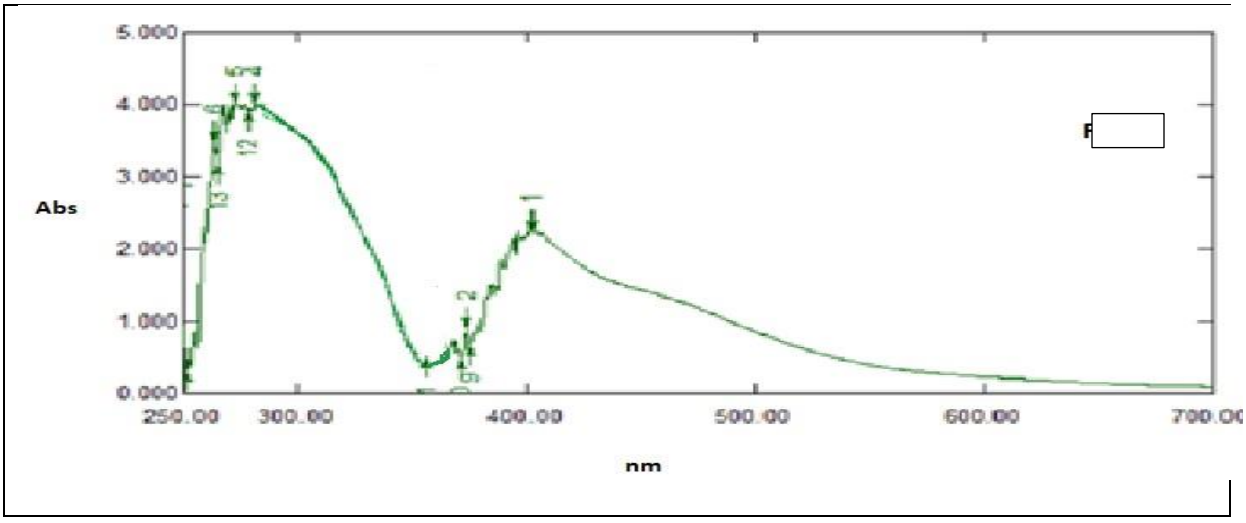

Figure (3-31) Electronic Spectra of Ferrous Complex [Fe $(HL_2)_2$]

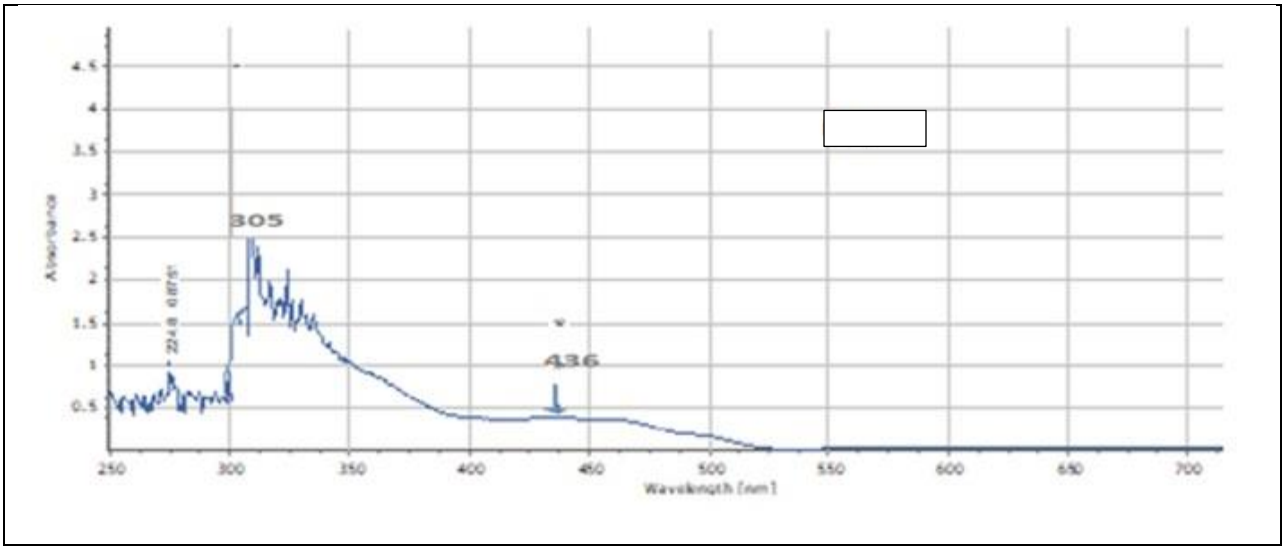

Figure (3-32) Electronic Spectra of iron Complex [Fe (HL_3)]

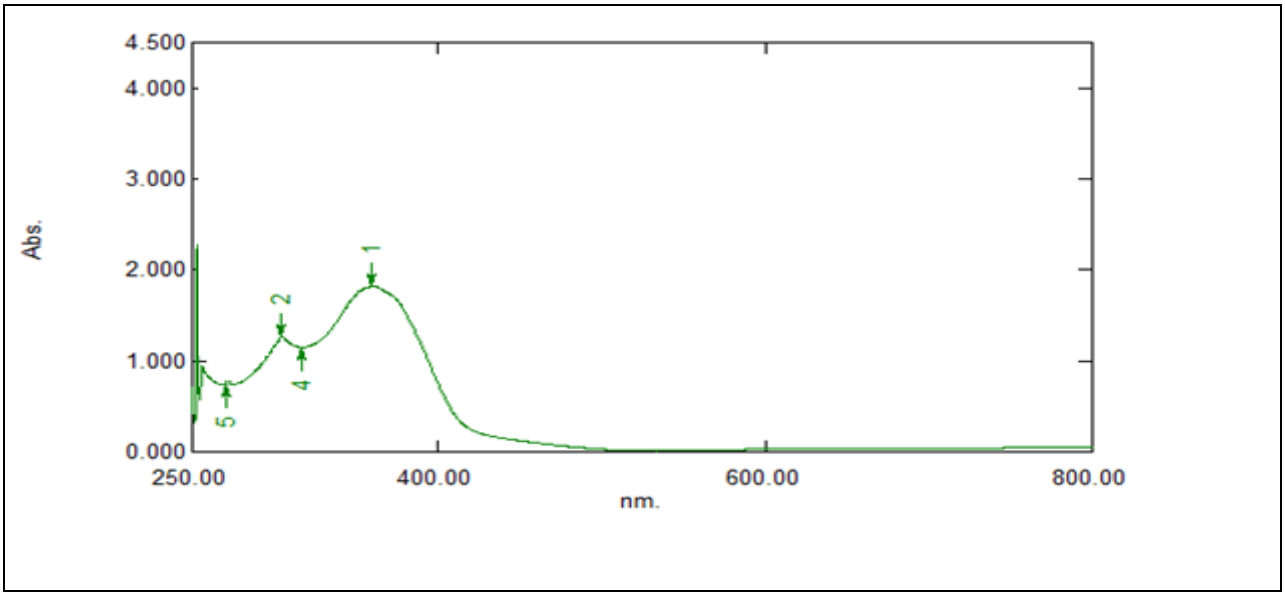

Figure (3-33) Electronic Spectra of Iron Complex [Fe (HL_4) $_2$]

3.7 Nuclear Magnetic Resonance Spectrum

The nuclear magnetic Resonance phenomenon is one of the physical phenomena that depend on the quantum mechanical magnetic properties of the nucleus of an atom. Nuclear magnetic resonance is used to indicate a group of scientific methodologies and techniques [130].

This phenomenon is used to study molecules in terms of structure and configuration. The phenomenon mainly depends on the fact that all atomic nuclei that have an odd number of protons or neutrons have an intrinsic magnetic moment and angular momentum. The most common nucleus used in these techniques is the nucleus of the hydrogen ^{1}H atom as it is the most abundant isotope of hydrogen in nature [131]. Each molecule shows several adsorbents that express the electronic environments surrounding each nucleus, which determine the type of bond and the other atoms attached to this nucleus. Therefore, this technique is considered one of the important techniques that use nuclear magnetic resonance analysis to identify the structural components of molecules [132].

The spectrum of the three ligands (HL_1, HL_3, and HL_4) was recorded in the DMSO-d^6 solvent. The first ligand (HL_1) showed a singlet peak at δ = 13.8 ppm

equivalent proton of the carboxylic acid hydroxyl O–H and at the site δ= (11.8) ppm a signal attributed to phenolic hydroxyl group [133]. The signal obtained at δ =8.2 ppm was assigned to singlet peak due to proton of imine group N=C–H [134]. The multiple signals obtained in the range δ= (6.5-7.8) ppm are due to aromatic hydrogen of carbons [135]. A doublet peak presented by the CO–CH group of the β-lactam ring appeared at the range δ = (2.5, 3.9) ppm S–CH group on the dihydrothiazine ring which was observed in the site δ= (2.8) ppm as a doublet peak. Also, a single pea that appeared at δ = (1.3) ppm could be attributed to methyl groups of 5-membered dihydrothiazine ring as shown in Figure (3-34).

The ^{1}HNMR spectrum of ligand (HL_3) in DMSO-d^6 showed a signal at the site δ= (9.9) ppm attributed to phenolic hydroxyl group signal [136]. The single peak obtained at δ= 8.2 ppm was due to proton of imine group CH=N in the ligand. This gives evidence of the formation of the imine group [137]. The multiple signals obtained in the range δ= (6.2-7.5) ppm are due to aromatic hydrogen of carbons [138]. A doublet peak presented by the CO–CH group of the β-lactam ring appeared at the range δ = (3.4, 3.6) ppm. Besides, the S–CH group on the dihydrothiazine ring was observed in the range δ= (2.5) ppm as doublet peak.

Lastly, a single peak that appeared at δ =1.57 ppm could be attributed to methyl groups of 5-membered dihydrothiazine rings as shown in Figure (3-35).

The ^{1}H-NMR spectrum of ligand (HL_4) showed a singlet peak at δ = (11.8) ppm equivalent proton of the carboxylic acid hydroxyl O–H [139]. The signal at the site δ= (9.6) ppm was attributed to the phenolic hydroxyl group signal [140]. The single peak obtained at δ= (8.4) ppm was due to proton of imine group CH=N in the ligand [141]. The multiple signals obtained in the range δ= (6.5-7.5) ppm are due to aromatic hydrogen of carbons [142]. The methyl groups of P-N, N -di methylbenzyldehyde appeared at δ= (3.2) ppm. The peak presented by the CO–CH group of the β-lactam ring also appeared at δ = (2.5) ppm. A single peak that appeared at δ = (1.3) ppm could be attributed to methyl groups of 5-membered dihydrothiazine rings as shown in Figure (3-36).

From this technique it can be dictated that Ligand behaved like un anion .

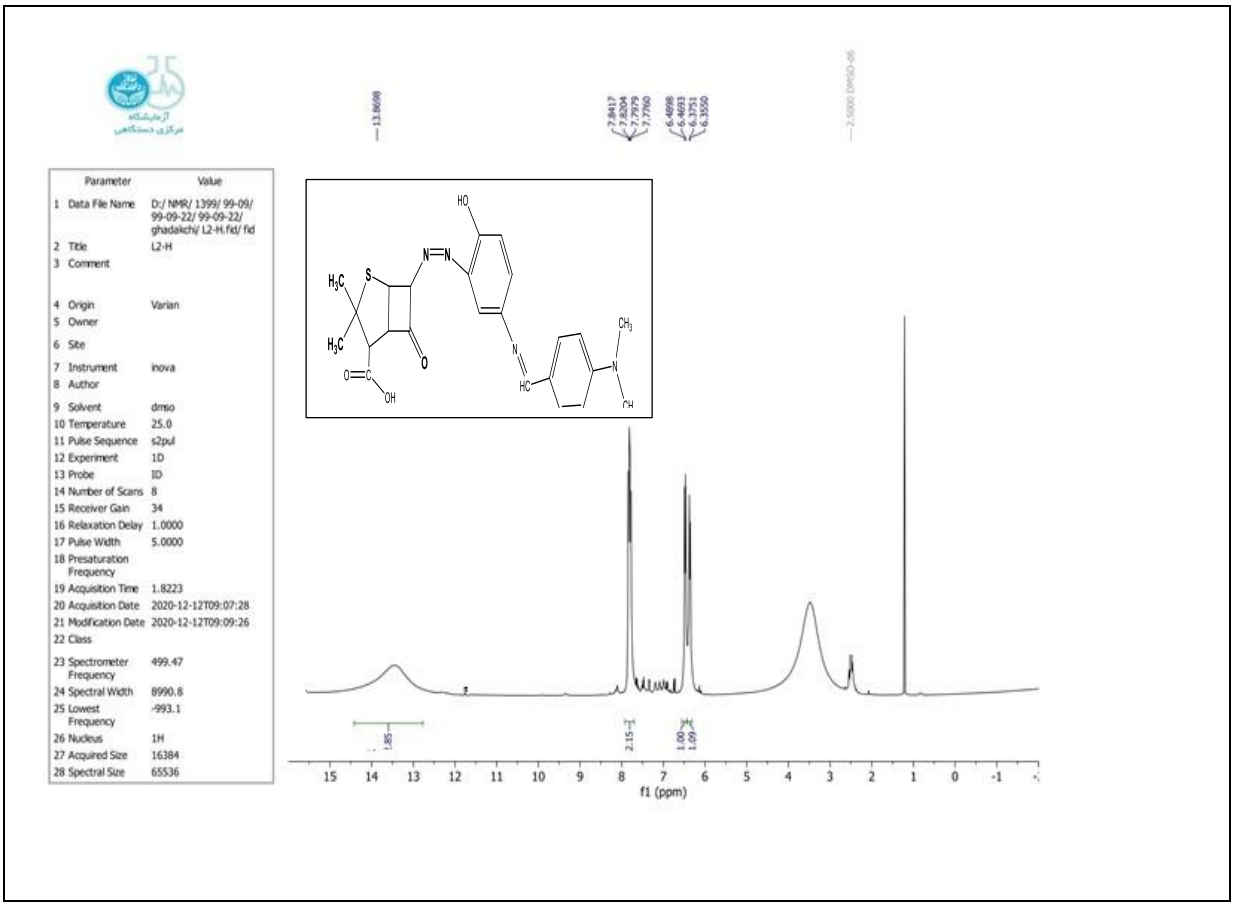

Figure (3-34) HNMR spectrum of HL_1 ligand

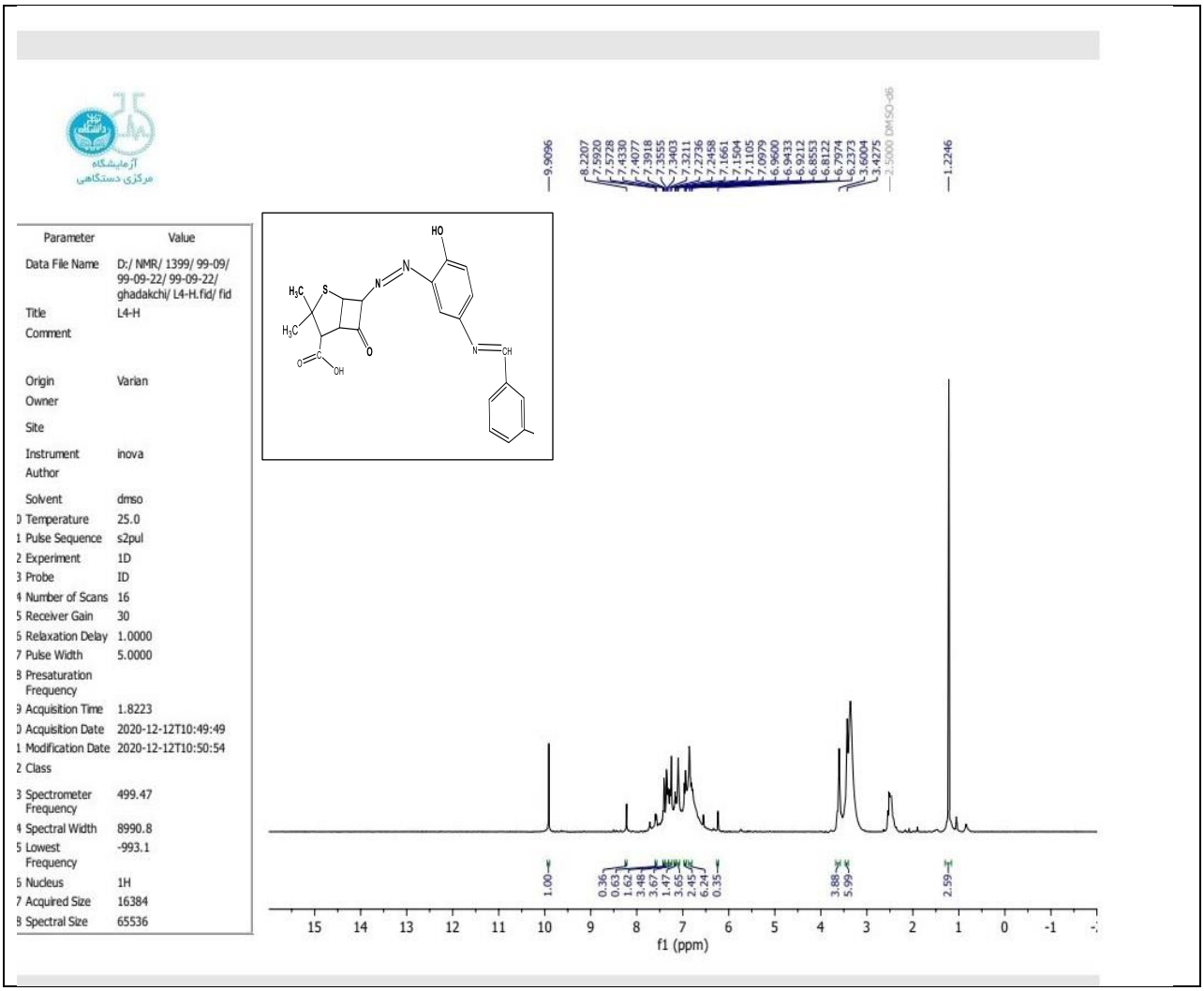

Figure (3-35) HNMR spectrum of HL_3 ligand

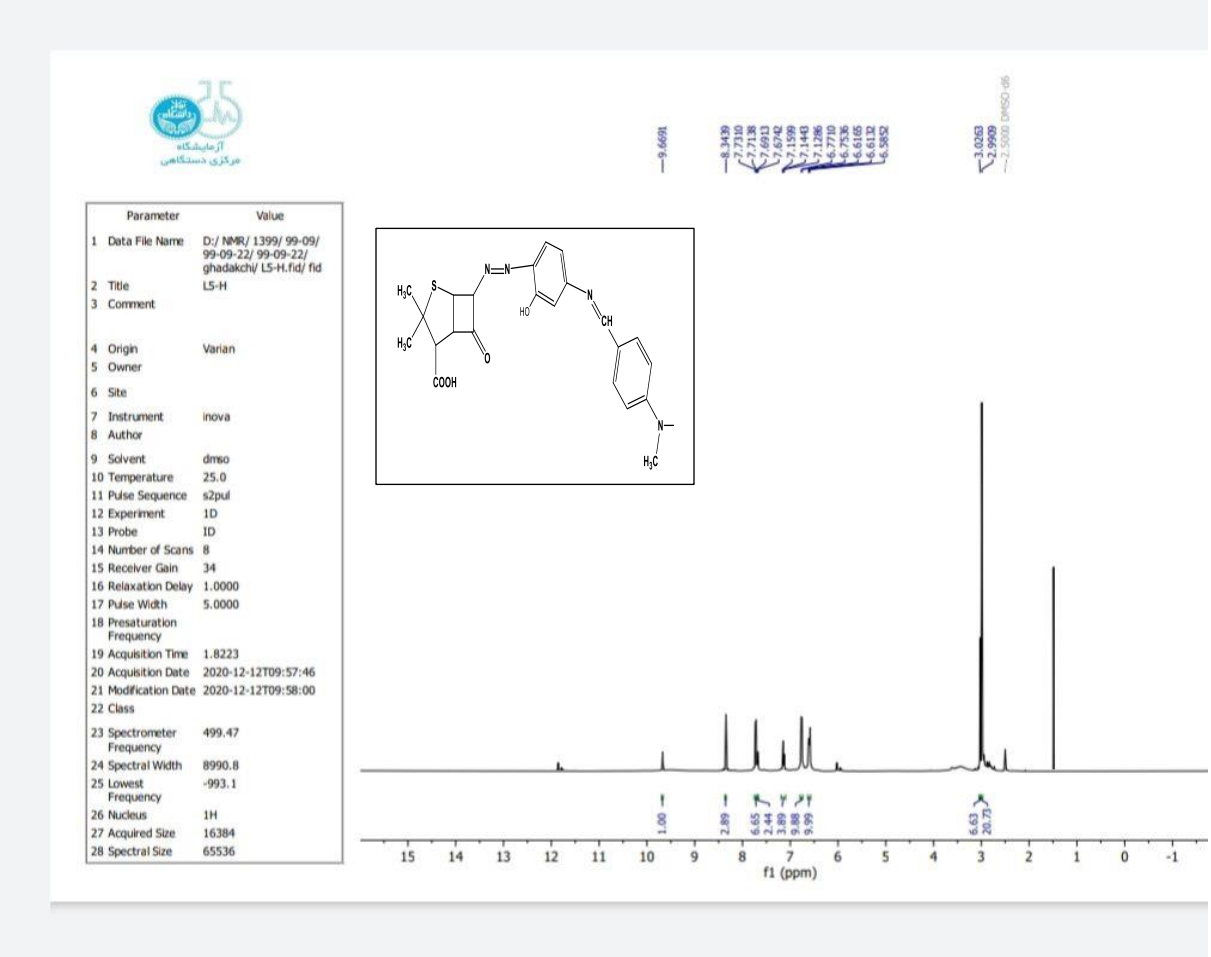

Figure (3-36) HNMR Spectrum of HL_4 Ligand

3.8 Mass Spectroscopy:

The mass spectrum differs from other technologies. According to this technique, the particles of the substance to be analyzed are passed out to a high amount of energy more than the energy required for the electronic transitions or vibrations to occur in UV-visible or infrared analysis [143]. The substance is bombarded by a beam of rapidly moving electrons, as this absorption energy leads to the separation of one or more electrons from the molecule, meaning the ionization process of the molecule takes place. Positive ions are formed in the original molecule along with breaking some of the weak bonds in the molecule, which leads to the formation of other small ions called fragments [144].

Due to the molecule's exposure to this tremendous energy resulting from a beam of electrons, several positive ions are formed that differ in mass (m) and charge (e).

Therefore, these ions are separated based on their difference in the ratio of mass to charge (m / e) using a magnetic field [145]. Results recorded as a mass spectrum showed the mass of these ions. In light of these recoded results, it is found that using a mass spectrometer depends on two basic processes that occur to the compound after being bombarded with a beam of electrons:

1. Ionization: it is the loss of one electron from the molecule, and a molecular ion is formed. The mass of this ion is equal to the mass of the molecule because the electron mass is very small and does not affect the molecular mass of the compound.
2. Fragmentation: it is when weak bonds in a molecular ion are broken into smaller fragment ions [146].

To prove the structural formula of organic ligands (HL_1), (HL_2), (HL_3), and (HL_4), the mass spectrum was recorded for them as shown in Figures (3-37), (3-38), (3-39), and (3-40), and the fragment patrons were (3-41), (3-42), (3-43), and (3-44). The molecular structures of ligands were exposed to be correct due to the appearance of peaks of the parent molecular ion at (465.4), (437.8), (437.4), and (465.5) (m / e). With a very high relative abundance, ligands have taken multiple fractionation paths, as the most important ligands are carbonyl, azo, and azomethine combined with the formation of positive molecular ions and other positively charged fractions [147]. From the previous, it can be confirmed from the composition of a ligand.

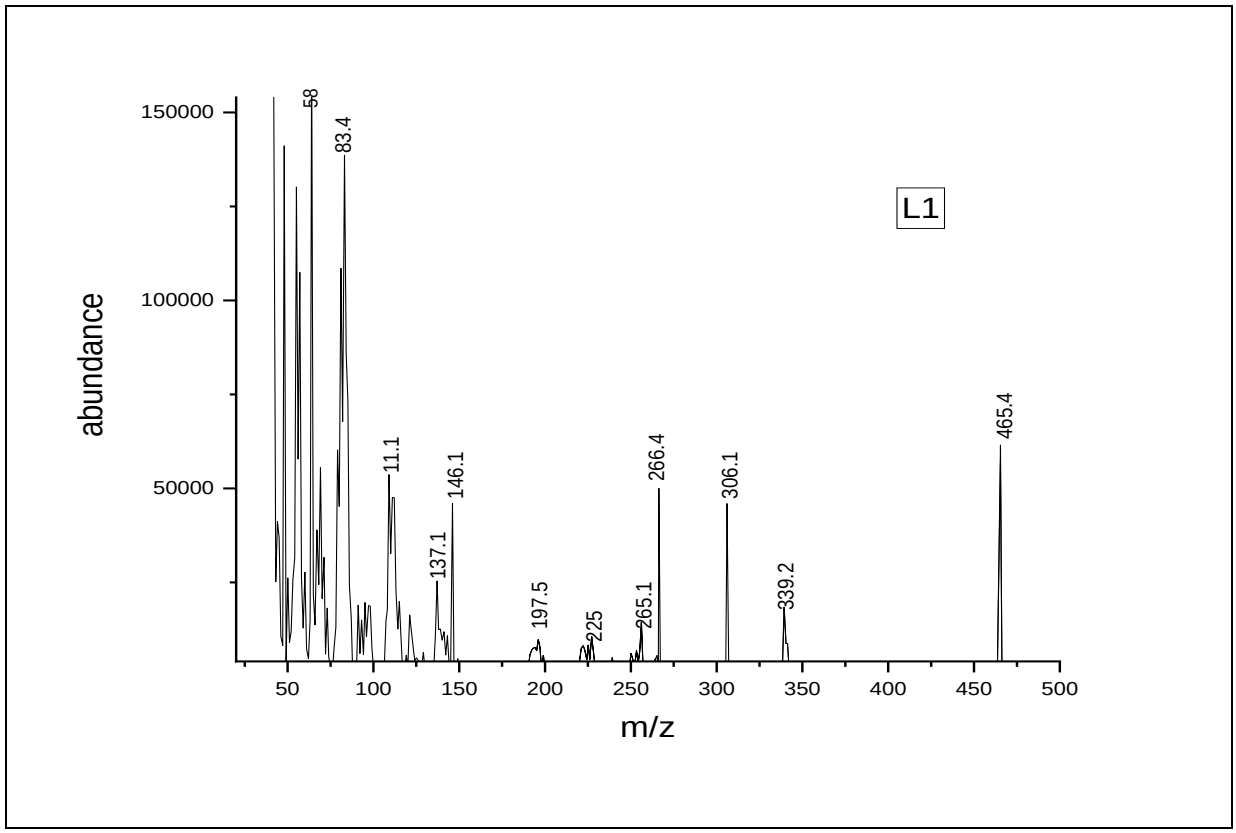

Figure (3-37) Mass Spectrum of Ligand (L1)

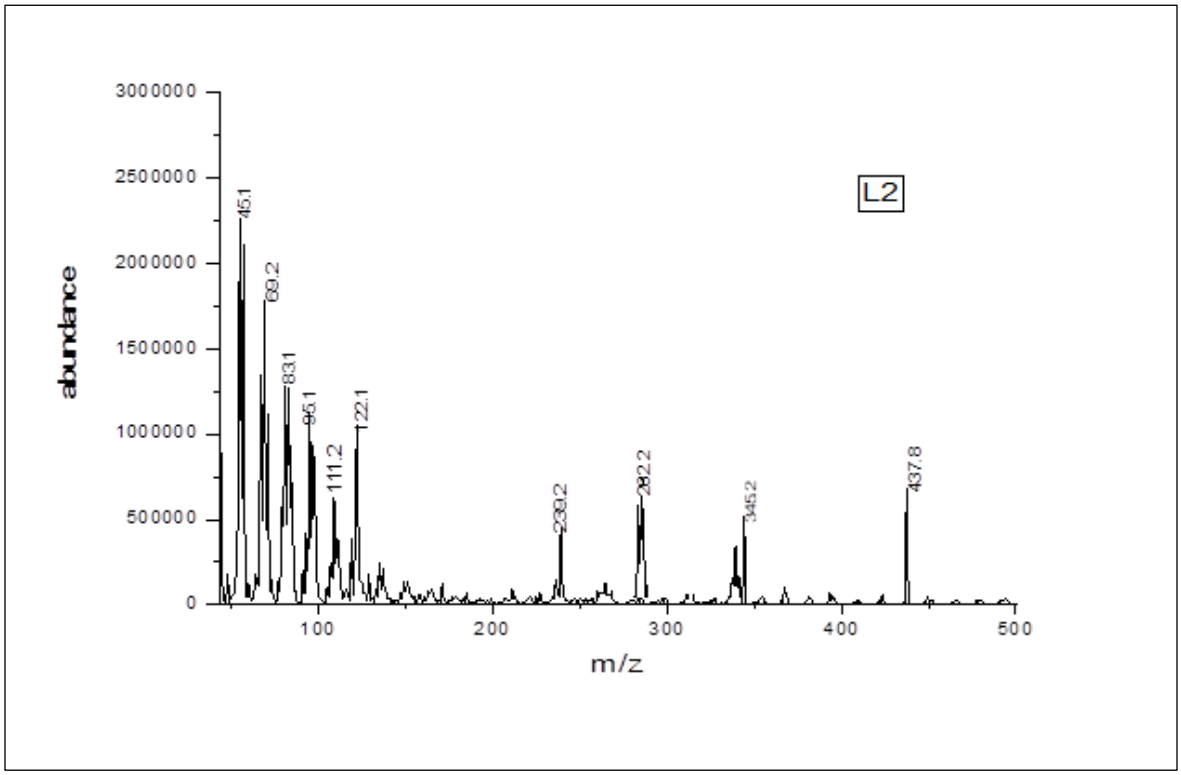

Figure (3-37) Mass Spectrum of Ligand (L2)

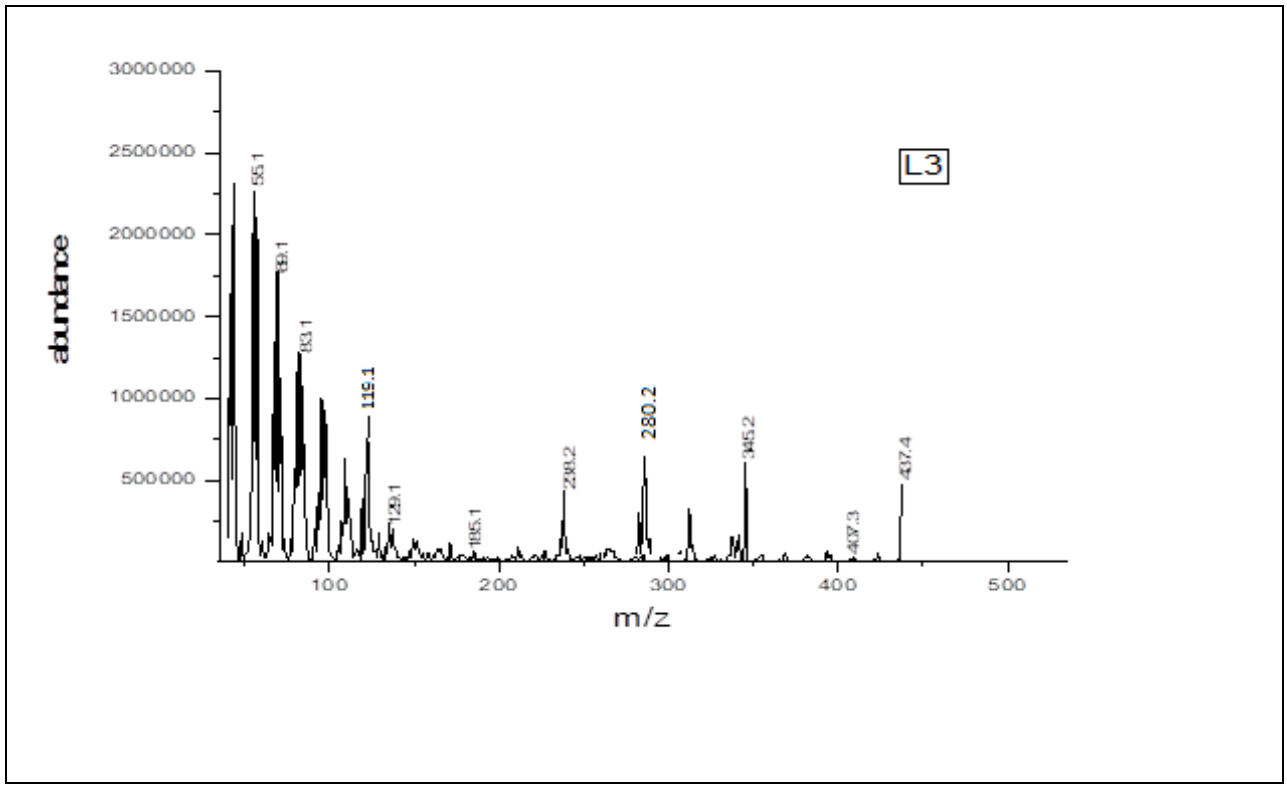

Figure (3-39) Mass Spectrum of Ligand (L_3)

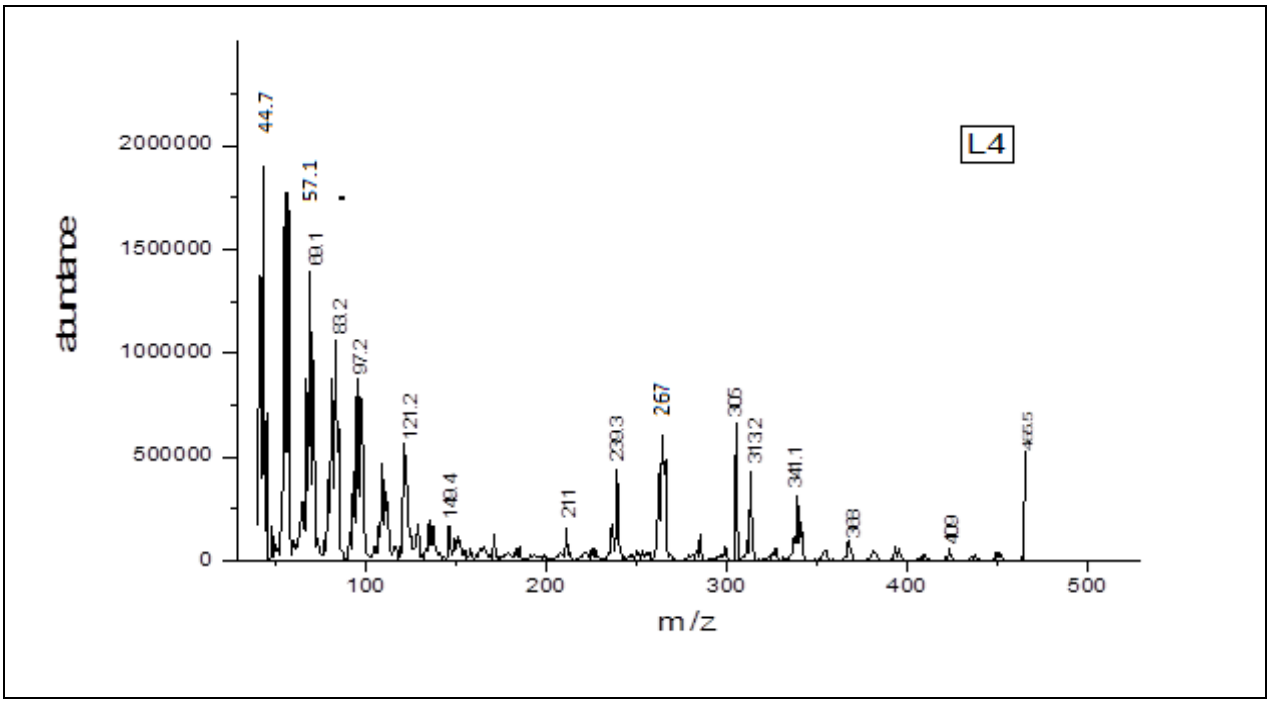

Figure (3-40) Mass Spectrum of Ligand (L_4)

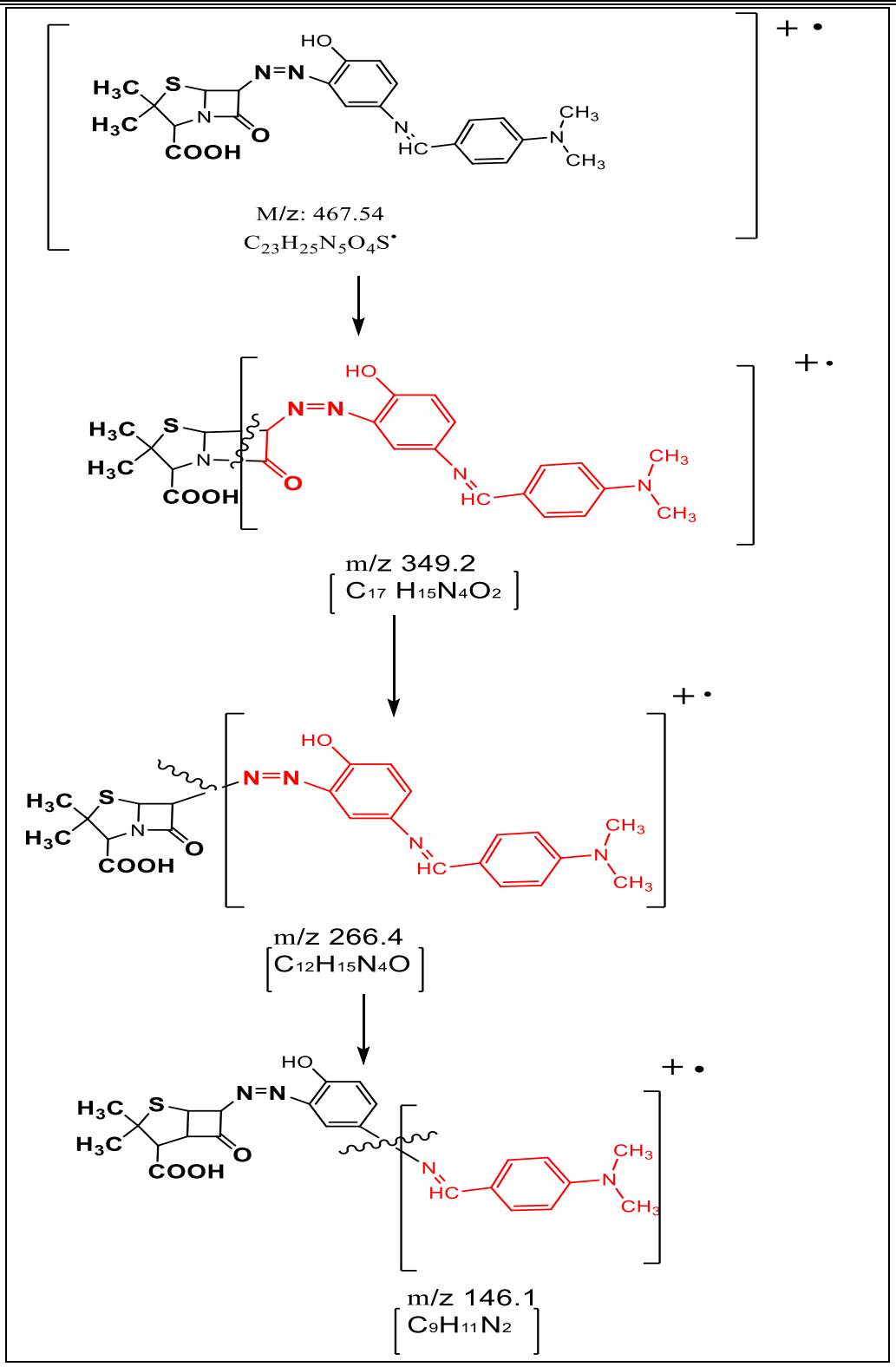

Figure (3-41) Fragmentation Pattern of Ligand (L_1)

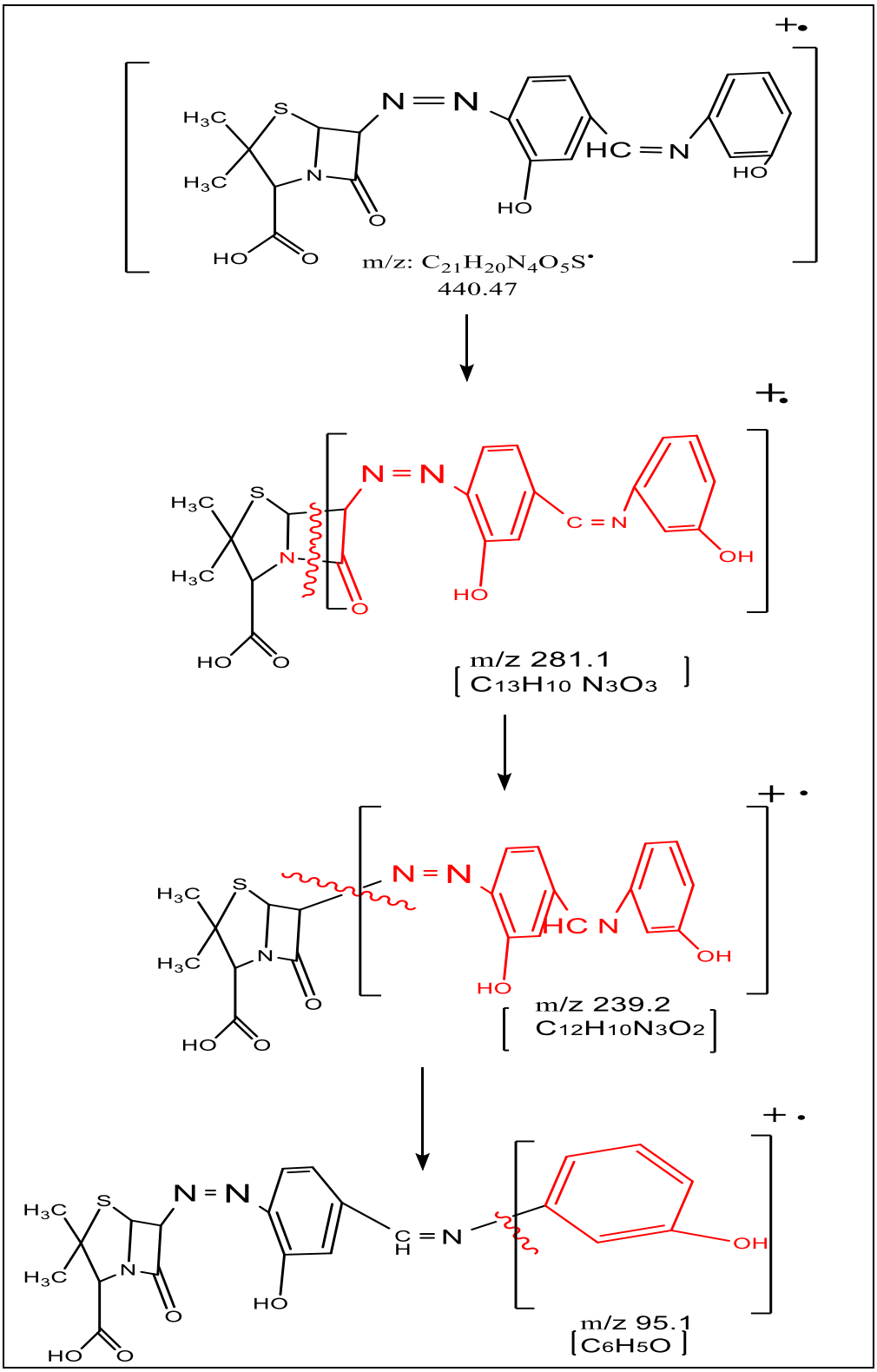

Figure (3-42) Fragmentation Pattern of Ligand (L_2)

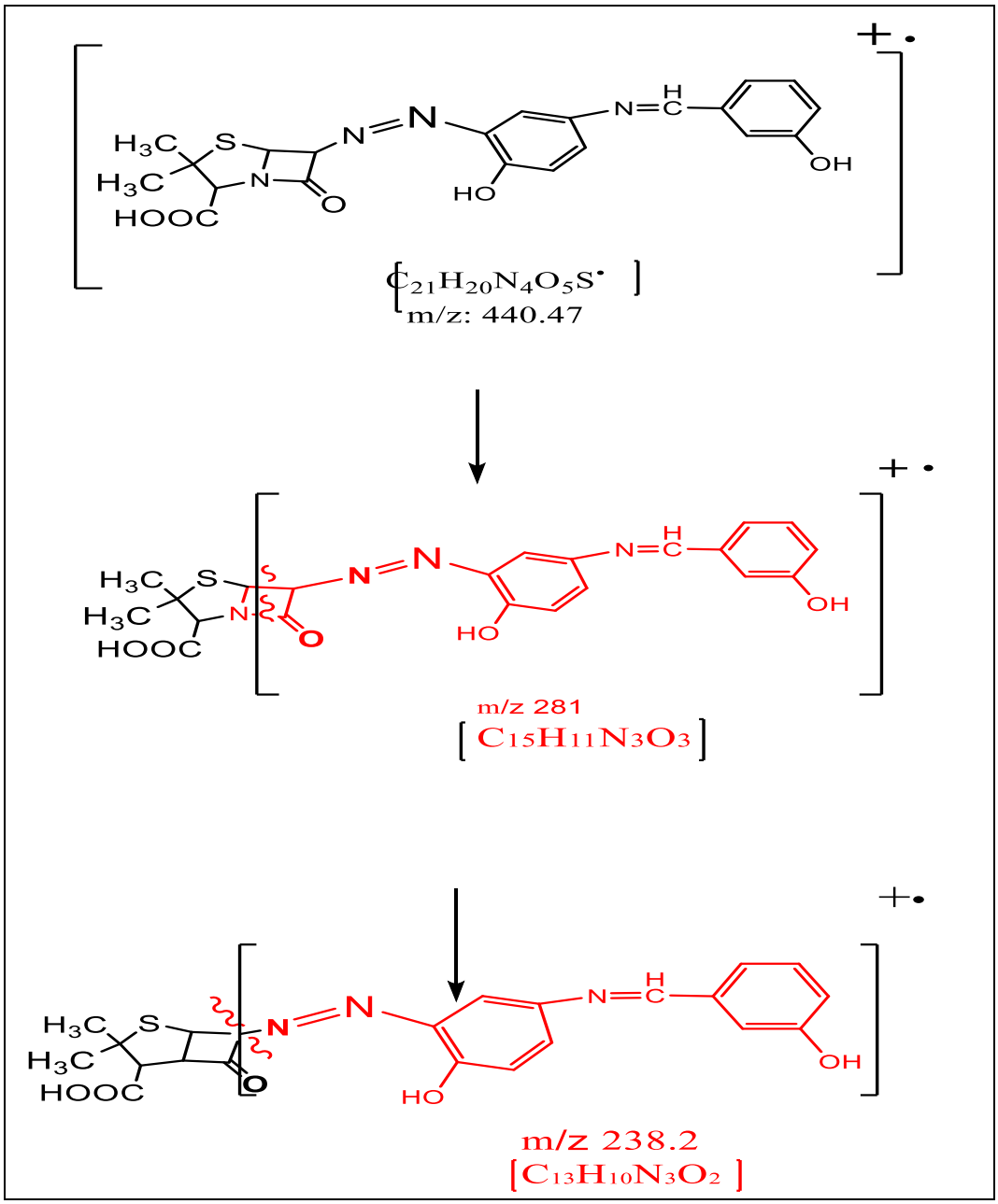

Figure (3-43) Fragmentation Pattern of Ligand (L_3)

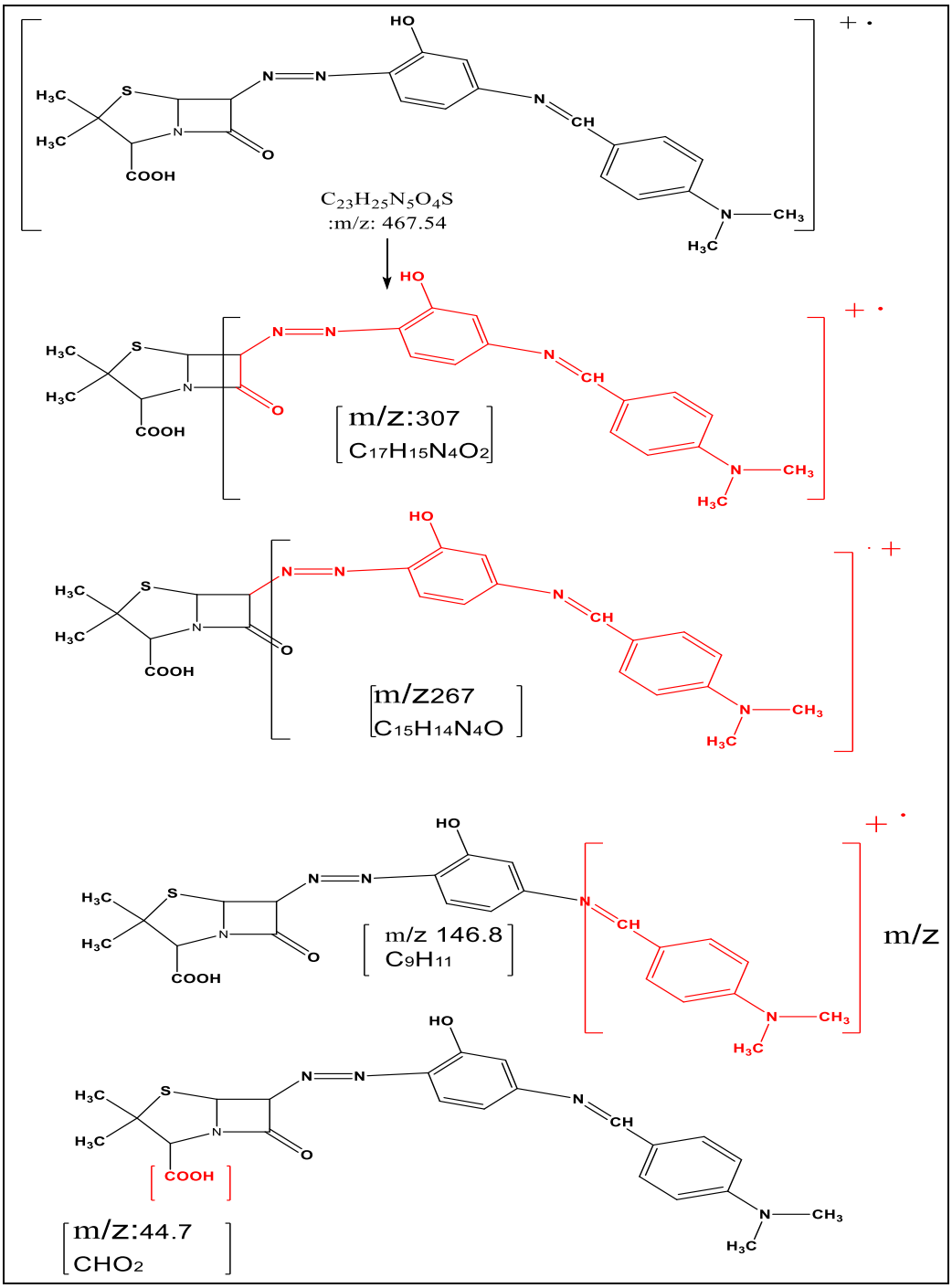

Figure (3-44) Fragmentation Pattern of Ligand (L_4)

3.9 Proposed Molecular Structures of Ligands Complexes:

The results of the analysis and measurement showed that the organic compounds used as ligands which are the subject of the study can be coordinated with metal ions through the oxygen atom of the hydroxyl of carboxyl group, carbonyl of lactam group, and nitrogen of azo group in the ligand (HL_1). The ligand (HL_2) is coordinated with the metal ion through carbonyl of lactam group, azo group, and hydroxyl of benzaldehyde. As for the third ligand, it was bound by the oxygen atom of the carboxylic hydroxyl group, oxygen atom of carbonyl group, and nitrogen atom of azo group. The ligand (HL_4) is coordinated with the metal ion through hydroxyl group, azo group, and azomethine group.

Accordingly, it can be said that the four molecules behave as tridentate ligands and negative ion. When these ligands were bond with metal ion, they formed 5-member ring with each of the first ligand (HL_1) and the second ligand (HL_2). They also formed 6-member ring with the third ligand (HL_3) and fourth ligand (HL_4). The suggestion of the spatial shapes can be gained through the following explanations:

3.9.1 Copper, Nickel and Iron Complexes Derived from Ligand (HL_1)

The infrared spectrum is a record shift of the carboxylic hydroxyl group, carbonyl of lactam group, and azo group. This is supported by the appearance of new metal-ligand peaks for both types M-N and M-O with all the metal complexes. As for molar conductivity, these values were recorded for the complexes (6.84, 15.4, 14.8, and S.mol $^{-1}$.cm ^{2}), respectively. The evidence that complexes exist in the form (1: 2) molar ratio lies in the fact that was no chlorine atom outside the coordination ball. The UV-visible spectrum played a key role in attaining the suggestion of the structural formula of the complexes through the displacement of peaks with the appearance of new peaks of electronic d-d transitions. From the magnetic susceptibility, the magnetic moments of copper, nickel, and iron complexes were found as follows: (1.83, 2.9, and 5.7 BM), respectively. The information obtained for the techniques used can be found at the octahedral shape for the complexes. Figure (3-45) shows the proposed spatial structure of the complexes.

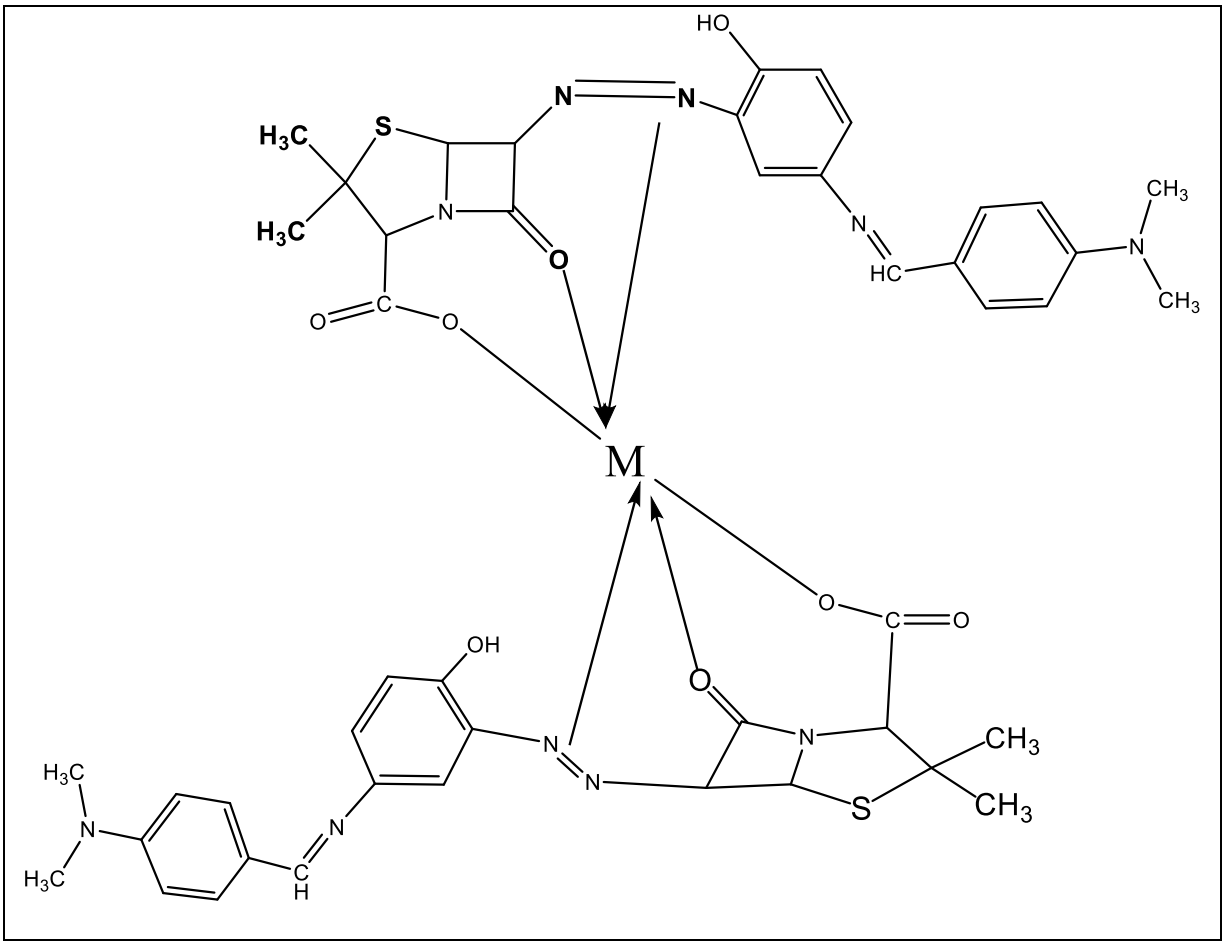

Figure (3-45) Structure Suggested of the Copper (II), Nickel (II), and Iron (II) Complex [M $(L_1)_2$]

3.9.2 Complexes of Copper, Nickel, and Iron of Ligand (HL_2)

The information obtained from infrared spectroscopy techniques showed that the band of hydroxyl, carbonyl of lactam, and azo was shifted to the lower wavelength such as complexes of copper, nickel, and iron respectively. It was also observed that the medium-strength bands which appeared were attributed to a metal-ligand bond of two types of bonds (M-N, M-O). Molar conductivity values indicated that the non-electrolyte solutions are equal to (11.1, 16, and 24.8 $S.mol^{-1}.cm^{2}$) which is equivalent to the (1:2) molar ratio. However, it indicates that there is no chlorine atom outside the coordination ball. When the UV-visible spectrum of complexes is compared with the ligand spectra, it showed redshift with the appearance of new peaks due to the d-d transitions. The magnetic moments were extracted equal to (1.8, 3.2, 5.4 BM, and Para magnetic) from the magnetic susceptibility values, respectively. Also, the atomic absorption supported the prepared structures of the

complexes. The information of the techniques showed that the octahedral complexes can be proposed. Figure (4-46) shows the suggested spatial structure of the complexes.

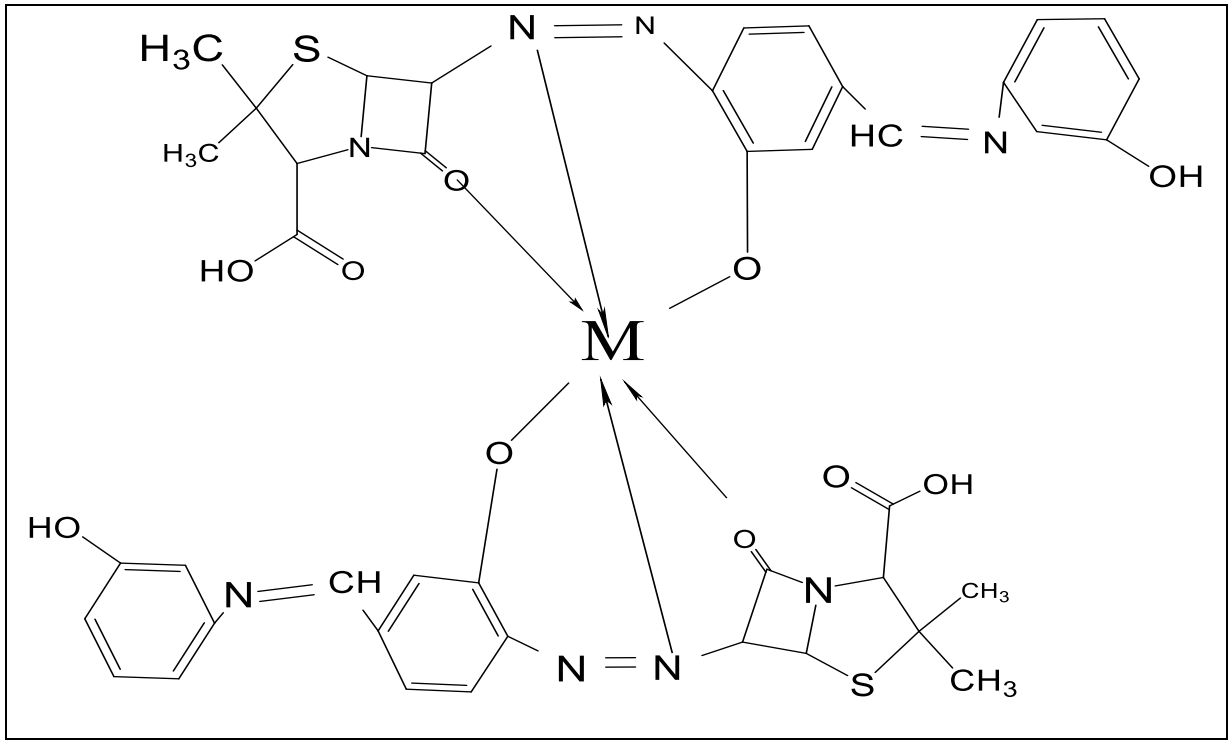

Figure (3-46) Structure Suggested of the Copper (II), Nickel (II), and Iron (II) complex [M $(L_2)_2$]

3.9.3 Copper, Nickel and Iron Complexes Derived from Ligand (HL_3)

The infrared spectrum is a record shift of the hydroxyl group and carbonyl of the lactam group, and azo group. This is supported by the appearance of new metal-ligand peaks for both types M-N and M-O with all the metal complexes. As for molar conductivity, these values were recorded (12.4, 15.3, 19.6) S.mol $^{-1}$.cm ^{2}) for the complexes, respectively. The evidence that complexes exist in the form (1: 2) molar ratio showed that there is no chlorine atom outside the coordination ball. The

UV-visible spectrum played a key role in attaining the suggestion of the structural formula of the complexes through the displacement of peaks with the appearance of new peaks of electronic d-d transitions. From the magnetic Susceptibility, the magnetic moments of copper, nickel, and iron complexes were found as follows: (1.7, 2.7, and 5.4) BM) respectively. The information obtained for the techniques used showed the attainment of the octahedral shape for the complexes. Figure (3-47) shows the proposed spatial structure of the complexes.

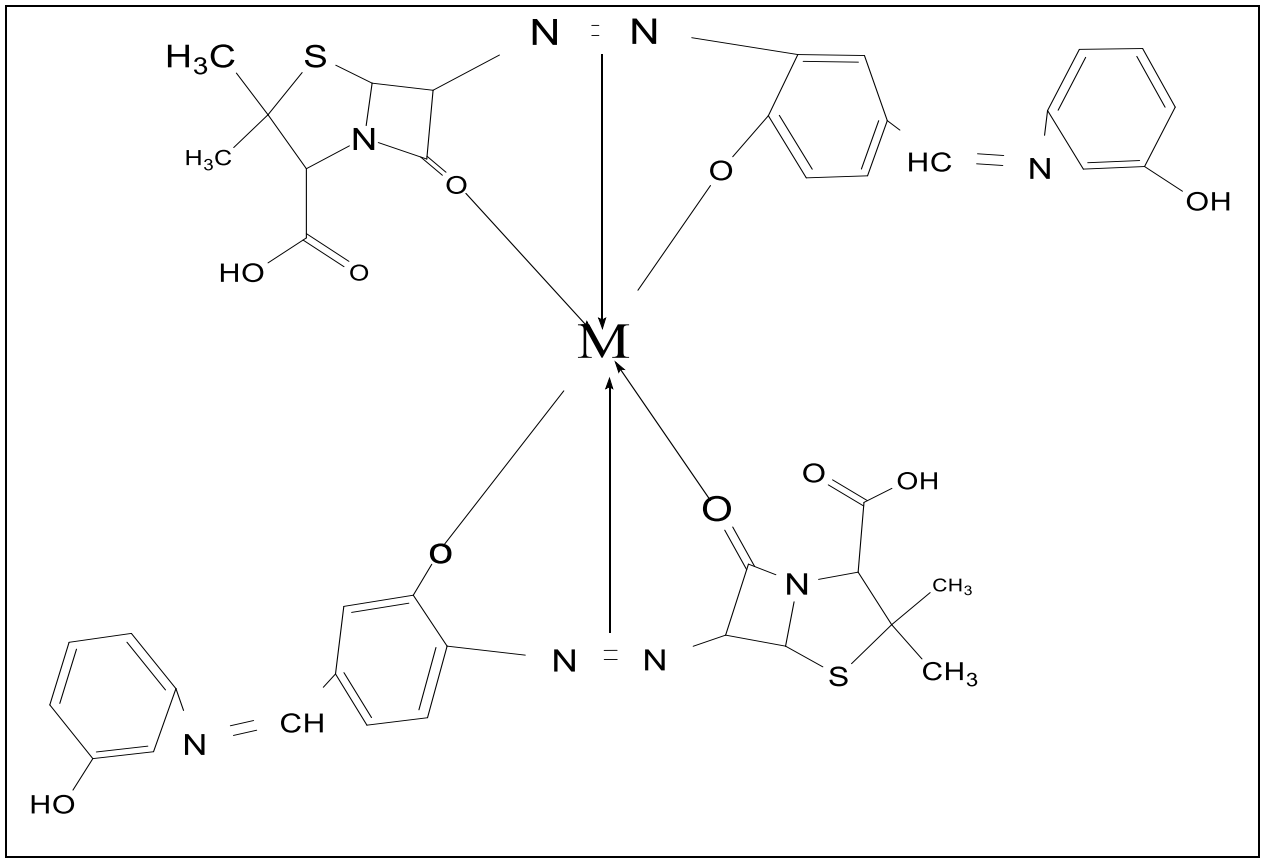

Figure (3-47) Structure Suggested of the Copper (II), nickel (II), and iron (II) complex [M $(L_3)_2$]

3.9.4 Complexes of Copper, Nickel, and Iron of Ligand (HL_4)

The information obtained from infrared spectroscopy techniques showed that the band of hydroxyl ,azo and azomethine was shifted to the higher wavelength such as copper, nickel, and iron, respectively. It was observed that the medium-strength bands, which appeared, were attributed to a metal-ligand bond of two types of bonds (M-N, M-O). Molar conductivity values also indicate that the non-electrolyte solutions are equal to (6.8, 15.2, 14.6 S.mol -1.cm 2) which is equivalent to the (1:2) molar ratio. However, there is no chlorine atom outside the coordination ball. When the UV-visible spectrum of complexes is compared with the ligand spectra, it showed redshift with the appearance of new peaks due to the d-d transitions. The magnetic moments were extracted equal to (1.69, 3.0, 5.6 BM, and Para magnetic) from the magnetic susceptibility values, respectively. Also, the atomic absorption supported the prepared structures of the complexes. The information of the previous techniques showed the octahedral complexes can be proposed. Figure (3-48) shows the suggested spatial structure of the complexes.

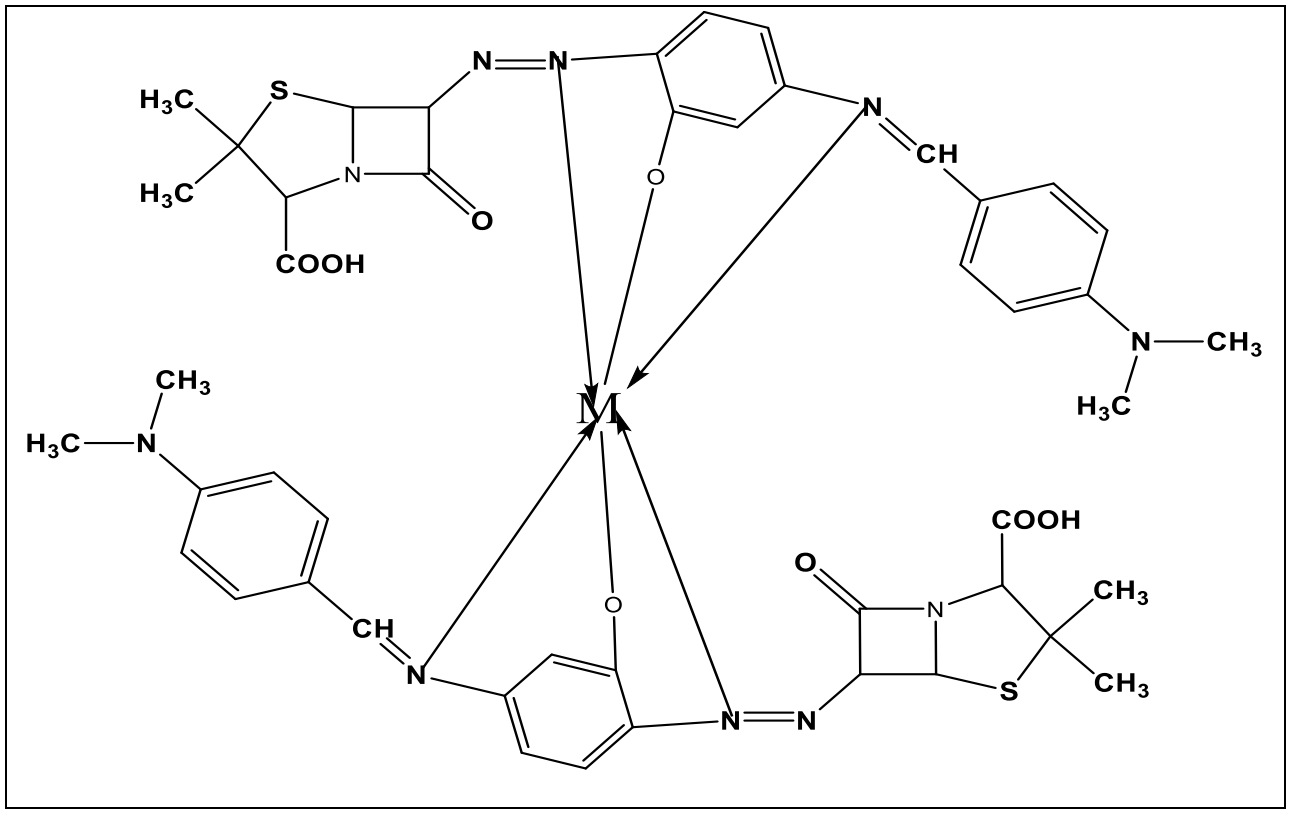

Figure (3-48) Structure Suggested of the Copper (II), Nickel (II), and Iron (II) complex [M $(L_4)_2$]

3.10 Biological Activity of Ligands and Complexes:

3.10.1 Determination of the Minimum Inhibition Concentration (MIC) for Ligand and Complexes

The Agar dilution method was used to detect MIC of the ligand and complexes. All compound solutions were diluted to obtain several concentrations ranging between 0.01 g/ml and 0.1 g/ml. The results of this study showed that the highest MIC of the solutions was 0.06 g/ml. However; it was 0.005 g/ml for the aqueous solution. This indicates that the Complexes solutions more have more biological activities than ligands as shown in table (3-8).

Table (3-8) Minimum Inhibition Concentration (MIC) for Ligand and Complexes

Name of pathogen	No	Comp	Minimum Inhibition Concentration MIC
	1	L_1	0.06
	2	$[Cu(L_1)_2]$	0.005
S.aureus	3	$[Ni(L_1)_2]$	0.02
	4	$[Fe(L_1)_2]$	_
	5	L_2	0.06
	6	$[Cu(L_2)_2]$	0.005
	7	$[Ni(L_2)_2]$	_
	8	$[Fe(L_2)_2]$	0.02
	9	L_3	0.04
	10	$[Cu(L_3)_2]$	0.04

	11	$[Ni(L_3)_2]$	0.04
	12	$[Fe(L_3)_2]$	_
	13	L_4	0.06
	14	$[Cu(L_4)_2]$	0.005
	15	$[Ni(L_4)_2]$	0.02
	16	$[Fe(L_4)_2]$	_

3.10.2 Antibacterial Activity of Ligands and Complexes

The ability of ligands and complexes to inhibit the growth of *S. aureus* bacteria was studied by agar's well diffusion method. The result clearly showed that the ligands and complexes were active against *S. aureus* bacteria in comparison to distilled water as a negative control. The antimicrobial property of the ligands (HL_1, HL_2, HL_3, and HL_4) and their complexes Cu(II), Ni (II), and Fe(II) metal ions was due to the specific properties of the azo-azomethine ligand that had donor atoms such as N, S, and O, where these structures can be found in various modes and bonding with metal ions. The minimum inhibitory concentration MIC for ligands and complexes was followed up. The results in Table (3-9) showed the minimum inhibitory concentration (MIC) g/ml of ligands and complexes. The inhibition zone diameter of S. aureus isolation for the ligands increased as the concentration of solution increased to reach 1.8cm against S. aureus in the high concentration of the solution 0.1 g/ml, but it was 1.0 cm only in low concentration 0.01 g/ml. As the inhibition zone diameter against S. aureus bacteria with the complex [Ni $(L_2)_2$] solutions was 3.0cm, This complex had more activity than other compounds due to reduction in the polarity of the metal ion by partial positive charge with donor groups,the [Cu $(L_2)_2$] showed that the inhibition zone was 1.9 cm. It also became apparent that the [Cu $(L_3)_2$] complex's diameter of inhibitory is 1.4 cm. Moreover, as the [Ni $(L_3)_2$] complex was equal to 1.5cm, the [Cu $(L_4)_2$] showed 2.4 cm, and [Ni $(L_4)_2$] was equal to 1.9cm. The complexes facilitate their diffusion through the lipid layer of spore membranes to the site of action, ultimately killing them by combining with OH groups of certain cell enzymes. The variation in the effectiveness of different biocidal agents against different organisms mainly depends on the impermeability of the cell. The hydrocarbon acts as a lipophilic group to drive the compound through the semipermeable membrane

of the cell. Likewise, Chelation mainly reduces the polarity of the central ion because of the partial sharing of its positive charge with the donor groups and possible π-electron delocalization within the whole chelate ring. This chelation

increases the lipophilic nature of the central atom which favors its permeation through the lipid layer of the membrane in the high and low concentration respectively [149], [150], and [151] as shown in Table (3-9) and Figures (3-49) and (3-50).

Table (3-9) Antibacterial Activity of Ligands and Complexes against *S. aureus* Bacteria

Name of pathogen	**No**	**Compound**	**Minimum Inhibition Zone (Cm)**
	1	**L_1**	**1cm**
	2	**$[Cu(L_1)_2]$**	**1cm**
	3	**$[Ni(L_1)_2]$**	**_**
	4	**$[Fe(L_1)_2]$**	**_**
	5	**L_2**	**1cm**
S.aureus.	**6**	**$[Cu(L_2)_2]$**	**1.9cm**
	7	**$[Ni(L_2)_2]$**	**3cm**
	8	**$[Fe(L_2)_2]$**	**1cm**
	9	**L_3**	**_**
	10	**$[Cu(L_3)_2]$**	**1.4cm**
	11	**$[Ni(L_3)_2]$**	**1.5cm**
	12	**$[Fe(L_3)_2]$**	**1cm**
	13	**L_4**	**_**
	14	**$[Cu(L_4)_2]$**	**2.4cm**

	15	**$[Ni(L_4)_2]$**	**1.9cm**
	16	**$[Fe(L_4)_2]$**	**_**

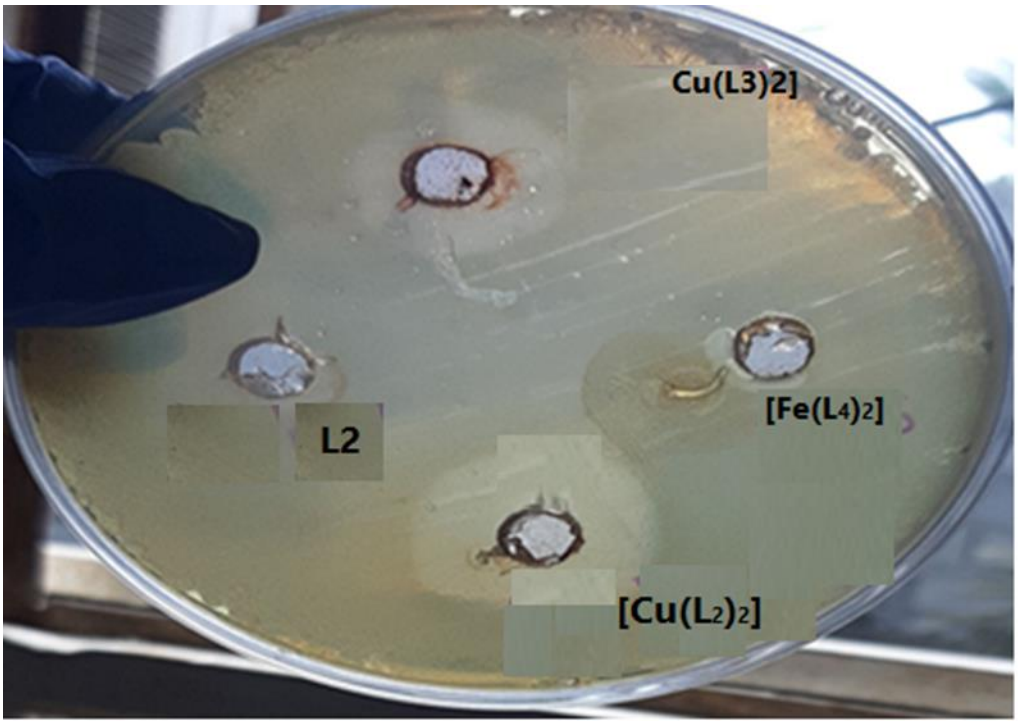

Figure (3-49) Inhibition Zone Diameter of Ligand and Complexes

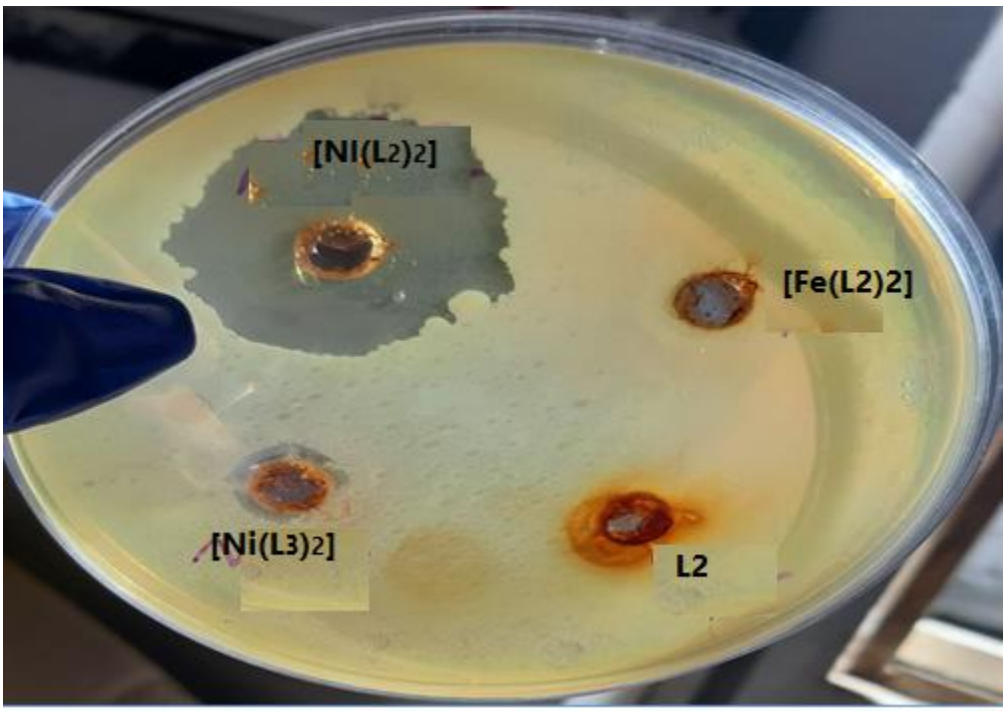

Figure (3-50) Inhibition Zone Diameter of Ligand and Complexes

3.10 .3 Effect of the Ligand and Complexes on Biofilm Formation

The *S. aureus* strain of bacteria was in detail studied to produce biofilm distinguished by its ability to produce virulence factors. The following figures showed the S. bacteria production of virulence factors after treatment with MIC from the prepared ligand and complexes. The current results obviously explained that these bacteria strains were active producers for these virulence factors after treating them with these bacterial suspensions, along with MIC of ligand and complexes. It is noted that S. aurous bacteria lost their capacity to provide these virulence factors (biofilm) after their treatment with the MIC bacteria as shown in Figures (3-51), (3-52),(3-53), (3-54), (3-55), (3-56), and (3-57) where the ligands (HL_1, HL_2, HL_3, and HL_4) and their complexes reduced the biofilm. Accordingly, this proposes that Chelation can make the complex's capacity decreases the virulence factor formation due to reduction in the polarity of the metal ion by partial positive charge with donor groups. The results of this study explained that ligand and complexes of the MIC solutions possess strong antibacterial activity against *S .aureus* biofilms.

Figure (3-51) Antibacterial Activity of $[Cu(L_1)_2]$ against *S .aureus* Biofilm

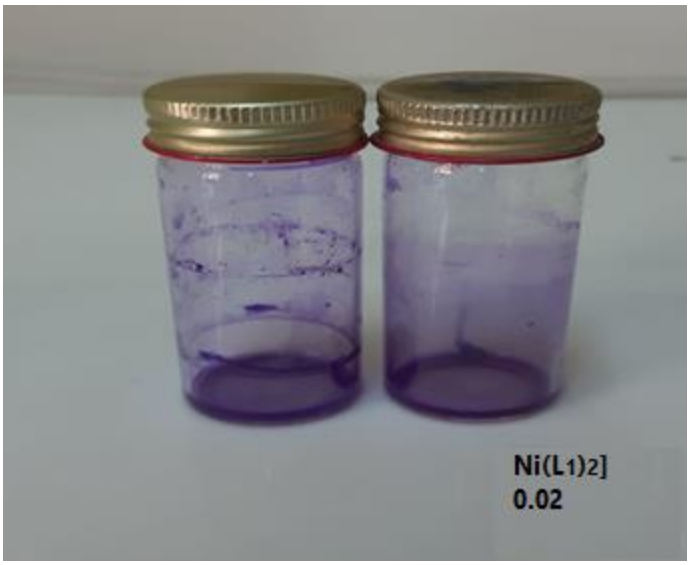

Figure (3-52) Antibacterial Activity of $[Ni(L_1)_2]$ against *S .aureus* Biofilm

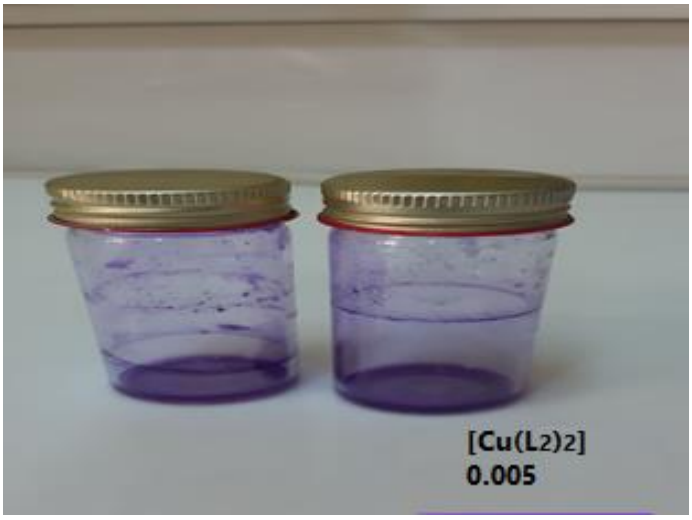

Figure (3-53) Antibacterial Activity of $[Cu(L_2)_2]$ against *S .aureus* Biofilm

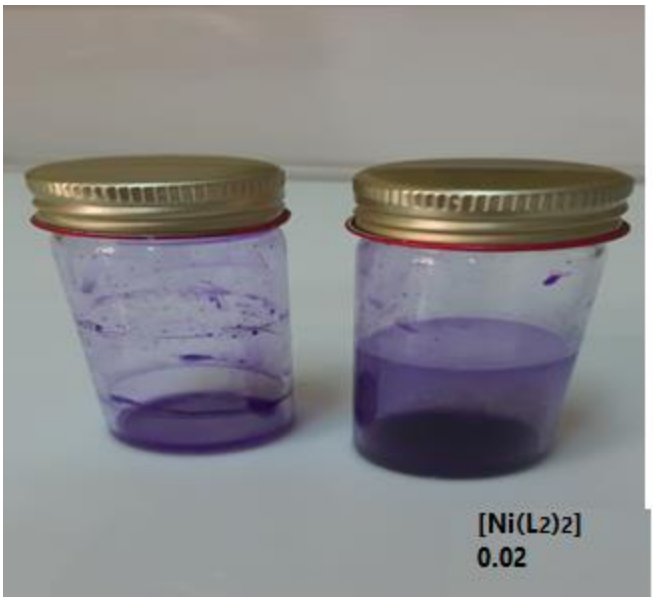

Figure (3-54) Antibacterial Activity of $[Ni(L_2)_2]$ against *S .aureus* Biofilm

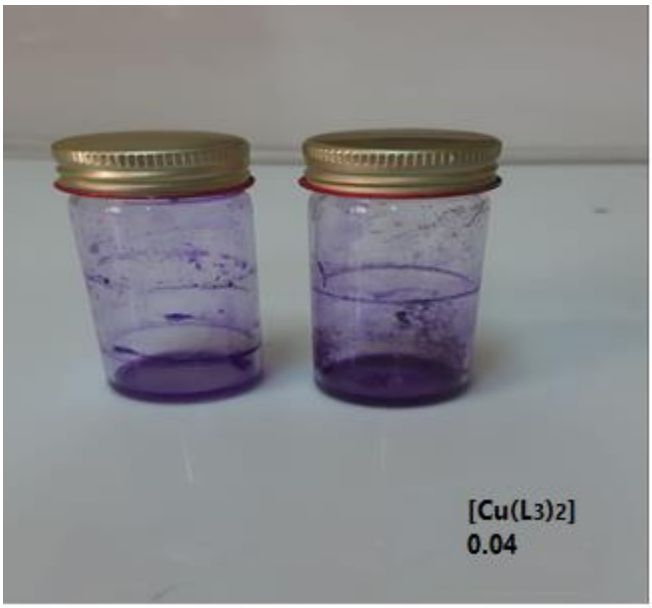

Figure (3-55) Antibacterial Activity against $[Cu(L_3)_2]$ *S .aureus* Biofilm

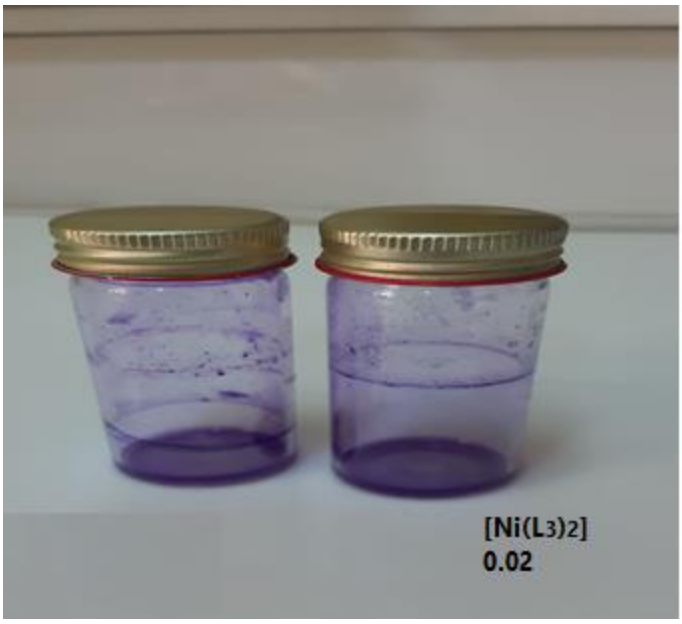

Figure (3-56) Antibacterial Activity $[Ni(L_3)_2]$against *S .aureus* Biofilm

Figure (3-57) Antibacterial Activity$[Fe(L_3)_2]$ against *S .aureus* Biofilm

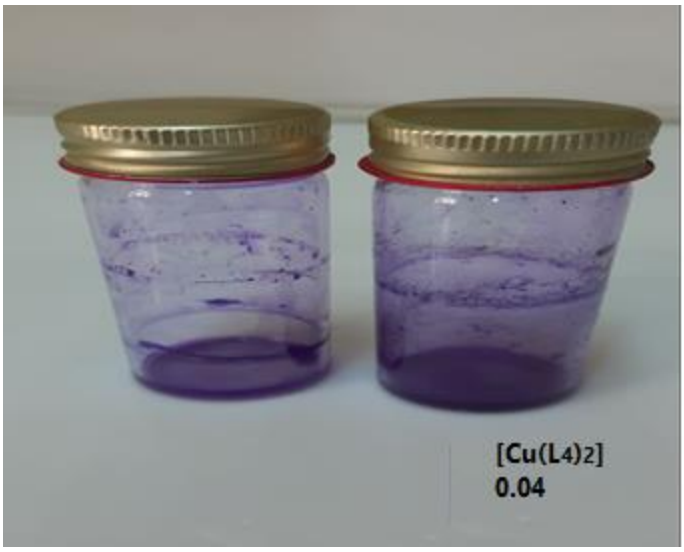

Figure (3-58) Antibacterial Activity $[Cu(L_4)_2]$against *S .aureus* Biofilm

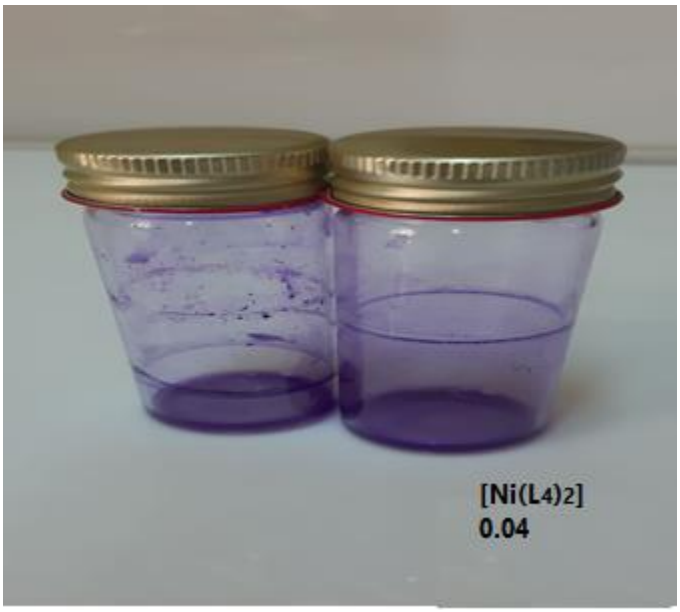

Figure (3-59) Antibacterial Activity $[Ni(L_4)_2]$against *S .aureus* Biofilm

3.10.4 Effect of the Ligand and Complexes on Hymolysin Formation

The results of this study explained that ligand and complexes of the MIC solutions possess strong antibacterial activity against *S .aureus* bacteria. The examined bacteria, which could produce the virulence factor (hemolysin), were treated with the (MIC) of $[Ni\ (L_2)_2]$ and $[Cu\ (L_3)_2]$, then the capacity of producing hemolysin

was assayed after the required incubation period with these MIC solutions. The results explained that the capacity of *S .aureus* bacteria to produce hemolysin toxin was good and effective. In detail, it partially lost its ability to produce hemolysin compared with the control due to reduction in the polarity of the metal ion by partial positive charge with donor groups [152] and [153] as shown in Figures (3-60) and (3-61).

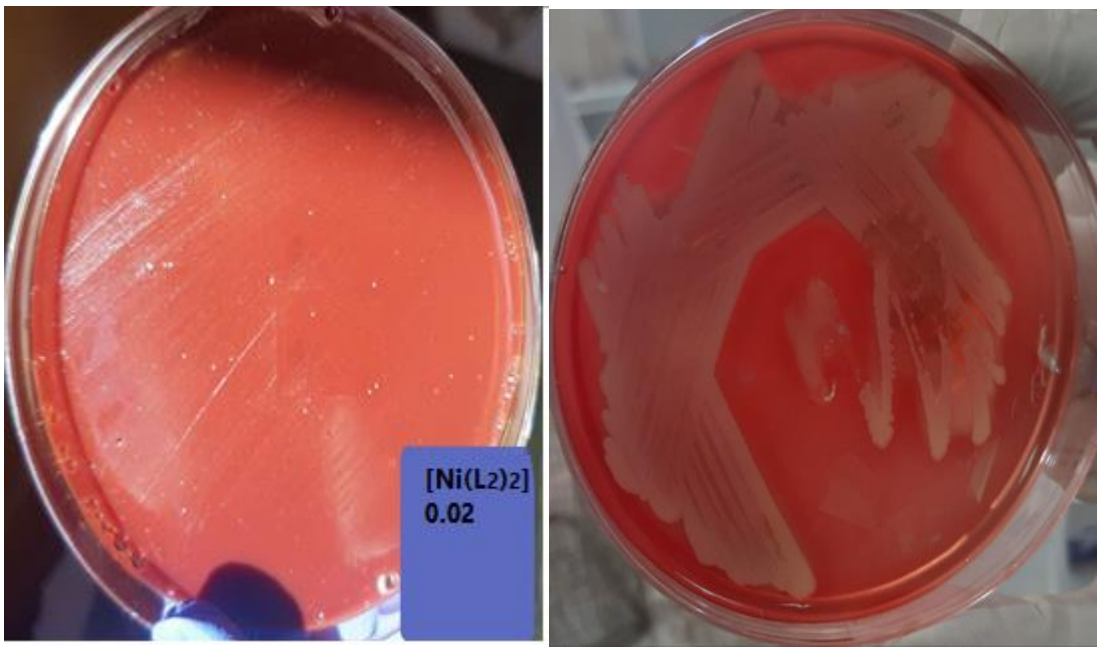

Figure (3-60) Effect of MIC of [Ni $(L_2)_2$]

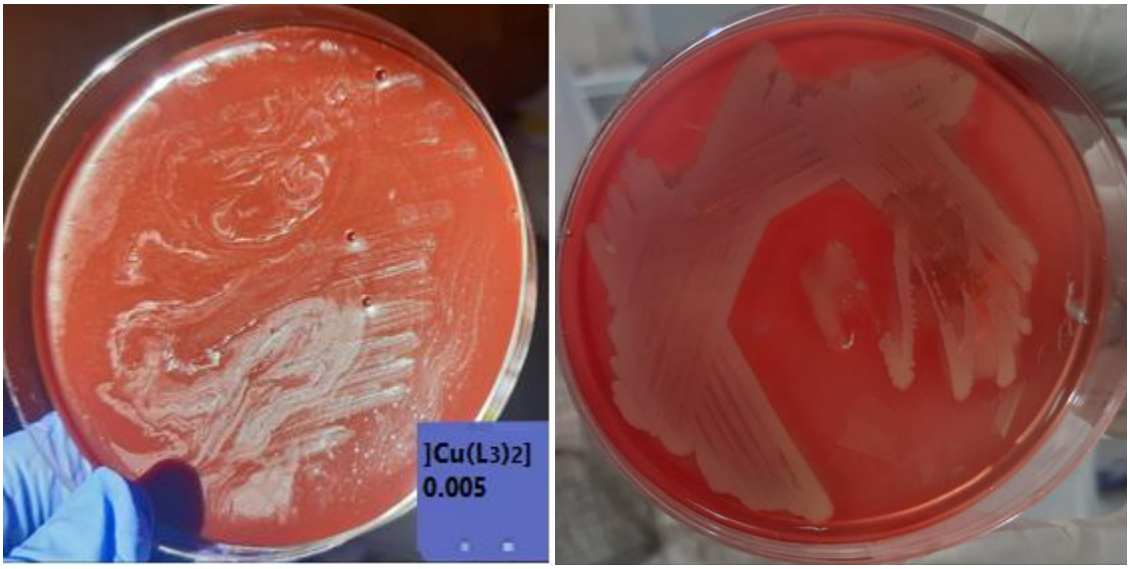

Figure (3-61) Effect of MIC of [Cu $(L_3)_2$]

3.11 Conclusion

In a nutshell, the current thesis presents the four new ligands prepared by the reaction of 6-amino penicillanic acid (6-APA) with Schiff bases to produce azo-azomethine ligands HL_1, HL_2, HL_3, and HL_4 respectively. the results of analyzes and measurement of organic compounds that uses as ligands can be co-ordinated with metal ions Through the oxygen atoms of the Hydroxyl ,carboxylic hydroxyl groups ,carbonyl of lactam group and nitrogen atom of the azo , azomethine groups, where the ligands acts as a tridentate ligands to form the octahedral shape complexes with sp^3d^2, d^2sp^3 hybridization were The prepared ligands and there complexes, the newly prepared ligands and their demonstrated a good inhibitory ability towards the (*Staphylococcus aureus*) bacteria. Also, the presence of the metal ions in the complexes reduces the biofilm & hemolysin enzyme. Thus, the prepared compounds could be good replacements for the public drugs used in the treatment of ulcers and other related diseases.

3.12 Suggestion for future work:

1. Synthesis of new Schiff base derivatives using different aldehydes.
2. Synthesis of new sets of complexes for all ligands using other set of metal
3. Evaluation of antibacterial activity of synthesized compounds in vivo
4. Evaluation of antibacterial of synthesized compounds activity against (Gram Positive and Gram Negative).
5. Isolation and identification of *S.aurues* bacteria from Ulcers then determine the effect of ligand and complexes on isolated bacteria .
6. Evaluation of cytotoxic effect, in study of interaction with various biological systems.

References

References

1. Drew, M. G. Structures of high coordination complexes. Coordination Chemistry Reviews, 24(2-3), 179-275. (1977).
2. Wells, A. F. Structural inorganic chemistry. Oxford university press. (2012).
3. Garnovskii, A. D., & Kharissov, B. I. (Eds.). Synthetic coordination and organometallic chemistry. CRC Press. (2003).
4. Gispert, J. R. Coordination chemistry (Vol. 483). Weinheim: Wiley-VCH. (2008).
5. Davies, J. A. Synthetic coordination chemistry: principles and practice. World Scientific. (1996).
6. Xavier, A., & Srividhya, N. (Synthesis and study of Schiff base ligands. IOSR Journal of Applied Chemistry, 7(11), 06-15. (2014).
7. M,Radi, M. F., Husain, S. S., Zaki, A. N. M., Sultan, A. A., Hamed, W. M., & Khamis, W. M. Synthesis and Characterization of some new Schiff base Compounds derived from 4-Amino benzoic acid and study their Biological activity. Research Journal of Pharmacy and Technology, 12(5), 2207-2212. (2019).
8. Schiff, H. Mittheilungen aus dem Universitätslaboratorium in Pisa: eine neue Reihe organischer Basen. Justus Liebigs Annalen der Chemie, 131(1), 118-119. (1864).
9. Ambika, S., Manojkumar, Y., Arunachalam, S., Gowdhami, B., Sundaram, K. K. M., Solomon, R. V., ... & Sundararaman, M. Biomolecular interaction, anti-cancer and anti-angiogenic properties of cobalt (III) Schiff base complexes. Scientific reports, 9(1), 1-14. (2019).
10. Cordes, E. H., & Jencks, W. P. On the mechanism of Schiff base formation and hydrolysis. Journal of the American Chemical Society, 84(5), 832-837. (1962).
11. El-Ajaily, M. M., Maihub, A. A., Mahanta, U. K., Badhei, G., Mohapatra, R. K., & Das, P. K. Mixed ligand complexes containing schiff bases and their biological activities: a short review. Rasayan J. Chem, 11(1), 166-174. (2018).
12. Qin, W., Long, S., Panunzio, M., & Biondi, S. Schiff bases: A short survey on an evergreen chemistry tool. Molecules, 18(10), 12264-12289. (2013).

13. . Gao, X., Wang, P., Wang, Q., Chen, J., & Lei, A. Electrochemical oxidative annulation of amines and aldehydes or ketones to synthesize polysubstituted pyrroles. Green Chemistry, 21(18), 4941-4945. (2019).
14. Langa, F., de la Cruz, P., de la Hoz, A., Díaz-Ortiz, A., & Díez-Barra, E. Microwave irradiation: more than just a method for accelerating reactions. Contemporary organic synthesis, 4(5), 373-386. (1997).
15. Gedye, R., Smith, F., Westaway, K., Ali, H., Baldisera, L., Laberge, L., & Rousell, J. Tetrahedron Lett 27: 279; b) Giguere RJ. Bray TL, Duncan SM, Majetich G Tetrahedron Lett, 27, 4945. (1986)
16. Priecel, P., & Lopez-Sanchez, J. A. Advantages and limitations of microwave reactors: From chemical synthesis to the catalytic valorization of biobased chemicals. ACS Sustainable Chemistry & Engineering, 7(1), 3-21. (2018).
17. Alhaidry, W. A. A. H., & Jamel, H. O. Synthesis and characterization of new benzothiazole-derived ligand and its complexes with some transitional metal ions with evaluation of their biological activities. Journal of Pharmaceutical Sciences and Research, 10(12), 3241. (2018).
18. Li, C. H., & Zuo, J. L. Self-Healing Polymers Based on Coordination Bonds. Advanced Materials, 1903762. (2019).
19. Wu, X., & Tamm, M. Transition metal complexes supported by highly basic imidazolin-2-iminato and imidazolin-2-imine N-donor ligands. Coordination Chemistry Reviews, 260, 116-138. (2014).
20. Joseph, J., Nagashri, K., & Rani, G. A. B. Synthesis, characterization and antimicrobial activities of copper complexes derived from 4-aminoantipyrine derivatives. Journal of Saudi Chemical Society, 17(3), 285-294. (2013).
21. Malik, M. A., Dar, O. A., Gull, P., Wani, M. Y., & Hashmi, A. A. Heterocyclic Schiff base transition metal complexes in antimicrobial and anticancer chemotherapy. MedChemComm, 9(3), 409-436. (2018).
22. Rani, C. V., Kesavan, M. P., Haseena, S., Varatharaj, R., Rajesh, J., & Rajagopal, G. Bidentate Schiff Base Ligands Appended Metal (II) Complexes as Probes of DNA and Plasma Protein: In Silico Molecular Modelling Studies. Applied Biochemistry and Biotechnology, 1-18. (2020).

23. Azam, M., Al-Resayes, S. I., Trzesowska-Kruszynska, A., Kruszynski, R., Shakeel, F., Soliman, S. M. & Wabaidur, S. M. Zn (II) complex derived from bidentate Schiff base ligand: Synthesis, characterization, DFT studies and evaluation of anti-inflammatory activity. Journal of Molecular Structure, 1201, 127177. (2020).
24. Abdi, K., Nowroozi, A., Mansouri-Torshizi, H., & Malekmohammadi, R. A Zn (II) complex of tetraaza macrocyclic Schiff base ligand. Synthesis, characterization, its experimental and therotical interaction studies with CT-DNA and BSA. Nashrieh Shimi va Mohandesi Shimi Iran. (2020).
25. Ansari, K. R., Chauhan, D. S., Quraishi, M. A., Mazumder, M. A., & Singh, A. Chitosan Schiff base: an environmentally benign biological macromolecule as a new corrosion inhibitor for oil & gas industries. International Journal of Biological Macromolecules, 144, 305-315. (2020).
26. Liu, X., Manzur, C., Novoa, N., Celedón, S., Carrillo, D., & Hamon, J. R. Multidentate unsymmetrically-substituted Schiff bases and their metal complexes: Synthesis, functional materials properties, and applications to catalysis. Coordination Chemistry Reviews, 357, 144-172. (2018).
27. Liu, X., & Hamon, J. R. Recent developments in penta-, hexa-and heptadentate Schiff base ligands and their metal complexes. Coordination Chemistry Reviews, 389, 94-118. (2019).
28. Wei, Z., Liao, W. Q., Tang, Y. Y., Li, P. F., Shi, P. P., Cai, H., & Xiong, R. G. Discovery of an antiperovskite ferroelectric in [(CH3) 3NH] 3 (MnBr3)(MnBr4). Journal of the American Chemical Society, 140(26), 8110-8113. (2018).
29. Berhanu, A. L., Mohiuddin, I., Malik, A. K., Aulakh, J. S., Kumar, V., & Kim, K. H. A review of the applications of Schiff bases as optical chemical sensors. TrAC Trends in Analytical Chemistry, 116, 74-91. (2019).
30. Fakhari, A. R., Khorrami, A. R., & Naeimi, H. Synthesis and analytical application of a novel tetradentate N2O2 Schiff base as a chromogenic reagent for determination of nickel in some natural food samples. Talanta, 66(4), 813-817. (2005).
31. Wang, Y., Ma, Z. Y., Zhang, D. L., Deng, J. L., Chen, X., Xie, C. Z. & Xu, J. Y. Highly selective and sensitive turn-on fluorescent sensor for detection of Al3+ based on quinoline-base Schiff base. Spectrochimica Acta Part A: Molecular and Biomolecular Spectroscopy, 195, 157-164. (2018).

32. Ritter, E., Przybylski, P., Brzezinski, B., & Bartl, F. Schiff bases in biological systems. Current Organic Chemistry, 13. (2009).
33. Al-Khathami, N. D., Al-Rashdi, K. S., Babgi, B. A., Hussien, M. A., Arshad, M. N., Eltayeb, N. E., ... & Al-Jahdali, M. Spectroscopic and biological properties of platinum complexes derived from 2-pyridyl Schiff bases. Journal of Saudi Chemical Society, 23(7), 903-915. (2019).
34. Hamzah, M. A. M., Jebur, I. K., & Ahmed, A. K. Synthesis, Characterization and Biological Activity Evaluation of Some New Azo Derivatives from 2-Amino Benzothiazole and Their Derivatives. kirkuk university journal for scientific studies, 13(1), 212-227. (2018).
35. Zollinger, H. Color chemistry: syntheses, properties, and applications of organic dyes and pigments. John Wiley & Sons. (2003).
36. Hamzah, M. A. M., Jebur, I. K., & Ahmed, A. K. Synthesis, Characterization and Biological Activity Evaluation of Some New Azo Derivatives from 2-Amino Benzothiazole and Their Derivatives. kirkuk university journal for scientific studies, 13(1), 212-227. (2018).
37. Benkhaya, S., M'rabet, S., & El Harfi, A. Classifications, properties, recent synthesis and applications of azo dyes. Heliyon, 6(1), e03271. (2020).
38. Hosseinnezhad, M., & Shaki, H. Investigation of photovoltaic properties of dye-sensitized solar cells based on azo dyes contain various anchoring groups. Pigment & Resin Technology. (2019).
39. Hakkou, K., Molina-Pinilla, I., Rangel-Núñez, C., Suárez-Cruz, A., Pajuelo, E., & Bueno-Martínez, M.Synthesis of novel (bio) degradable linear azo polymers conjugated with olsalazine. Polymer Degradation and Stability, 167, 302-312. . (2019).
40. Ali, Y., Hamid, S. A., & Rashid, U. Biomedical applications of aromatic azo compounds. Mini reviews in medicinal chemistry, 18(18), 1548-1558. (2018).
41. Al-Rubaie, L. A. A. R., & Mhessn, R. J. Synthesis and characterization of azo dye para red and new derivatives. Journal of Chemistry, 9(1), 465-470. (2012).
42. Çanakçı, D., & Serin, S. Synthesis of new azo dye polymers based on naphthol by oxidative polycondensation: antimicrobial activity and fastness studies. Journal of Polymer Research, 27(1), 1-23. (2020).

43. Rahman, M. M., Haque, T. M. A., Sourav, N. S., Rahman, S., Yesmin, S., Mia, R & Begum, K. Synthesis and investigation of dyeing properties of 8-hydroxyquinoline-based azo dyes. Journal of the Iranian Chemical Society, 1-10. (2020).
44. Au, W. W. Susceptibility of children to environmental toxic substances. International journal of hygiene and environmental health, 205(6), 501-503. (2002).
45. Al-Muhanaa, S. S., & Al-Khafagy, A. H. Preparation and Biological Activities of New Heterocyclic Azo Ligand and Some of Its Chelate Complexes. Nano Biomed. Eng, 10(1), 46-55. (2018).
46. Rana, M., Cho, H. J., Roy, T. K., Mirica, L. M., & Sharma, A. K. Azo-dyes based small bifunctional molecules for metal chelation and controlling amyloid formation. Inorganica chimica acta, 471, 419-429. (2018).
47. Pasha, C. Determination of paracetamol in pharmaceutical samples by spectrophotometric method. Eclética Química Journal, 45(3), 37-46. (2020).
48. Sarkar, S., Banerjee, A., Halder, U., Biswas, R., & Bandopadhyay, R. Degradation of synthetic azo dyes of textile industry: a sustainable approach using microbial enzymes. Water Conservation Science and Engineering, 2(4), 121-131. (2017).
49. Azam, M., Al-Resayes, S. I., Wabaidur, S. M., Altaf, M., Chaurasia, B., Alam, M. & Park, S. Synthesis, structural characterization and antimicrobial activity of Cu (II) and Fe (III) complexes incorporating azo-azomethine ligand. Molecules, 23(4), 813. (2018).
50. Sahan, F., Kose, M., Hepokur, C., Karakas, D., & Kurtoglu, M. New azo-azomethine-based transition metal complexes: Synthesis, spectroscopy, solid-state structure, density functional theory calculations and anticancer studies. Applied Organometallic Chemistry, 33(7), e4954. (2019).
51. Anwar, A., Shah, M. R., Muhammad, S. P., Ali, K., & Khan, N. A. Synthesis of 4-formyl pyridinium propylthioacetate stabilized silver nanoparticles and their application in chemosensing of 6-aminopenicillanic acid (APA). International Journal of Environmental Science and Technology, 16(3), 1563-1570. (2019).

52. Soleimanpour Moghadam, N., Azadmehr, A., & Hezarkhani, A. Extended release of 6-aminopenicillanic acid by silanol group functionalized vermiculite. Journal of Dispersion Science and Technology, 1-14. (2020).
53. Alabdali, A. J., Sabah, Y. H., & Mohsien, R. A. Synthesis, Characterization and Biological Evaluation of Penicillin Derivatives Complexes with Some Transition Metal Ions. Int. J. Curr. Microbiol. App. Sci, 5(12), 321-332. (2016).
54. Özdemir, Ö., Gürkan, P., Özçelik, B., & Oyardı, Ö. Synthesis and antimicrobial activities of new higher amino acid Schiff base derivatives of 6-aminopenicillanic acid and 7-aminocephalosporanic acid. Journal of Molecular Structure, 1106, 181-191. (2016).
55. Jasim, R. H., Said, M. H., & Ali, B. Q. Preparation, characterization and Biological Evaluation of β-lactam Derived from 6-Amino penicillinic Acid and Salicyldehyde. Pharm Anal Chem, 3, 125. (2017).
56. Xavier, A., & Srividhya, N. Synthesis and study of Schiff base ligands. IOSR Journal of Applied Chemistry, 7(11), 06-15. (2014).
57. Majeed, H., Al-Ahmad, A., & Hussain, K. The preparation, characterization and the study of the linear optical properties of a new azo compound. Journal of Basrah Researches ((Sciences)), 37(2). (2011).
58. Salehi, M., Rahimifar, F., Kubicki, M., & Asadi, A. Structural, spectroscopic, electrochemical and antibacterial studies of some new nickel (II) Schiff base complexes. Inorganica Chimica Acta, 443, 28-35. (2016).
59. Baron, E. J. Bailey and Scott's diagnostic microbiology. (2002).
60. Kateete, D. P., Kimani, C. N., Katabazi, F. A., Okeng, A., Okee, M. S., Nanteza, A., ... & Najjuka, F. C. Identification of Staphylococcus aureus: DNase and Mannitol salt agar improve the efficiency of the tube coagulase test. Annals of clinical microbiology and antimicrobials, 9(1), 1-7. (2010).
61. Sun, Z., Huang, S., Zhu, P., Yue, F., Zhao, H., Yang, M., ... & Xu, J. A microbiome-based index for assessing skin health and treatment effects for atopic dermatitis in children. Msystems, 4(4), e00293-19. (2019).
62. Collee, J. G., Mackie, T. J., & McCartney, J. E. Mackie & McCartney practical medical microbiology. Harcourt Health Sciences. (1996).
63. Kendall, R. J., Presley, S. M., Austin, G. P., & Smith, P. N. Advances in biological and chemical terrorism countermeasures. CRC Press. (2008).

64. Collee, J. G., Mackie, T. J., & McCartney, J. E. Mackie & McCartney practical medical microbiology. Harcourt Health Sciences. (1996).
65. Adwan, G., & Mhanna, M. Synergistic effects of plant extracts and antibiotics on Staphylococcus aureus strains isolated from clinical specimens. Asian Pacific Journal of Tropical Medicine, 2(3), 46-51. (2009).
66. Aiyegoro, O., Adewusi, A., Oyedemi, S., Akinpelu, D., & Okoh, A. Interactions of antibiotics and methanolic crude extracts of Afzelia Africana (Smith.) against drug resistance bacterial isolates. International journal of molecular sciences, 12(7), 4477-4487. (2011).
67. Saheed, Y., Nasir, M. U., Abbas, B., & Bello, R. Y. GC-MS Analysis and Antimicrobial Spectrum of Stem Bark Extracts of Ficus sycomorus. Microbiology Research Journal International, 118-128. (2020).
68. Mathur, T., Singhal, S., Khan, S., Upadhyay, D. J., Fatma, T., & Rattan, A. Detection of biofilm formation among the clinical isolates of staphylococci: an evaluation of three different screening methods. Indian journal of medical microbiology, 24(1), 25. (2006).
69. Buxton, R. Blood agar plates and hemolysis protocols. American Society for Microbiology, 1-9. (2005).
70. Porchia, M., Pellei, M., Del Bello, F., & Santini, C. Zinc Complexes with Nitrogen Donor Ligands as Anticancer Agents. Molecules, 25(24), 5814. (2020).
71. Malinowski, J., Zych, D., Jacewicz, D., Gawdzik, B., & Drzeżdżon, J. Application of Coordination Compounds with Transition Metal Ions in the Chemical Industry—A Review. International Journal of Molecular Sciences, 21(15), 5443. (2020).
72. Sorak, D., Herberholz, L., Iwascek, S., Altinpinar, S., Pfeifer, F., & Siesler, H. W. New developments and applications of handheld Raman, mid-infrared, and near-infrared spectrometers. Applied Spectroscopy Reviews, 47(2), 83-115. (2012).
73. Günzler, H., & Gremlich, H. U. IR spectroscopy. An introduction. (2002).
74. Kumar, S. Infrared spectroscopy: Method development and ligand binding studies (Doctoral dissertation, No Idea, Could be any). (2010).
75. Mahdi, S. M., & Ismail, A. K. Preparation and Identification of new azo-schiff base ligand (NASAR) and its divalent transition metal Complexes.

Journal of Pharmaceutical Sciences and Research, 10(9), 2175-2178. (2018).

76. Hassan, A., Macedo, L. J., de Souza, J. C., Lima, F. C., & Crespilho, F. N. A combined Far-FTIR, FTIR Spectromicroscopy, and DFT Study of the Effect of DNA Binding on the [4Fe4S] Cluster Site in EndoIII. Scientific reports, 10(1), 1-12. (2020).
77. Özdemir, Ö., Gürkan, P., Özçelik, B., & Oyardı, Ö. Synthesis and antimicrobial activities of new higher amino acid Schiff base derivatives of 6-aminopenicillanic acid and 7-aminocephalosporanic acid. Journal of Molecular Structure, 1106, 181-191. (2016).
78. Yousif, E., Majeed, A., Al-Sammarrae, K., Salih, N., Salimon, J., & Abdullah, B. Metal complexes of Schiff base: preparation, characterization and antibacterial activity. Arabian Journal of Chemistry, 10, S1639-S1644. (2017).
79. Naderi, F., Orojloo, M., Jannesar, R., & Amani, S. Synthesis and spectroscopic studies of an azo-azomethine receptor for naked-eye detection of hydrogen carbonate ions in aqueous media. Polycyclic Aromatic Compounds, 1-15. (2019).
80. Nagesh, G. Y., Raj, K. M., & Mruthyunjayaswamy, B. H. M. Synthesis, characterization, thermal study and biological evaluation of Cu (II), Co (II), Ni (II) and Zn (II) complexes of Schiff base ligand containing thiazole moiety. Journal of molecular structure, 1079, 423-432. (2015).
81. Sapna, K., Sharma, N. K., & Kohli, S. Synthesis, Characterization and Antimicrobial Studies of Copper (II) Complexes of Semicarbazone and Thiosemicarbazone of m-Hydroxy Benzaldehyde and p-Hydroxy Benzaldehyde. Oriental journal of chemistry, 28(2), 969. (2012).
82. Alabdali, A. J., Sabah, Y. H., & Mohsien, R. A. Synthesis, Characterization and Biological Evaluation of Penicillin Derivatives Complexes with Some Transition Metal Ions. Int. J. Curr. Microbiol. App. Sci, 5(12), 321-332. (2016).
83. Yousif, E., Majeed, A., Al-Sammarrae, K., Salih, N., Salimon, J., & Abdullah, B. Metal complexes of Schiff base: preparation, characterization and antibacterial activity. Arabian Journal of Chemistry, 10, S1639-S1644. (2017).

84. Kasare, M. S., Dhavan, P. P., Jadhav, B. L., & Pawar, S. D. Synthesis of Azo Schiff Base Ligands and Their Ni (II), Cu (II) and Zn (II) Metal Complexes as Highly-Active Antibacterial Agents. Chemistry Select, 4(36), 10792-10797. (2019).
85. Mazhar, N., Aftab, M., Mahmud, T., Basra, M. R., Akhtar, M., & Mitu, L. Synthesis, Characterization and Biological Evaluation of New Schiff Base Ligand derived from 3-hydroxy-benzaldehyde and p-toluidine and its Divalent Metal Ions.(2018).
86. Jawad, A. A., & Alabdali, A. J. Synthesis, Characterization and Antibacterial Activity of Some Penicillin Derivatives. Al-Nahrain Journal of Science, 23(4), 29-34. (2020).
87. Sahan, F., Kose, M., Hepokur, C., Karakas, D., & Kurtoglu, M. New azo-azomethine-based transition metal complexes: Synthesis, spectroscopy, solid-state structure, density functional theory calculations and anticancer studies. Applied Organometallic Chemistry, 33(7), e4954. (2019).
88. Warad, I., Ali, O., Al Ali, A., Jaradat, N. A., Hussein, F., Abdallah, L. & Alharthi, F. A. Synthesis and spectral Identification of three Schiff bases with a 2-(piperazin-1-yl)-N-(thiophen-2-yl methylene) ethanamine moiety acting as novel pancreatic lipase inhibitors: Thermal, DFT, antioxidant, antibacterial, and molecular docking investigations. Molecules, 25(9), 2253. (2020).
89. Mubark, H. M. H., Witwit, I. N., & Ali, A. A. M. Synthesis of new azo imidazole ligand and fabricating it with chelate complexes with some metallic ions. In Journal of Physics: Conference Series (Vol. 1660, No. 1, p. 012031). IOP Publishing. (2020, November).
90. Hossain, M. S., Zakaria, C. M., & Zahan, M. K. (2017). Synthesis and characterization with antimicrobial activity studies on some transition metal complexes of N, O donor novel schiff base ligand. Journal of Scientific Research, 9(2), 209-218.
91. Jawad, A. A., & Alabdali, A. J. Synthesis, Characterization and Antibacterial Activity of Some Penicillin Derivatives. Al-Nahrain Journal of Science, 23(4), 29-34. (2020).
92. Andiappan, K., Sanmugam, A., Deivanayagam, E., Karuppasamy, K., Kim, H. S., & Vikraman, D. In vitro cytotoxicity activity of novel Schiff base ligand–lanthanide complexes. Scientific reports, 8(1), 1-12. (2018).

93. Witwit, I. N., Mubark, H. M. H., & Ali, A. A. M. Synthesis and studying the coordination behavior of a new heterocyclic imidazole azo ligand with some of the first series transition and (IIB) ions. In AIP Conference Proceedings (Vol. 2290, No. 1, p. 030025). AIP Publishing LLC. (2020, December).
94. Salehi, M., Faghani, F., Kubicki, M., & Bayat, M. New complexes of Ni (II) and Cu (II) with tridentate ONO Schiff base ligand: synthesis, crystal structures, electrochemical and theoretical investigation. Journal of the Iranian Chemical Society, 15(10), 2229-2240. (2018).
95. Salehi, M., Faghani, F., Kubicki, M., & Bayat, M. New complexes of Ni (II) and Cu (II) with tridentate ONO Schiff base ligand: synthesis, crystal structures, electrochemical and theoretical investigation. Journal of the Iranian Chemical Society, 15(10), 2229-2240. (2018).
96. Salehi, M., Faghani, F., Kubicki, M., & Bayat, M. New complexes of Ni (II) and Cu (II) with tridentate ONO Schiff base ligand: synthesis, crystal structures, electrochemical and theoretical investigation. Journal of the Iranian Chemical Society, 15(10), 2229-2240. (2018).
97. Mandour, H. S., Abouel-Enein, S. A., Morsi, R. M., & Khorshed, L. A. Azo ligand as new corrosion inhibitor for copper metal: Spectral, thermal studies and electrical conductivity of its novel transition metal complexes. Journal of Molecular Structure, 1225, 129159. (2021).
98. Mondal, S., Chakraborty, M., Mondal, A., Pakhira, B., Blake, A. J., Sinn, E., & Chattopadhyay, S. K. Cu (II) complexes of a tridentate N, N, O-donor Schiff base of pyridoxal: synthesis, X-ray structures, DNA-binding properties and catecholase activity. New Journal of Chemistry, 42(12), 9588-9597. (2018).
99. Anacona, J. R., & Lopez, M. Mixed-ligand nickel (II) complexes containing sulfathiazole and cephalosporin antibiotics: synthesis, characterization, and antibacterial activity. International Journal of Inorganic Chemistry, (2012).
100. Wilcox, L. V. Electrical conductivity. Journal-American Water Works Association, 42(8), 775-776. (1950).
101. Yousif, E., Majeed, A., Al-Sammarrae, K., Salih, N., Salimon, J., & Abdullah, B. Metal complexes of Schiff base: preparation, characterization

and antibacterial activity. Arabian Journal of Chemistry, 10, S1639-S1644. (2017).

102. Chaudhary, N. K., & Mishra, P. Metal complexes of a novel Schiff base based on penicillin: characterization, molecular modeling, and antibacterial activity study. Bioinorganic chemistry and applications, 2017. (2017).

103. Carlin, R. L., & van Duyneveldt, A. J. Magnetic properties of transition metal compounds (pp. 91-92). New York: Springer-Verlag(1977).

104. Robins, D. A. (The magnetic susceptibility and electrical resistivity of some transition metal silicides. Philosophical Magazine, 3(28), 313-327. 1958).

105. Stewart, A. M. General gauge independence of diamagnetism plus paramagnetism. Australian Journal of Physics, 53(4), 613-629. (2000).

106. Hussain, A., AlAjmi, M. F., Rehman, M. T., Amir, S., Husain, F. M., Alsalme, A., ... & Khan, R. A. Copper (II) complexes as potential anticancer and Nonsteroidal anti-inflammatory agents: In vitro and in vivo studies. Scientific reports, 9(1), 1-17. (2019).

107. Elango, G., Arumugam, A. P., & Guhanathan, S. Co (II), Ni (II) and Cu (II) Complexes with Schiff Base Ligand: Syntheses, Characterization, Antimicrobial Studies and Molecular Docking Studies. SOJ Mater Sci Eng, 5(2), 1-12. (2017).

108. Turan, N., Buldurun, K., Çolak, N., & Özdemir, İ. Preparation and spectroscopic studies of Fe (II), Ru (II), Pd (II) and Zn (II) complexes of Schiff base containing terephthalaldehyde and their transfer hydrogenation and Suzuki-Miyaura coupling reaction. Open Chemistry, 17(1), 571-580. (2019).

109. Herburger, A., Barwa, E., Ončák, M., Heller, J., van der Linde, C., Neumark, D. M., & Beyer, M. K. Probing the Structural Evolution of the Hydrated Electron in Water Cluster Anions (H2O) n–, n≤ 200, by Electronic Absorption Spectroscopy. Journal of the American Chemical Society, 141(45), 18000-18003. (2019).

110. Dena, A. S. A., Muhammad, Z. A., & Hassan, W. M. Spectroscopic, DFT studies and electronic properties of novel functionalized bis-1, 3, 4-thiadiazoles. Chemical Papers, 73(11), 2803-2812. (2019).

111. Knaak, T., González, C., Dappe, Y. J., Harzmann, G. D., Brandl, T., Mayor, M., ... & Gruber, M. Fragmentation and distortion of terpyridine-based spin-crossover complexes on Au (111). The Journal of Physical Chemistry C, 123(7), 4178-4185. (2019).

112. Bonhommeau, S., Pontius, N., Cobo, S., Salmon, L., de Groot, F. M., Molnar, G., ... & Eberhardt, W. Metal-to-ligand and ligand-to-metal charge transfer in thin films of Prussian blue analogues investigated by X-ray absorption spectroscopy. Physical Chemistry Chemical Physics, 10(38), 5882-5889. (2008).

113. Gispert, J. R. Coordination chemistry (Vol. 483). Weinheim: Wiley-VCH. (2008).

114. Jena, V.. Electronic Spectra of Transitions Metal Complexes. Lulu. com. (2015)

115. Carlin, R. L. Inorganic electronic spectroscopy (Lever, ABP). (1969).

116. Bougossa, I., Aggoun, D., Ourari, A., Berenguer, R., Bouacida, S., & Morallon, E. Synthesis and characterization of a novel non-symmetrical bidentate Schiff base ligand and its Ni (II) complex: electrochemical and antioxidant studies. Chemical Papers, 74, 3825-3837. (2020).

117. Althobiti, H. A., & Zabin, S. A. (2020). New Schiff bases of 2-(quinolin-8-yloxy) acetohydrazide and their Cu (II), and Zn (II) metal complexes in vitro antimicrobial potentials and in silico physicochemical and pharmacokinetics properties. Open Chemistry, 18(1), 591-607.

118. Awad, A. A., Hasson, M. M., & faron Alfarhani, B. September). Synthesis and characterization of a new Schiff base ligand type N2O2 and their cobalt (II), nickel (II), copper (II), and zinc (II) complexes. In Journal of Physics: Conference Series (Vol. 1294, No. 5, p. 052040). IOP Publishing. (2019),

119. Warad, I., Ali, O., Al Ali, A., Jaradat, N. A., Hussein, F., Abdallah, L., ... & Alharthi, F. A. Synthesis and spectral Identification of three Schiff bases with a 2-(piperazin-1-yl)-N-(thiophen-2-yl methylene) ethanamine moiety acting as novel pancreatic lipase inhibitors: Thermal, DFT, antioxidant, antibacterial, and molecular docking investigations. Molecules, 25(9), 2253. (2020).

120. Al-Riyahee, A. A., Hadadd, H. H., & Jaaz, B. H. Novel Nickel (II), Copper (II) and Cobalt (II) complexes of Schiff bases A, D and E:

Preparation, Identification, Analytical and Electrochemical Survey. Oriental Journal of Chemistry, 34(6), 2927. (2018).

121. Witwit, I. N., Mubark, H. M. H., & Ali, A. A. M. Synthesis and studying the coordination behavior of a new heterocyclic imidazole azo ligand with some of the first series transition and (IIB) ions. In AIP Conference Proceedings (Vol. 2290, No. 1, p. 030025). AIP Publishing LLC. (2020, December).
122. Mahmoud, W. A., Hassan, Z. M., & Ali, R. W. Synthesis and spectral analysis of some metal complexes with mixed Schiff base ligands 1-[2-(2-hydroxybenzylideneamino) ethyl] pyrrolidine-2, 5-dione (HL1) and (2-hydroxybenzalidine) glycine (HL2). In Journal of Physics: Conference Series (Vol. 1660, No. 1, p. 012027). IOP Publishing. (2020, November).
123. Yeğiner, G., Gülcan, M., Işık, S., Ürüt, G. Ö., Özdemir, S., & Kurtoğlu, M. Transition metal (II) complexes with a novel azo-azomethine Schiff base ligand: Synthesis, structural and spectroscopic characterization, thermal properties and biological applications. Journal of fluorescence, 27(6), 2239-2251. (2017).
124. Mumtazm, A., & Mahmud, T. Structural investigation of some novel synthesized Schiff base Transition metal complexes derived from drug together with Antimicrobial study. Pakistan journal of pharmaceutical sciences, 32(3). (2019).
125. Kareem, I. K., & Hadi, M. A. Synthesis and Characterization Of Some transition Metal Complexes with New Azo-Schiff base ligand 3, 4-bis (((1E, 2E)-2-((2-((4-((Z)-(3-hydroxyphenyl) diazenyl) naphthalen-1-yl) amino) ethyl) imino)-1, 2-diphenylethylidene) amino) phenyl)(phenyl) methanone. Egyptian Journal of Chemistry, 63(1), 301-313. (2020).
126. Darari, M., Francés-Monerris, A., Marekha, B., Doudouh, A., Wenger, E., Monari, A, & Gros, P. C. Towards Iron (II) Complexes with Octahedral Geometry: Synthesis, Structure and Photophysical Properties. Molecules, 25(24), 5991. (2020).
127. Turan, N., Buldurun, K., Çolak, N., & Özdemir, İ. Preparation and spectroscopic studies of Fe (II), Ru (II), Pd (II) and Zn (II) complexes of Schiff base containing terephthalaldehyde and their transfer hydrogenation and Suzuki-Miyaura coupling reaction. Open Chemistry, 17(1), 571-580. (2019).

128. Alsabra, R., & Radwan, L. Synthesis of Metal Complexes Fe (II), Co (II), Ni (II) of Monodentate Schiff Bases Derived from Aromatic Aldehyde. Synthesis, 8(7). (2016).

129. Rani, C. V., Kesavan, M. P., Haseena, S., Varatharaj, R., Rajesh, J., & Rajagopal, G. Bidentate schiff base ligands appended metal (II) complexes as probes of DNA and plasma protein: in silico molecular modelling studies. Applied biochemistry and biotechnology, 191(4), 1515-1532. (2020).

130. Barth, H. G., & Mays, J. W. (Eds.). Modern methods of polymer characterization John Wiley & Sons. (Vol. 115).(2019)

131. Ratcliffe, L. P., Derry, M. J., Ianiro, A., Tuinier, R., & Armes, S. P. A single thermoresponsive diblock copolymer can form spheres, worms or vesicles in aqueous solution. Angewandte Chemie, 131(52), 19140-19146. (2019).

132. Hore, P. J. Nuclear magnetic resonance. Oxford University Press, USA. (2015).

133. Salem, Z. Synthesis and Study of an Azo-azomethine Dyes with NO Donor Set of Atoms and Their Cu (II), Co (II) and Ni (II) Complexes. Chemistry and Materials Research, 9(3). (2017).

134. Kareem, I. K., & Hadi, M. A. Synthesis and Characterization Of Some transition Metal Complexes with New Azo-Schiff base ligand 3, 4-bis (((1E, 2E)-2-((2-((4-((Z)-(3-hydroxyphenyl) diazenyl) naphthalen-1-yl) amino) ethyl) imino)-1, 2-diphenylethylidene) amino) phenyl)(phenyl) methanone. Egyptian Journal of Chemistry, 63(1), 301-313. (2020).

135. Borase, J. N., Mahale, R. G., Rajput, S. S., & Shirsath, D. S. Design, synthesis and biological evaluation of heterocyclic methyl substituted pyridine Schiff base transition metal complexes. SN Applied Sciences, 3(2), 1-13. (2021).

136. Ahmad, N., Alam, M., Wahab, R., Ahmed, M., & Ahmad, A. Synthesis, spectral and thermo-kinetics explorations of Schiff-base derived metal complexes. Open Chemistry, 18(1), 1304-1315. (2020).

137. Gönül, İ. Synthesis and structural characterization of ONO type tridentate ligands and their Co (II) and Ni (II) complexes: Investigation of electrical conductivity and antioxidant properties. Inorganica Chimica Acta, 495, 119027. (2019).

138. Kholoud, R. Synthesis, physicochemical characterization and cytotoxic activity of p-methoxyphenyl and p-fluorophenyl maleanilic acid and their corresponding Cr, Mo and W metal carbonyl novel Organometallic Chelates. Journal of Transition Metal Complexes, 2020. (2020).

139. Hussain, G., Abass, N., Shabir, G., Athar, M., Saeed, A., Saleem, R., ... & Khan, M. A.New acid dyes and their metal complexes based on substituted phenols for leather: Synthesis, characterization and optical studies. Journal of applied research and technology, 15(4), 346-355. . (2017).

140. Warad, I., Ali, O., Al Ali, A., Jaradat, N. A., Hussein, F., Abdallah, L. & Alharthi, F. A. Synthesis and spectral Identification of three Schiff bases with a 2-(piperazin-1-yl)-N-(thiophen-2-yl methylene) ethanamine moiety acting as novel pancreatic lipase inhibitors: Thermal, DFT, antioxidant, antibacterial, and molecular docking investigations. Molecules, 25(9), 2253. (2020).

141. Bougossa, I., Aggoun, D., Ourari, A., Berenguer, R., Bouacida, S., & Morallon, E. Synthesis and characterization of a novel non-symmetrical bidentate Schiff base ligand and its Ni (II) complex: electrochemical and antioxidant studies. Chemical Papers, 74, 3825-3837. (2020).

142. Soso, S. B., & Koziel, J. A. Analysis of odorants in marking fluid of Siberian tiger (Panthera tigris altaica) using simultaneous sensory and chemical analysis with headspace solid-phase microextraction and multidimensional gas chromatography-mass spectrometry-olfactometry. Molecules, 21(7), 834. (2016).

143. Rubakhin, S. S., & Sweedler, J. V. A mass spectrometry primer for mass spectrometry imaging. In Mass Spectrometry Imaging (pp. 21-49). Humana Press, Totowa, NJ. (2010).

144. Awad, H., Khamis, M. M., & El-Aneed, A. Mass spectrometry, review of the basics: ionization. Applied Spectroscopy Reviews, 50(2), 158-175. (2015).

145. Horita, T., Yamaji, K., Ishikawa, M., Sakai, N., Yokokawa, H., Kawada, T., & Kato, T. Active Sites Imaging for Oxygen Reduction at the La0. 9Sr0. 1MnO3− x/Yttria-Stabilized Zirconia Interface by Secondary-

Ion Mass Spectrometry. Journal of the Electrochemical Society, 145(9), 3196. (1998).

146. Warad, I., Ali, O., Al Ali, A., Jaradat, N. A., Hussein, F., Abdallah, L. & Alharthi, F. A. Synthesis and spectral Identification of three Schiff bases with a 2-(piperazin-1-yl)-N-(thiophen-2-yl methylene) ethanamine moiety acting as novel pancreatic lipase inhibitors: Thermal, DFT, antioxidant, antibacterial, and molecular docking investigations. Molecules, 25(9), 2253. (2020).

147. Hussain, A., AlAjmi, M. F., Rehman, M. T., Amir, S., Husain, F. M., Alsalme, A. & Khan, R. A. Copper (II) complexes as potential anticancer and Nonsteroidal anti-inflammatory agents: In vitro and in vivo studies. Scientific reports, 9(1), 1-17. (2019).

148. Andersson, B., Gustafson, G., & Söderberg, B. A general model for jet fragmentation. Zeitschrift für Physik C Particles and Fields, 20(4), 317-329. (1983).

149. El-Boraey, H. A., & EL-Gammal, O. A. Macrocyclic Cu (II) and Pd (II) complexes with new 16-membered tetradentate [N 4] ligand: synthesis, characterization, 3D molecular modeling and in vitro anticancer and antimicrobial activities. Journal of Inclusion Phenomena and Macrocyclic Chemistry, 90(1), 123-134. (2018).

150. Dahi, M. A., & Jarad, A. J. Synthesis, characterization and biological evaluation of thiazolyl azo ligand complexes with some metal ions. In Journal of Physics: Conference Series (Vol. 1664, No. 1, p. 012090). IOP Publishing. (2020, November).

151. Mulye, S. S., Maurya, A. S., Kamble, S. A., Deshmukh, P. V., Yadav, L. S., Mishra, R. K., & Jain, A. Medicinal and Phytochemical Analysis of Alcoholic Whole Fruit Extracts of Actinidia Deliciosa. Journal of Scientific Research, 64(1). (2020).

152. Bose, S., Khodke, M., Basak, S., & Mallick, S. K. Detection of biofilm producing staphylococci: need of the hour. Journal of clinical and diagnostic research, 3(6), 1915-1920. (2009).

153. Halim, R. M. A., Kassem, N. N., & Mahmoud, B. S. Detection of biofilm producing staphylococci among different clinical isolates and its relation to methicillin susceptibility. Open access Macedonian journal of medical sciences, 6(8), 1335. (2018).

الخلاصة

يتضمن هذا العمل تحضير اربع ليكندات جديده كمشتقات 6-امينو بنسيليينيك اسيد مع مركبات قواعد شيف لانتاج ليكندات(HL_1),(HL_2),(HL_3) على التوالي تم تحضير معقدات (HL_4),جديده من تفاعل 6-امينو بنسيلينك اسيد, الليكندات المذكوره مع ايونات الفلزات الانتقاليه Cu(II),Ni(II),Fe(II) حيث تم تفاعلها مع الايونات الفلزيه نسبه 1:2 ليكاند فلز تم تشخيص المركبات المحضره بواسط طيف الرنين النووي المغناطيسي للبروتون ,اطياف الاشعه تحت الحمراء , اطياف الالاشعه الفوق البنفسجيه والمرئيه, والتحليل الدقيق للمعادن والعناصر ,التوصيليه الكهربائيه ,الحساسيه المغناطيسيه للمعقدات فقد بينت هذه الدراسات ان الشكل الفراغي المقترح لجميع المعقدات هو ثماني السطوح كما تم دراسه الفعاليه البايولوجيه لليكندات المحضره ومعقداتها حيث تم دراستها ضد بكتيريا ال(*s.aureus*) باستخدام طريقه ال MICفقد اثبتت الدراسه كفائه المركبات المحضره في تثبيط الفعاليه البايولوجيه للبكتيريا (S.aureus)كما تم دراسه فعاليتها ضد عوامل الضراوه Biofilm and Hemolysin.

وزارة التعليم العالي والبحث العلمي
جامعة كربلاء
كلية العلوم
قسم الكيمياء

تحضير وتشخيص معقدات تحتوي على مجموعة البيتا-لاكتام مع بعض العناصر الانتقالية ودراسة فعاليتها ضد البكتيريا المرضيه الحيوية

رسالة مقدمة الى

مجلس كلية العلوم-جامعة كربلاء وهي جزء من متطلبات نيل شهاده الماجستير في الكيمياء

تقدمت بها

ابتسام محمد علي عبد الحسن

بأشراف

أ.د محمد حامد سعيد

أ.د فاء صادق محسن الوزني

2021 م **1442**